High Resolution Radio Frequency Measurements of Faraday Rotation and Differential Absorption with Rocket Probes

H. Knoebel, D. Skaperdas, J. Gooch,
B. Kirkwood and H. Krone

Edited by D. Skaperdas

REPORT R-273 DECEMBER, 1965

This work was supported in part by the Joint Services Electronics Programs (U. S. Army, U. S. Navy, and U. S. Air Force) under Contract No. DA 28 043 AMC 00073(E).

This work was also supported by the National Aeronautics and Space Administration under Grant NsG 504.

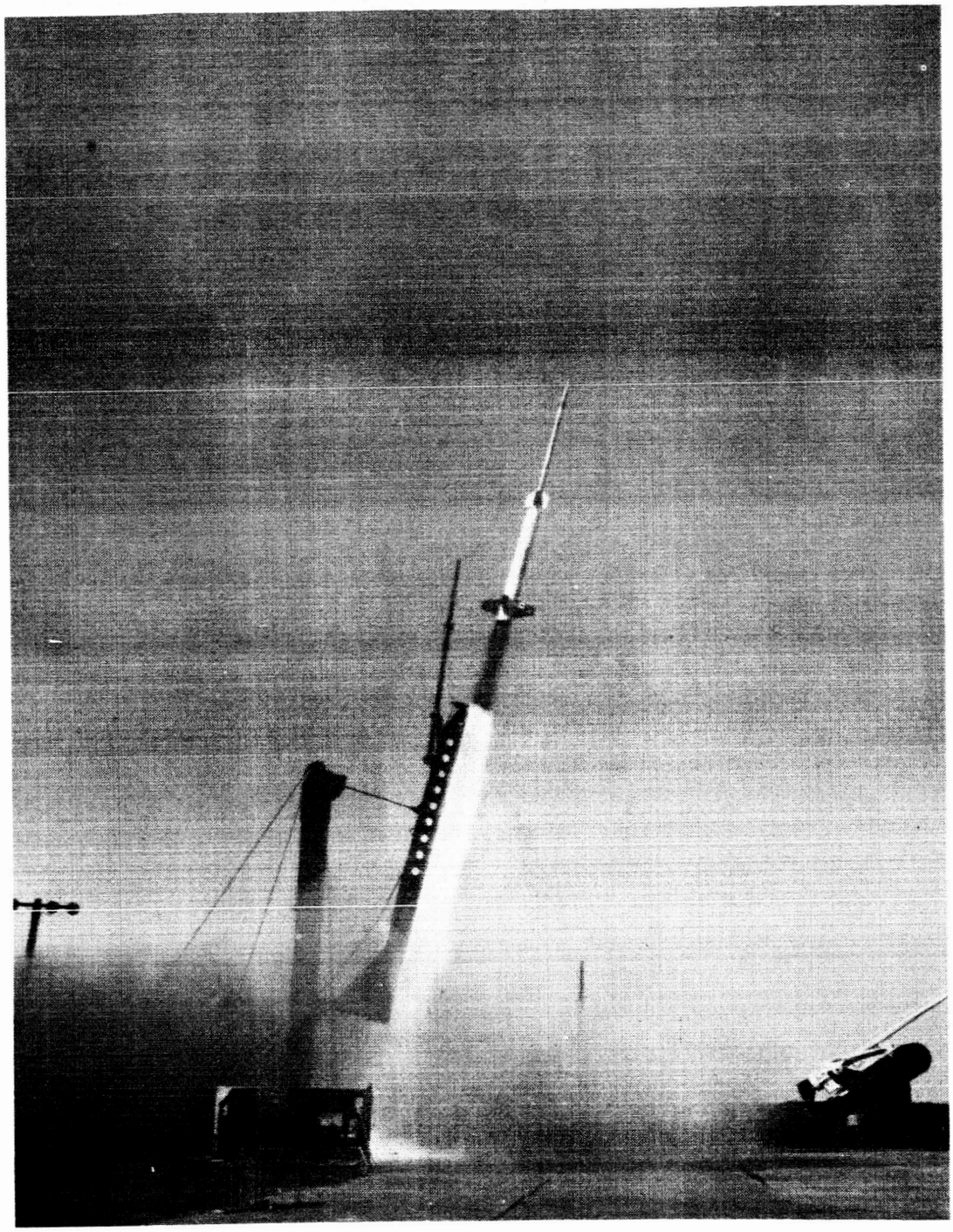

Nike-Apache Rocket with CSL Payload During Launch

Index

Preface

A highly essential system for lower ionosphere radio propagation measurements, using probe rockets, developed by the Coordinated Science Laboratory is described in detail. Unique features include (1) feedback around a closed loop consisting of the rocket and ground stations employed in a null-seeking technique, which increases absorption measurement accuracy and (2) artificial rotation of the ground based antenna which extends the range over which Faraday rotation can be resolved from layer reflection phenomena. The rocket borne and ground station equipment has been shown to work reliably during a series of 14 rocket measurements made from both land-based facilities and the NASA seagoing mobile launch platform during the International Quiet Sun Years. Complete engineering information is given in the hope that other investigators may easily duplicate the measurements. Data processing techniques for smoothing and improving the accuracy as well as some typical data are described.

This system was developed by a group of scientists and engineers who are primarily interested in aerospace instrumentation, measurement control, and data handling techniques working in cooperation with the ionosphere scientists at the University of Illinois Electrical Engineering Department, who were responsible for the basic research program. It is felt that the application of sound engineering principles to this program of basic measurement will greatly increase the fruitfulness of rocket probes in obtaining an understanding of our atmosphere.

H. Knoebel
Group Leader

I. Introduction

During the IQSY years of 1964 and 1965 the Coordinated Science Laboratory conducted ionospheric experiments at various geomagnetic latitudes using a series of fourteen Nike-Apache rocket probes under a synoptic IQSY program which is headed by Dr. Sidney Bowhill. The purpose of these experiments was to measure with improved techniques the differential absorption and Faraday rotation for the determination of electron density and collision frequency in the D region. Of the 14 rocket firings 13 were considered operationally successful. Failure of the fourteenth was due to malfunctioning of a commercial telemetry transmitter. These firings mark the end of CSL's participation in this phase of the project. This report is written to serve two purposes. The first is to serve as a final project report and the second is to provide a type of training manual whereby other groups can either use CSL's or build their own equipment to carry out similar ionospheric experiments. In a prototype system such as this, constructed to meet firing deadlines, there are certainly some engineering designs that can now be improved. Such known weak or marginal designs will be pointed out and suggestions given to improve the performance. This report, then, will describe the novel system and operating techniques developed by CSL used to measure differential absorption and Faraday rotation and will describe some representative data.

II. General Description

A. Theory

The presence of a magnetic field in a region of free electrons gives rise to a bi-refringent index of refraction, i.e., two indices of refraction exist, depending on the polarization of the electromagnetic waves within the region. This results in a relative polarization angle between two differently polarized waves (Faraday rotation) propagating within the medium. In addition, collisions between the electrons and neutral particles lead to power absorption from the propagating waves. The presence of absorption makes the two indices of refraction complex, with a resultant Faraday rotation and differential absorption between two differently polarized waves. The Appleton-Hartree equations which evaluate the index of refraction are quite complex and simplify greatly if the electromagnetic waves are propagated either in the direction of (quasi-longitudinal approximation) or perpendicular to (quasi-transverse approximation) the earth's magnetic field. In CSL's series of experiments, both propagations were conducted on separate rocket launchings.

The electron density versus height profile can be computed in regions of negligible loss by standing wave analysis or by the relative polarization angle (Faraday rotation) between two differently polarized waves (ordinary and extraordinary) propagated through the ionosphere either in or perpendicular to the earth's magnetic field. The Faraday rotation is proportional to $\int N dz$ where N is the electron density and z is the height. The electron density can also be measured independently by means of a probe on the rocket. The electron collision frequency ν can be computed at a given height by assuming a model $\nu=kp$ where p is the atmospheric

pressure at that height and k is a constant. This constant is determined from the appropriate Appleton-Hartree approximation using the relative absorption between the two differently polarized waves and the electron density determined from the Faraday rotation.

Most of CSL's rocket probes have taken place under conditions where the quasi-longitudinal approximation of the Appleton-Hartree equation holds; i.e., the direction of propagation of the transmitted wave is very nearly in the direction of the earth's magnetic field. Under this condition the refractive index $\eta=(\mu-i\chi)$ is given by

$$\eta^2 = (\mu-i\chi)^2 = 1 - \frac{X}{1-iZ\pm Y} \qquad (1)$$

where X is a measure of the electron density, Y is a measure of the earth's magnetic field, and Z is a measure of the electron collision frequency. The wave polarization ρ, defined by the ratio of the y and x components of the electric field intensity in the plane transverse to the direction of propagation z (where x, y, and z is a triad), is, for the quasi-longitudinal case,

$$\rho = \mp i. \qquad (2)$$

From the $\pm Y$ term in Eq.(1), it is seen that there are two values for the refractive index η in space, giving rise to two modes of propagation. From Eq.(2), it is seen that the resulting space and time quadratures cause the two modes to be oppositely circularly polarized waves, the ordinary and the extraordinary. In the northern hemisphere, Y in Eq.(1) is a positive number for ascending waves, negative in the southern hemisphere. Therefore, in the northern hemisphere, the counterclockwise wave looking up is the one which is more absorbed, whereas in the southern hemisphere

it is the clockwise one. These facts must be taken into consideration during firings in the southern hemisphere.

Some of the rocket firings took place at the magnetic equator. For this experimental condition, the direction of the propagated radio wave will be transverse to the earth's magnetic field. For this case, the "quasi-transverse" approximation of the Appleton-Hartree equation is valid, and, for the purely transverse case, one has

$$\eta^2 = 1 - \frac{X}{1-iZ} \qquad \text{with} \quad \rho = 0$$

for the ordinary wave, and

$$\eta^2 = 1 - \frac{X(1-X-iZ)}{(1-iZ)(1-X-iZ)-Y^2} \qquad \text{with} \quad \rho = \infty$$

for the extraordinary wave.

From these equations it can be shown that the ordinary wave is linearly polarized with its electric vector parallel to the earth's magnetic field, while the extraordinary wave is linearly polarized with its electric vector perpendicular to the earth's magnetic field (and to the direction of propagation). Hence, during equatorial rocket firings, the radiating system must be conveniently modified to change the transmitted waves from oppositely circularly polarized to mutually perpendicular linearly polarized, with the ability to position the two linear polarizations about the axis of propagation. A scheme for doing this will be described in section III A.

B. System

The differential absorption and total absorption, apart from the inverse square law attenuation, are functions of frequency. It is desirable to choose a frequency low enough to yield significant amounts of differential absorption and yet have enough extraordinary wave signal left to measure

Faraday rotation. Since it is difficult to predict well in advance the level of ionospheric ionization, and since the simultaneous success of both measurements is critically dependent on the choice of frequency, provision is made for two sets of equipment tuned in advance to different frequencies in the two to four megacycle range.

All of the ground-based equipment except the transmitting antennas are within a van. The system is designed to operate in any of three modes of increasing complexity. The least complex mode maintains the transmitted ordinary and extraordinary circularly polarized waves at constant values. This method makes the measurement of Faraday rotation difficult when the differential absorption becomes large at the higher altitudes, resulting in decreased signal modulation. Furthermore, the receiver output versus input characteristics must be accurately known in order to measure the differential absorption.

The second mode is to mechanically sweep the ordinary transmitted wave output power by means of an attenuator, traversing the entire range about once each second. This would insure appropriate measuring conditions at least once each second, corresponding to data points no more than one kilometer apart.

The third and most complex mode, and the one which was used successfully on all the experiments, is to control the extraordinary wave transmitted power by means of an attenuator actuated by feedback of the received signal telemetered from the rocket, keeping the ordinary transmitted power constant. As differential absorption appears, the attenuation is continuously reduced by a servomechanism to maintain the modulation of the received signal at a fixed 32 per cent, corresponding to a 10 db

difference in the intensity of the two received wave components. The attenuator settings are continuously recorded along with the other data, enabling subsequent determination of the differential absorption.

Figure 1 is a block diagram of the entire system used during the earlier firings. The CSL van equipment is shown within the dotted lines at the left. The two exciters X and O are crystal-controlled cw oscillators differing in frequency by 500 cps and operating 250 cps above and below the desired center frequency. Each exciter can be quickly switched to an alternate frequency in the 2-4 mc range if desired.

The output of each exciter is controlled by a waveguide-beyond-cutoff attenuator actuated in any of three ways as described above. Fig. 2 indicates the mechanical system controlling the attenuators. The output shaft of each differential controls an attenuator position. The input to one differential (extraordinary) consists of a time-dependent angle $\theta_1(t)$ coming from the servo motor via a slip clutch and speed reducer, and an angular position θ_2 (power level) set manually. The output of this differential, which controls the extraordinary wave attenuator, consists of $\theta_2 - \theta_1(t)$. The inputs to the second differential (ordinary) consist of the manually set angular position θ_2 (power level) and a fixed position θ_3, which is used only for calibration purposes. The output of this differential, which controls the ordinary wave attenuator, consists of $\theta_2 - \theta_3$. The voltage across a potentiometer connected to the output shaft of each differential is used to monitor the position of each attenuator. Photographs of the attenuator unit are shown in Fig. 3a, b.

In the earlier version the outputs of the attenuators, designated as X and O, are fed into a hybrid circuit consisting of two transformers arranged to form the outputs X + O and X - O. One of the outputs, X - O,

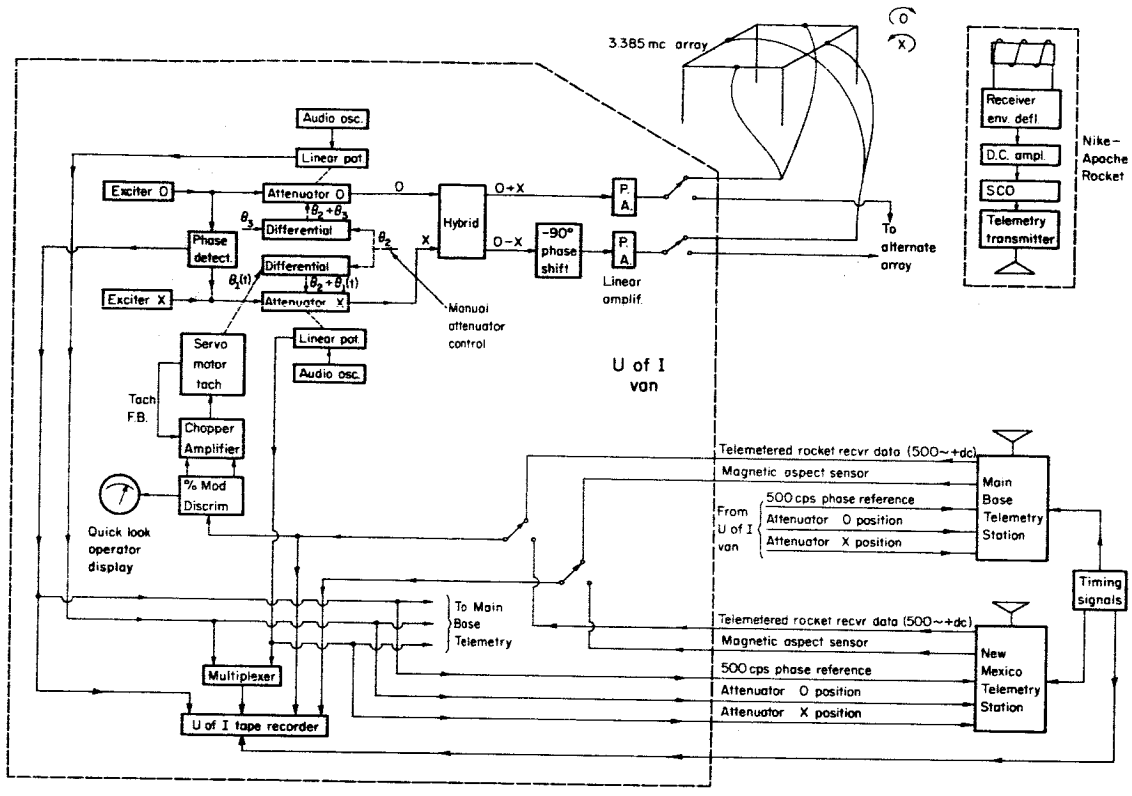

Figure 1

Early System Block Diagram

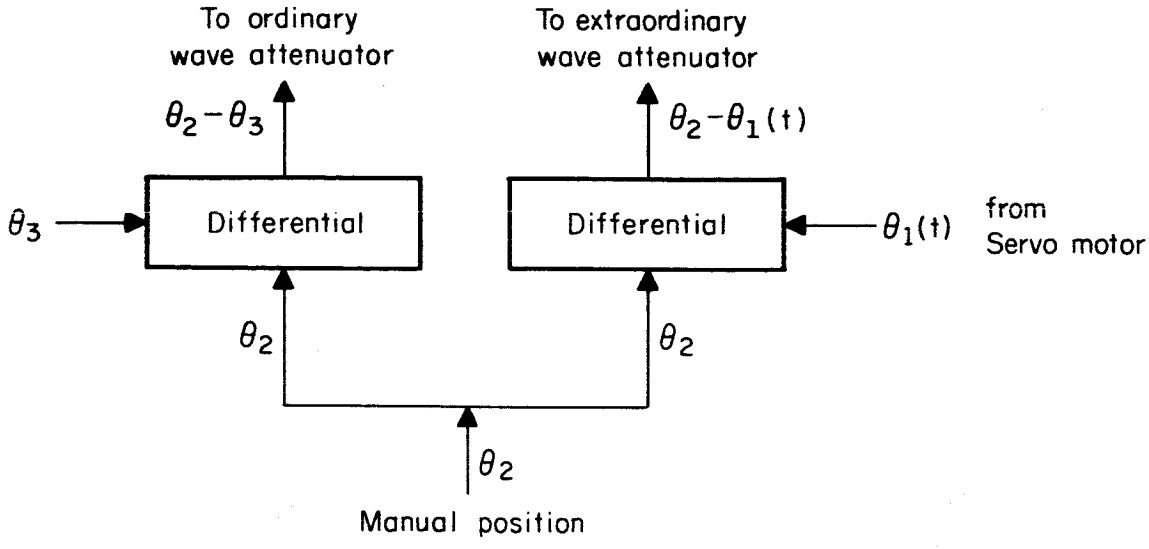

Figure 2

Rf Attenuator Drive

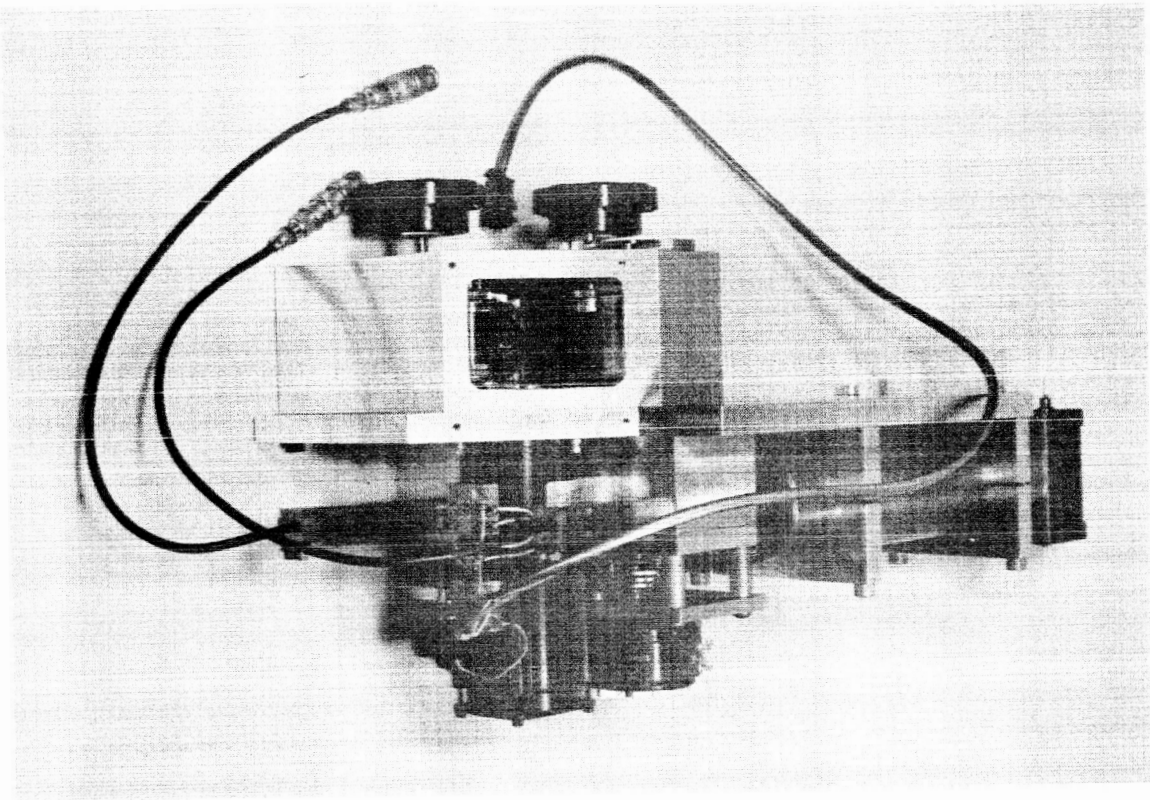

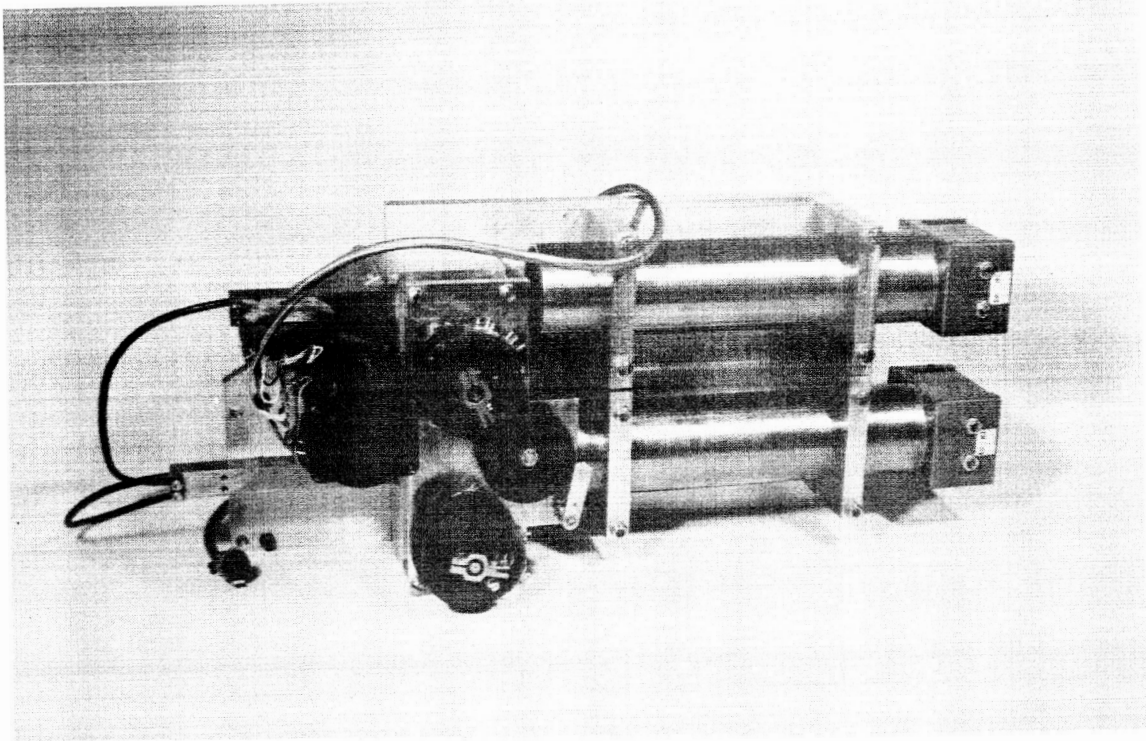

Figure 3
Waveguide-Beyond-Cutoff Attenuators and Servo Drive Mechanism

is phase shifted 90° with respect to the other by means of an extra quarter wavelength transmission line in its path. The other output is fed to an attenuator pad to equalize the attenuation of the delay line. The two outputs are then amplified by the linear power amplifiers, which are commercial one kilowatt transmitters made by the Technical Materiel Corporation, and then fed to the appropriate antenna array elements through balancing and matching networks. Each array consists of four horizontal half-wave dipoles elevated one-quarter wavelength above the ground plane and arranged as the sides of a square, with the inputs of the opposite pairs fed in phase, one pair being fed by $(O+X)/\underline{0°}$, the other by $(O-X)/\underline{-90°}$. The combined space and time quadrature results in two oppositely circularly polarized waves, X and O, which would degenerate to a simple linearly polarized wave if X and O were at the same frequency and amplitude. The difference of 500 cps between X and O results, instead, in a linearly polarized wave in which the plane of polarization rotates at 250 cps. Each dipole pair, moreover, gives an antenna gain over a single dipole of about 4 db, and the presence of the imperfect ground plane increases the gain by perhaps another few db. In order to test the antenna array, a horizontal ferrite rod antenna, placed at the center of the array and rotating at 600 rpm, is provided. If during tests the transmitting antenna array transmits anything but a circularly polarized wave, it is easily seen by this rotating antenna as a modulated rf signal.

For the later firings a scheme for obtaining either circular or linear polarizations was developed and incorporated into the system. The O and X waves can be independently adjusted for either circular or linear polarizations by variable attenuators and phase shifters. As seen in the new system block diagram of Fig. 4, the signal which is to be the ordinary

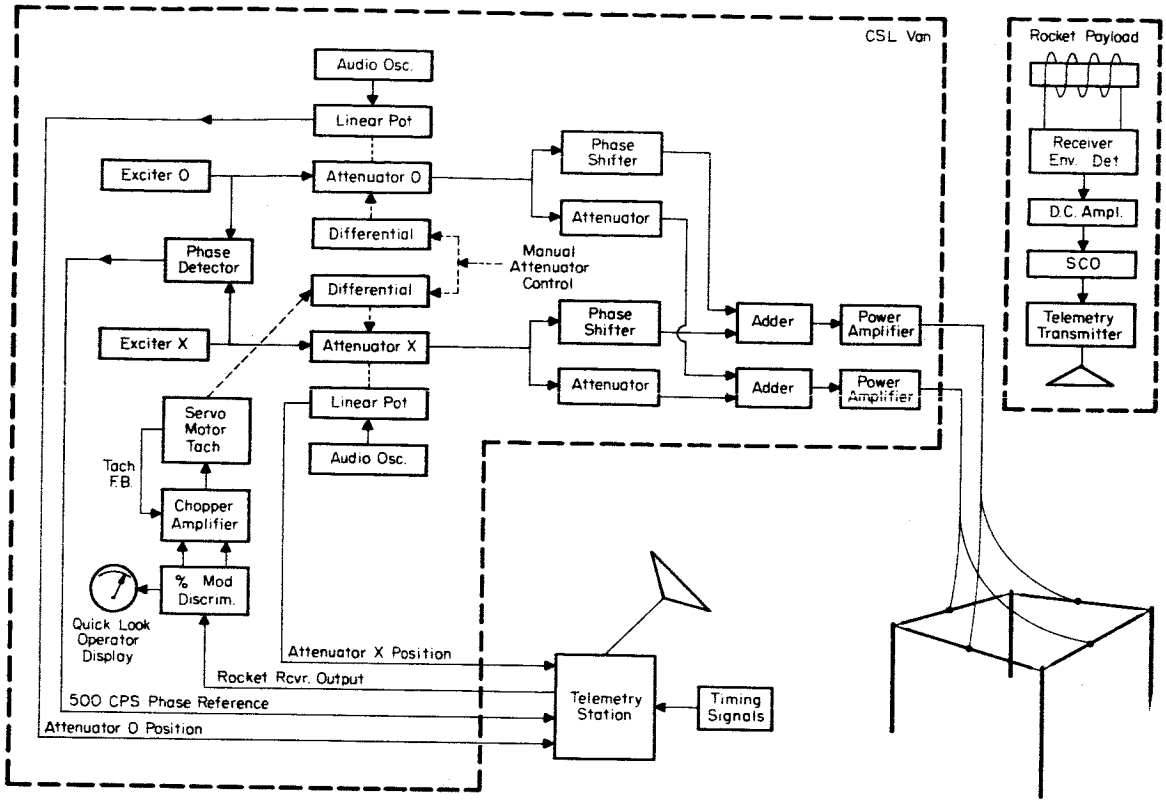

Figure 4

Present System Block Diagram

wave is passed through a power divider, half the power going through a variable phase shifter and half through a variable attenuator. The outputs are sent to adders which have 30 db isolation between adjacent channels, then are amplified and radiated. The extraordinary wave is treated identically. By observing a suitable indicator, such as a small land or airborne rotating dipole in the case of cw or reflections from the ionosphere in the case of pulsed transmissions, each transmitted mode can be set to circular or linear polarization by means of its corresponding phase shifter and attenuator, independently from the other mode. The purity of polarization is limited by the accuracy and resolution of the indicator.

The ferrite-rod antenna (see Fig. 5) located in the Nike-Apache rocket gives an rf signal output which is amplitude modulated in the region of 500 cps (which is twice the 250 cps rotation of the transmitted plane of polarization) plus twice the rotation of the rocket spin plus a small contribution from Faraday rotation. The rocket spin is independently measured by a magnetic aspect sensor contained in the payload.

The output of the antenna is fed to a transistorized, crystal-controlled superheterodyne receiver designed and developed by Space Craft, Incorporated (see Fig. 6). The sensitivity of the receiver for a 10 db signal-to-noise ratio and a signal which is 90 per cent modulated at 500 cps is -120 dbm or better. Its dynamic range is from threshold to -60 dbm with no more than 6 db change in output level. The receiver bandwidth is about 2 kc and the AGC time constant for the first payload was about 100 msec. The modulated rf signal is detected, dc coupled and amplified to a 5-volt level for feeding a standard FM-FM telemetry sub-carrier oscillator and telemetry transmitter.

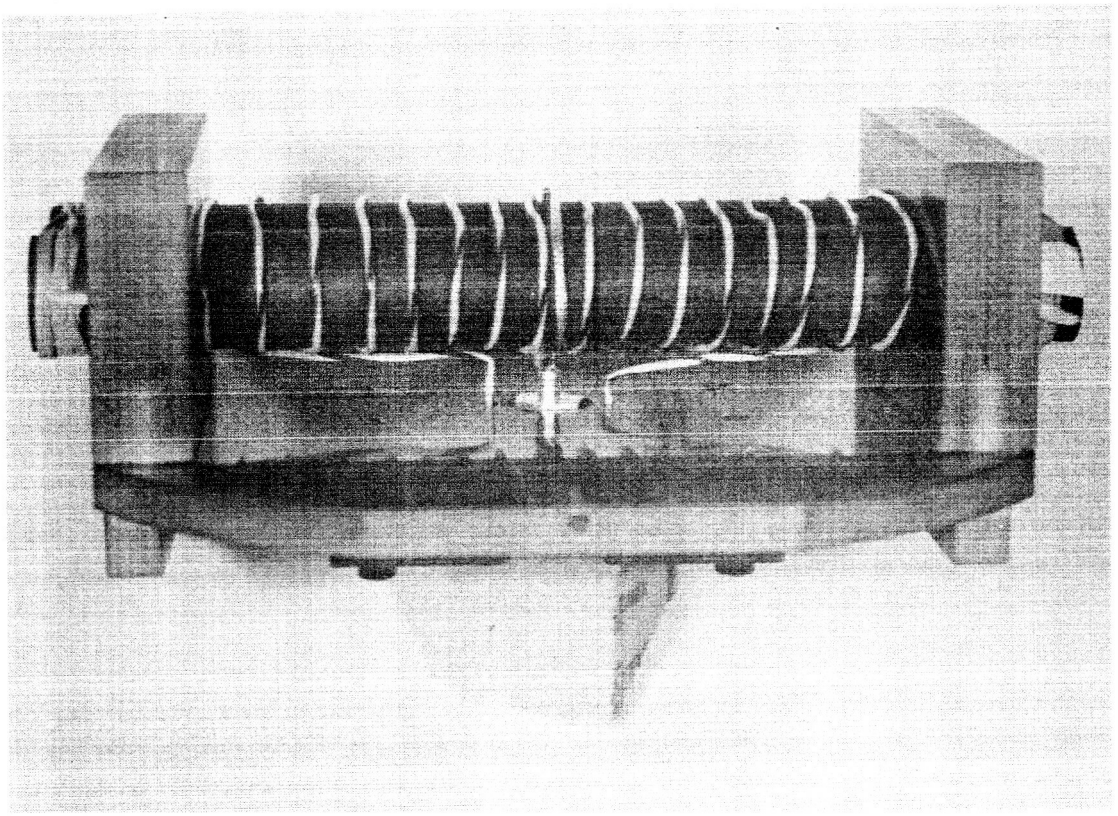

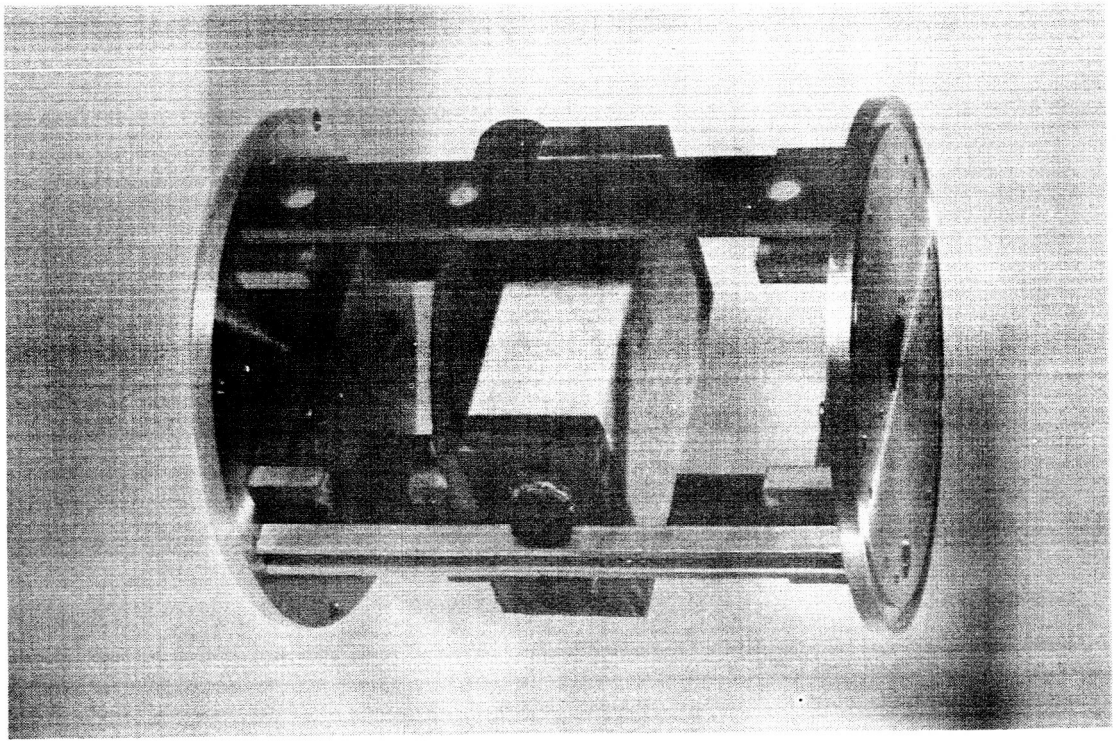

Figure 5
Ferrite Rod Rocket Antenna

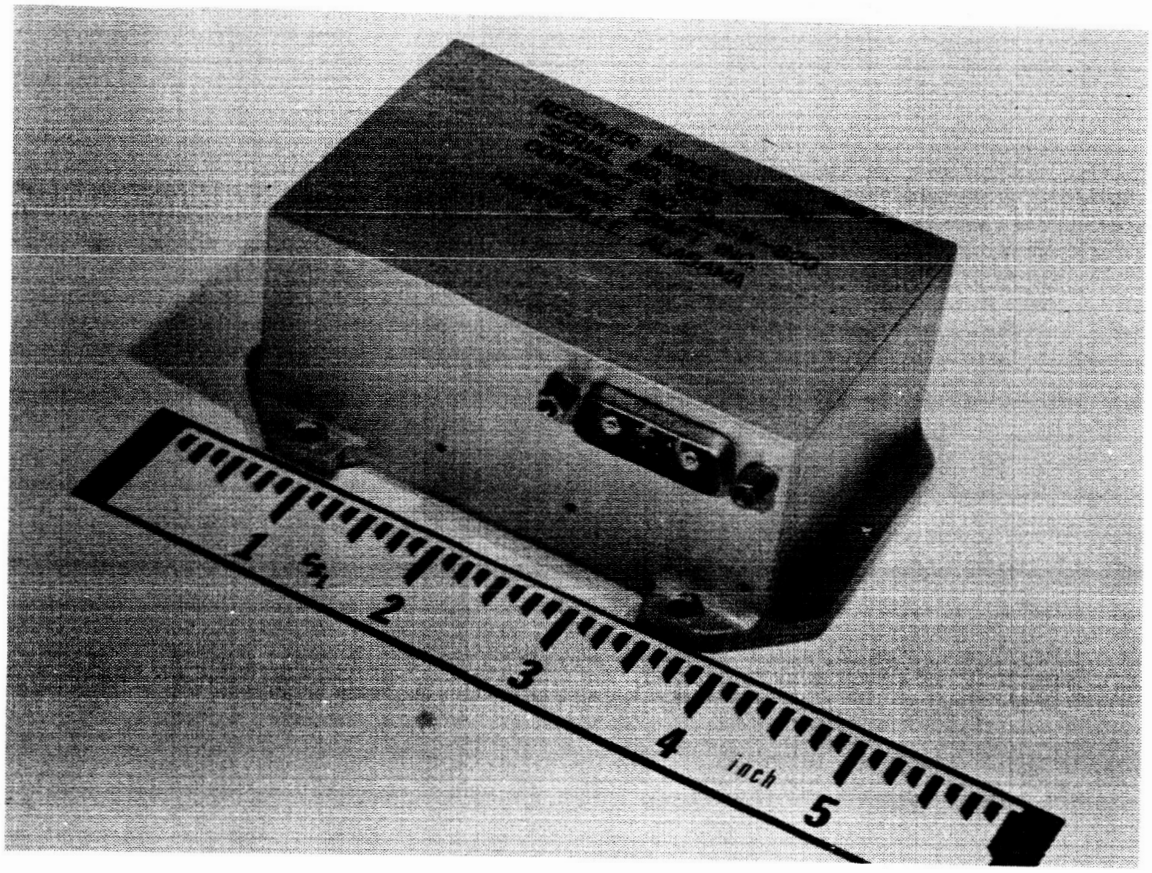

Figure 6

Rocket Receiver

The telemetry signal from the rocket is received and recorded, usually at two separate telemetry stations. Both stations re-transmit the telemetered receiver signal, which contains the 500 cps difference frequency and a dc component, to the CSL van via telephone lines where both are monitored. The better of the two signals is selected and fed to a circuit which separates the ac and dc components and compares their relative magnitudes as a measure of the per cent modulation. If this modulation is different from a predetermined value of 32 per cent, a dc error signal of appropriate polarity is developed. This is chopped at 60 cps, amplified and fed to a servo motor. The servo motor then controls the relative position of the extraordinary wave attenuator (X) in order to maintain a constant 32 per cent modulation at the rocket receiver. A tachometer is incorporated to stabilize the feedback loop.

Signals generated at the transmitter van and sent to the telemetry stations for recording are the 500 cps beat frequency of the two exciters used as a phase reference and the two rf attenuator position signals. Additional signals recorded at the telemetry stations of interest to this experiment include the telemetered rocket receiver signal, which is sent back to the van for closing the servo loop, the telemetered magnetic aspect sensor signal, the launch range timing signal and the rocket trajectory data obtained from radar tracking sites. In addition, part of the 500 cps reference frequency is added to the receiver signal and part is phase shifted 90° and added to the receiver signal and both recorded. These are used as an alternative way of extracting the Faraday rotation data.

C. Data

The advantages of the data obtained by CSL's system are as follows: First, a high sampling rate of Faraday rotation and differential absorption is obtained due to the 500 cps frequency difference between the extraordinary and ordinary waves. In the so-called quasi-longitudinal mode where the two waves are oppositely circularly polarized, this means that the linearly polarized transmitted wave is rotating at 250 cps. Second, the high sampling frequency is far removed from any spin modulation and from the standing wave modulation at all altitudes, thereby enabling the signal frequency to be clearly distinguished from the standing wave pattern. Third, the servo system, which maintains a constant ratio of ordinary to extraordinary power at the rocket, considerably reduces the non-linearity of the rocket receiver for measuring relative absorption between the two waves and transfers this measurement to a set of precision rf attenuators located on the ground. These refinements have enabled Faraday rotation and differential absorption measurements to be made to resolutions of about one degree and 0.2 db, respectively.

Representative data during a rocket probe is shown from CSL's first experiment, designated as Number 14.143. The Nike-Apache rocket reached an apogee of 105 statute miles and a horizontal range of 110 miles with a flight time of 406 seconds. All of the differential absorption and Faraday rotation during the ascent took place from about 60 seconds to 90 seconds after launch. Apogee occurred at 205 seconds.

A general picture of the experiment can be seen in Fig. 7a,b,c,d, which shows five recorded signals of interest during the entire rocket flight. The signals at the top and bottom edges are universal time signals. The second signal from the top is the telemetered rocket receiver output

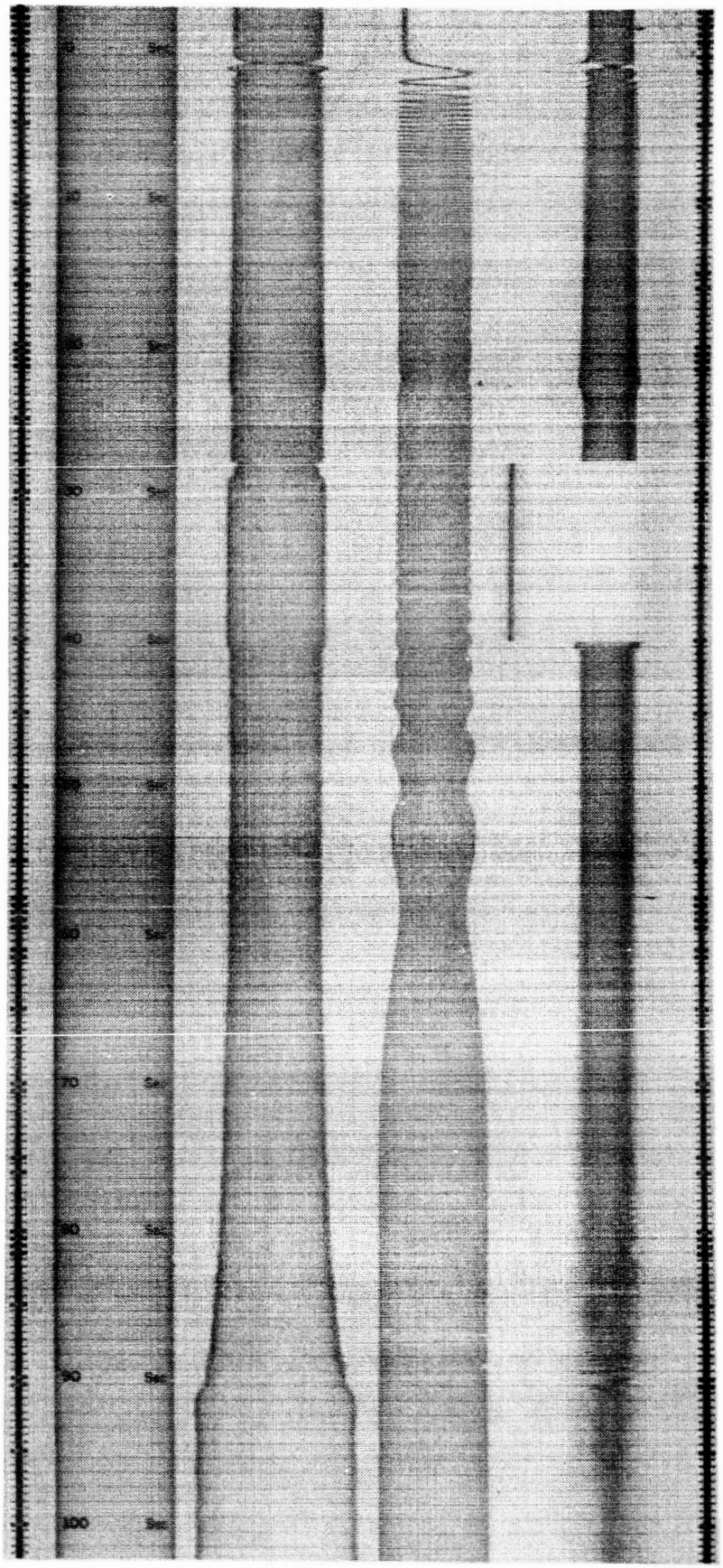

Figure 7a

Telemetry Chart Records for Experiment 14.143

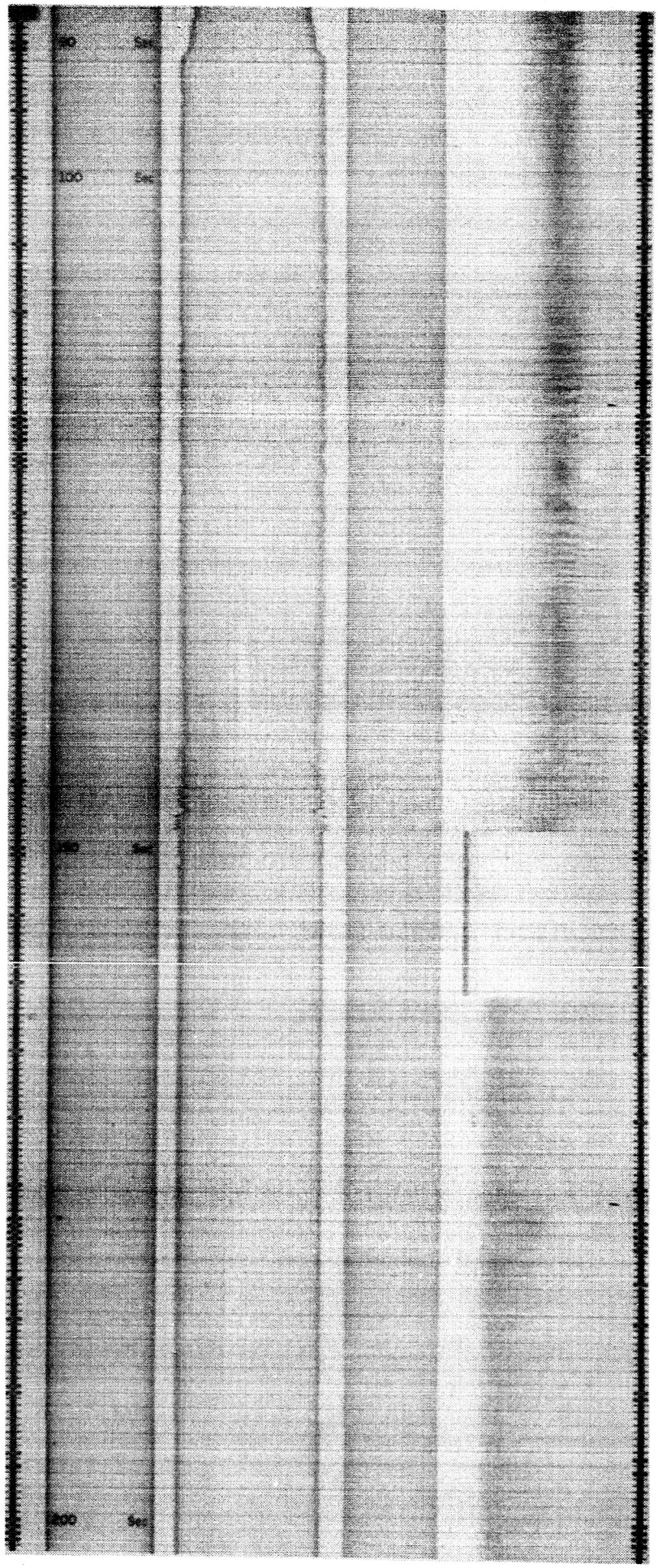

Figure 7b
Telemetry Chart Records for Experiment 14.143.

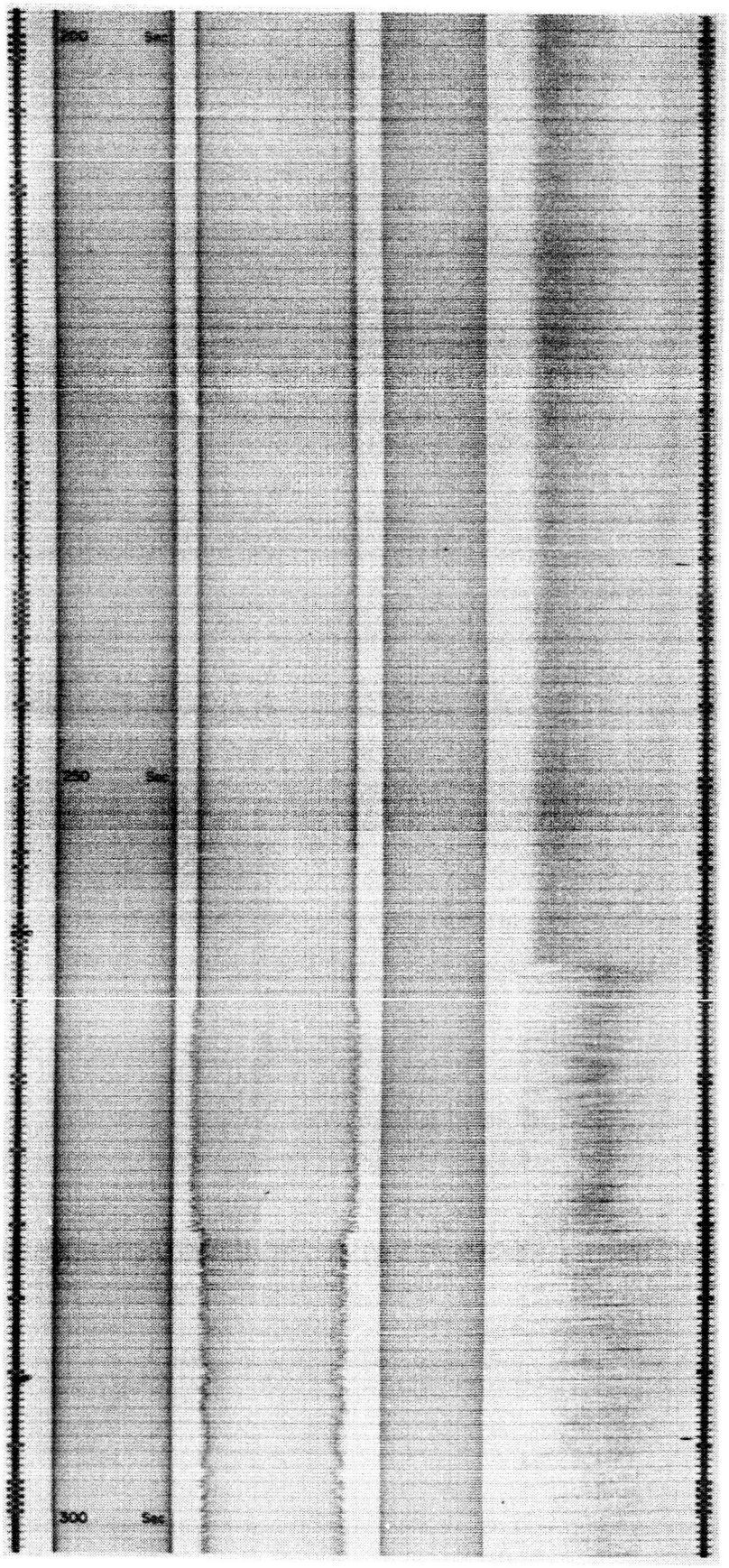

Figure 7c
Telemetry Chart Records for Experiment 14.143

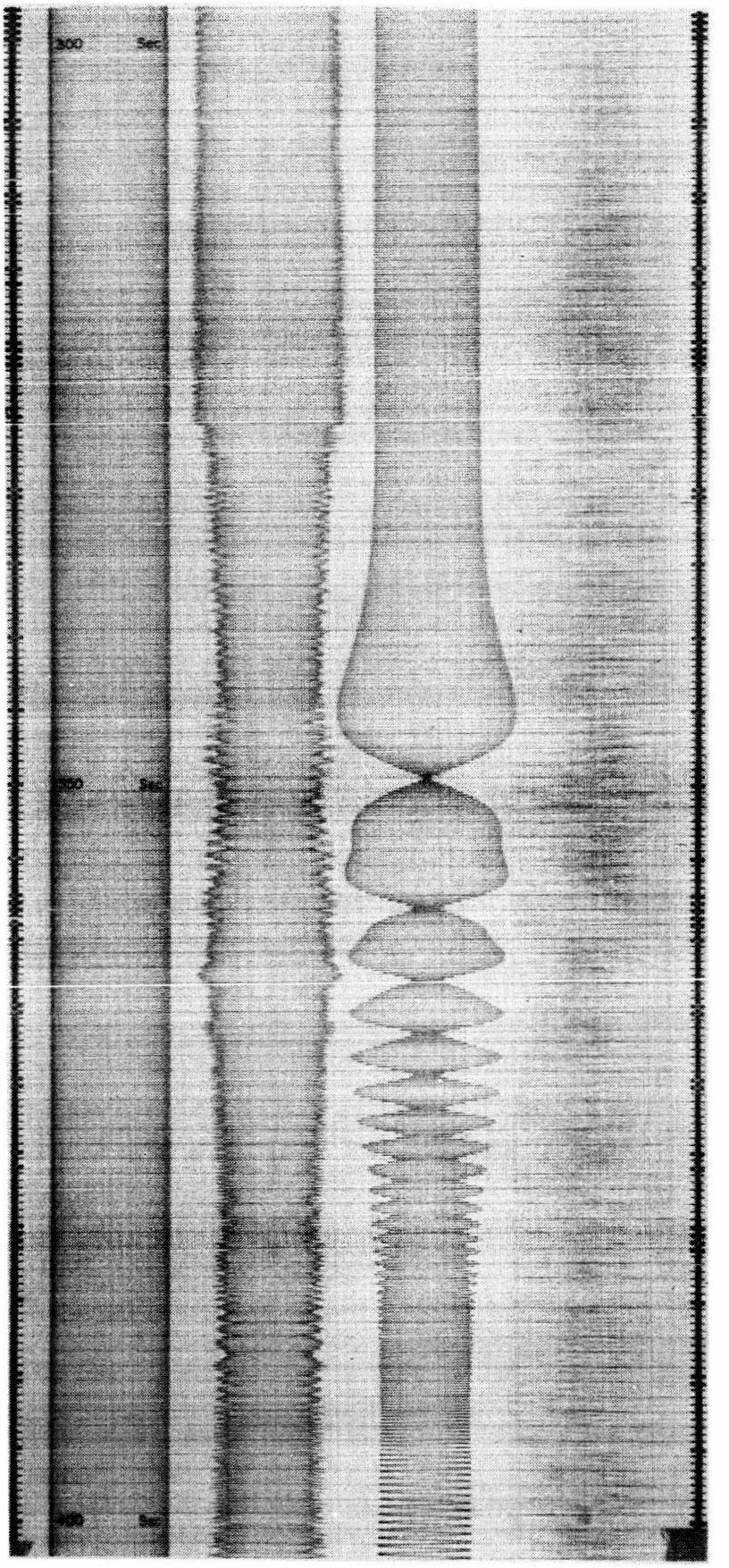

Figure 7d
Telemetry Chart Records for Experiment 14.143

consisting of a dc component and the 500 cps difference frequency, modified by the rocket spin frequency and Faraday rotation. The next lower signal is the telemetered magnetic aspect sensor which measures the transverse component of earth's magnetic field. Each period of this sinusoidal signal represents one rotation of the rocket. The next lower signal represents the magnitude of the extraordinary wave transmitted power. It consists of a 200 cps audio signal output of a linear potentiometer coupled to the servo-controlled attenuator. The second signal from the bottom represents the magnitude of the ordinary wave transmitted power as indicated by the amplitude of a 100 cps audio signal. The distance between vertical lines represents one second of time. It is seen from Fig. 7 that the ordinary wave power was kept constant (at about 10 watts) during the entire flight. The initial extraordinary wave power was about 1 watt. Time of launch (t=0 sec) can easily be discerned from the magnetic aspect sensor signal, as the rocket begins to spin at an increasing rate. No particular effect is observed at t = 3.5 sec, where the Nike first stage burned out. However, at about t = 20 sec, when the second stage (Apache) fired, a slowdown of the rocket spin occurred, a usual phenomena which cannot be explained by the Wallops Island personnel. At t = 28 sec, the Apache stage burned out and a precession of the rocket about its spin axis appears. At t = 40 sec, the ejectable doors covering apertures used in a separate radiation experiment conducted by GCA Corporation were released. The rocket precession damped out at about 70 sec, at which time the rocket spin rate stabilized at 6 rps. Apogee occurred at 205 sec and at t = 330 sec the rocket appears to have re-entered the earth's atmosphere at a point where frictional drag caused it to tip over and descend like a precessing bomb. At t = 340 sec, the

magnetic aspect sensor axis was perpendicular to the earth's magnetic field, resulting in zero signal output. At t = 406 sec the rocket descended below the horizon, resulting in loss of signal.

Returning to the other signals, at -60 sec < t < 0 sec, the servo loop was closed, with attenuator X at 32 db below one kilowatt and attenuator O at 20 db below one kilowatt. At t = 0, there was a sudden change of the rocket receiver signal, causing a servo impulse which quickly damped out, probably due to the rocket blast. Fig. 8a is a time-enlarged view of this event. In these figures, one second of time is represented by the light vertical lines (see Fig. 8b). In Fig. 8 are also shown, as the second and third records from the top, the sum of the rocket receiver signal (fourth from top) with the 500 cps reference signal and with the 500 cps reference signal phase shifted 90°. These traces together with the magnetic aspect sensor trace (fifth from top), are used to measure Faraday rotation. In Fig. 8a the rocket has not yet made one revolution. At t = 28 to 40 sec the rocket receiver was cut off in order to obtain a calibration signal. The signal in this interval represents zero dc receiver output voltage. In the interval t = 60 to 90 seconds, the output of attenuator X is increasing, showing that differential absorption is taking place. Fig. 8b is representative of the recorded signals near t = 66 sec, where the rocket is at an altitude of 77 km. The magnetic aspect sensor trace indicates that the rocket was spinning at about 6 cps. The rocket receiver difference frequency shows a modulation due to the rocket spin and standing wave caused by reflection of the extraordinary wave at a higher altitude. At t = 85 sec (100 km) Fig. 8c shows the standing wave ratio getting larger. At t = 90 sec (106 km) the differential absorption (and Faraday rotation) suddenly stop, signifying a reflection of the extraordinary wave at this point.

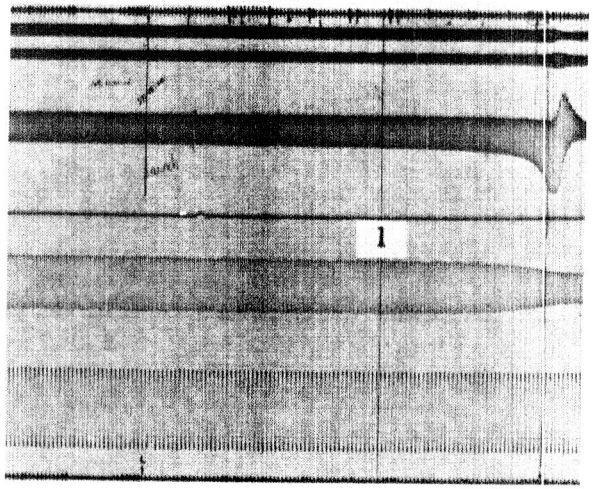

a

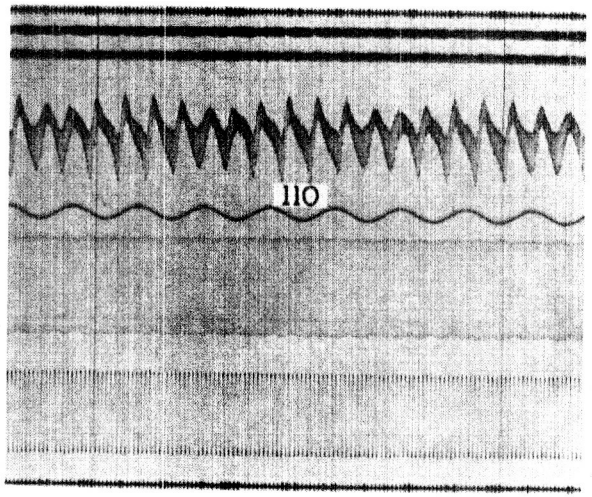

e

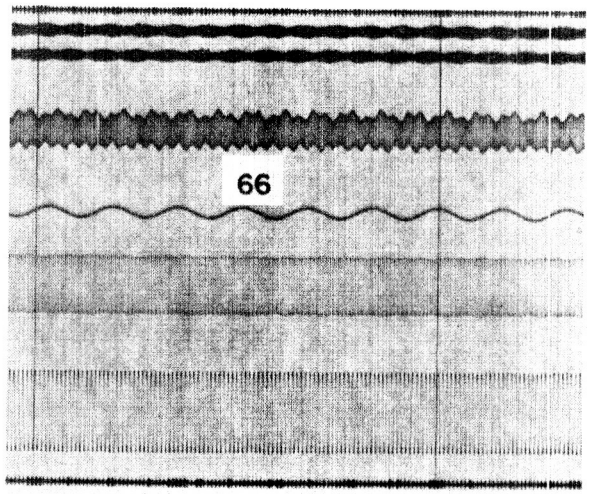

b

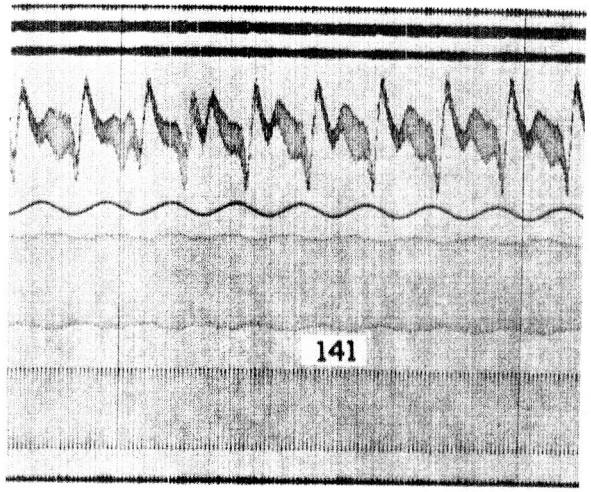

f

Figure 8
Expanded Telemetry Chart Records
at Points of Interest for Experiment 14.143

c

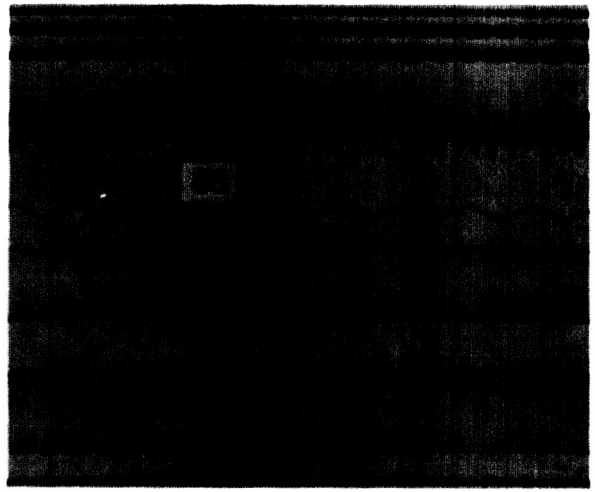

g

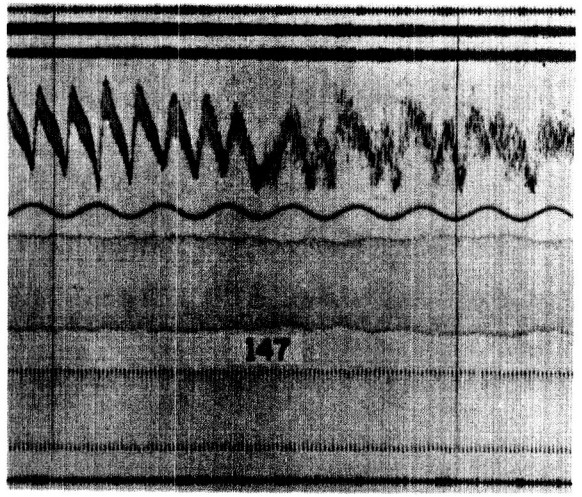

d

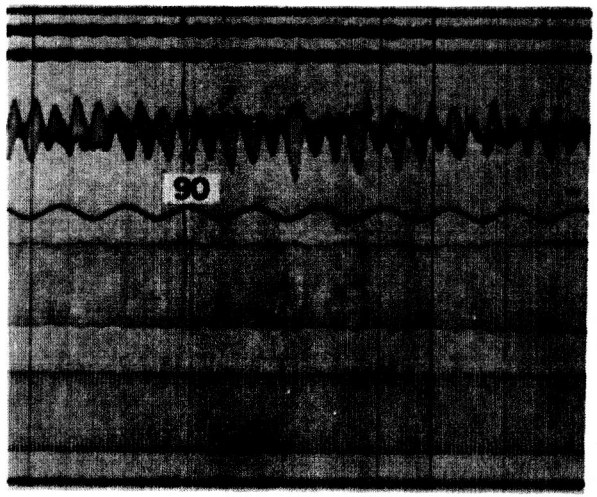

h

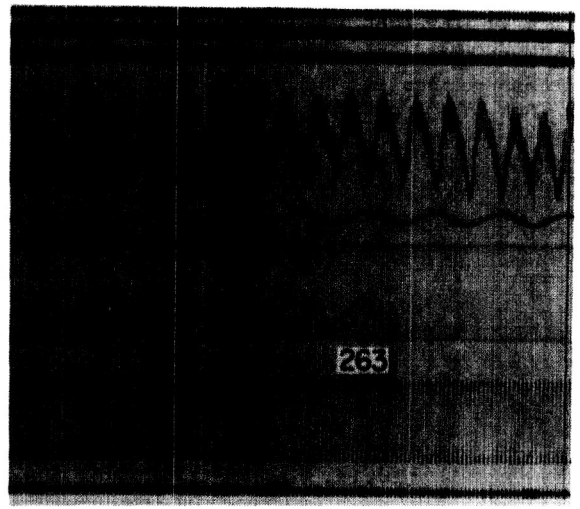

Figure 8
Expanded Telemetry Chart Records
at Points of Interest for Experiment 14.143

A further time expansion of Fig. 8d shows a sudden phase reversal of the receiver difference frequency, corroborating this reflection. At this altitude the maximum system resolution between clockwise and counterclockwise circularly polarized waves has been reached (about 26 db). Above this altitude only the standing waves are of interest. Fig. 8e shows the rocket receiver modulated by the standing wave at t = 110 sec (125 km). The receiver difference frequency in this case is due to some ordinary (clockwise) component being radiated at the extraordinary frequency due to a slightly elliptically polarized antenna system. It is interesting to note that at all altitudes higher than the extraordinary reflection level (106 km), the receiver difference frequency suddenly dropped to the value of 500 cps, the value it had before launch. This can be explained if the two circularly polarized waves are rotating in the same sense (clockwise in this case), thereby nullifying the effect of rocket spin.

A comparison of the standing wave wavelengths in Fig. 8b and 8d shows the effect of the decreasing index of refraction and consequent increasing phase velocity of propagation with increasing altitude. At t = 120 sec (134 km) a zero beat of the rocket receiver modulation envelope caused by the rocket spin and the standing wave pattern can be seen in Fig. 7. The effect of a very large standing wave ratio on the rocket receiver output is shown in Fig. 8f at t = 141 sec (149 km). Since the AGC feedback loop has an integrator at the standing wave frequency, the receiver closed loop differentiates the standing wave pattern (full wave rectified sine wave) to give the waveform shown in Fig. 8f. At t = 147 sec (152 km) a second reflection layer occurs. In Fig. 8g it is seen that the rocket receiver signal suddenly becomes noisy. One second later the second calibration signal occurred for a total of 12 sec, masking the presence of a

third reflection layer (Z-trace). This was later observed during the descent and is shown in Fig. 8h. At this point the system servo loop was opened. During the descent the combination of a large standing wave ratio and rocket precession and tilt made the data extremely noisy. However, at t = 262 sec (153 km) the rocket again broke through the third reflection level (Fig. 8h), and the system servo loop was again closed a few seconds later as seen by the jittering attenuator X record. The second reflection level with identical rocket receiver characteristics as in Fig. 8g was again passed at t = 281 sec (142 km). At this time attenuator X jumped to a new level and stayed there until the differential absorption region starting at t = 325 sec (102 km) was reached, at which point the extraordinary power started to decrease. Nine seconds later the rocket started to tumble, descending below the horizon at t = 406 sec. At this point the system servo loop was broken and the two attenuators were driven against their stops, as shown in Fig. 7d.

D. Data Analysis

The two main parameters derived from the data are differential absorption and Faraday rotation frequency or total relative phase versus time after launch or rocket height. The standing wave length at the higher altitudes can also be readily obtained versus time after launch. Other parameters that may be present are the height at which the first extraordinary reflection occurs, the height at which the ordinary reflection takes place and the height at which the second extraordinary reflection (Z-trace) occurs. At the time of this writing, manual methods of extracting the main parameters were used; however, completely automatic methods were being introduced.

The manual method of extracting the differential absorption consists of subtracting the instantaneous db readings of the rf waveguide-beyond-cutoff attenuators at given intervals of time. Immediately before each

rocket firing, as part of the count-down procedure, and again immediately after splash, a calibration is made of each rf attenuator. The calibration consists of manually stepping each attenuator by 10 db and recording the output audio voltage of the coupled linear potentiometers. As a result, a chart or scale can be made of rf attenuation in db versus audio voltage. From data such as Fig. 7a, the amplitudes of the lower two traces can be manually measured at given intervals of time and the amplitudes referred to the calibration scale to obtain db readings. The difference in the db readings is the uncorrected differential absorption. Minor corrections due to certain receiver characteristics, described in section III B can be applied, but have not yet been done so. In certain experiments, large fluctuations in differential absorption are present, as shown in Fig. 10. The reason for these fluctuations is not presently known.

The Faraday rotation can be manually extracted by one of three methods. Each method uses the fact that the rocket receiver signal contains the frequency components $(500 \pm 2f_s \pm 2f_F)$ cps where 500 cps represents the difference frequency of the O and X waves, f_s is the instantaneous rocket spin rate and f_F is the instantaneous Faraday rotation rate. Also, the magnetic aspect sensor signal contains the frequency component $\pm f_s$. In the simplest method, described in detail in section III J, the rocket receiver signal is multiplied with the 500 cps reference signal to get the difference frequency $\pm 2f_s \pm 2f_F$, where f_s is about 6 cps and f_F varies from zero to a maximum of about 5 cps. Starting from launch time, the total number of cycles of the resultant $\pm 2f_s \pm 2f_F$ signal is counted at regular intervals of time and divided by two. The total number of cycles of the magnetic aspect sensor signal $\pm f_s$ is also counted at corresponding times and subtracted from the first result to get the total Faraday rotation angle $\int f_F \, dt$ to an accuracy of about 0.1 cycle.

A second, more laborious method is to count the individual cycles of the rocket receiver signal $500 \pm 2f_s \pm 2f_F$ up to a particular time T and subtract twice the total number of cycles of the magnetic aspect sensor signal $\pm f_s$ and the total number of cycles of the 500 cps reference signal, which leaves $2\int_0^T f_F \, dt$. Of the two methods, the first is easier and somewhat more accurate.

The third method is the most laborious but gives Faraday rotation to resolutions of about one degree. It is described in detail in section III J. Briefly, the difference frequency $\pm 2f_s \pm 2f_F$ is obtained from magnetic tapes slowed down by a factor of 1/16 in real time and recorded versus time after launch by a pen recorder. On a second channel the pen recorder records the magnetic aspect sensor signal $\pm f_s$. The total number of cycles are counted for each wave as in the first method; however, the maximums of the two quasi-sinusoidal signals are used as reference points for the total number of cycles. These maximums are statistically determined to a high accuracy by averaging the center of approximately twenty pairs of points, each pair of equal amplitude, about each maximum. This method gives an uncorrect Faraday rotation of resolution high enough to be able to distinguish the effects of rocket precession, as shown in Fig. 11. In this figure, the rocket precession is indicated by the magnetic aspect sensor envelope variation. Because of the higher resolution, the data can be profitably corrected for signal propagation time lag.

The extracted differential absorption and Faraday rotation from CSL's first experiment is shown in Fig. 9. Differential absorption data for two later experiments is shown in Fig. 10. High resolution Faraday rotation data manually obtained from the first experiment is shown in Fig. 11.

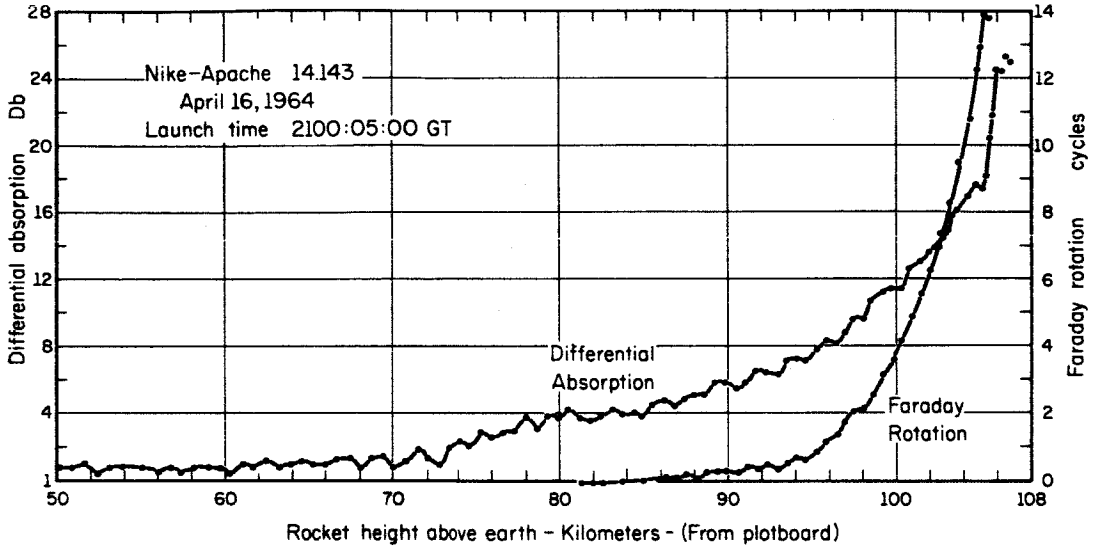

Figure 9

Differential Absorption and Faraday Rotation
vs Rocket Height for Experiment 14.143

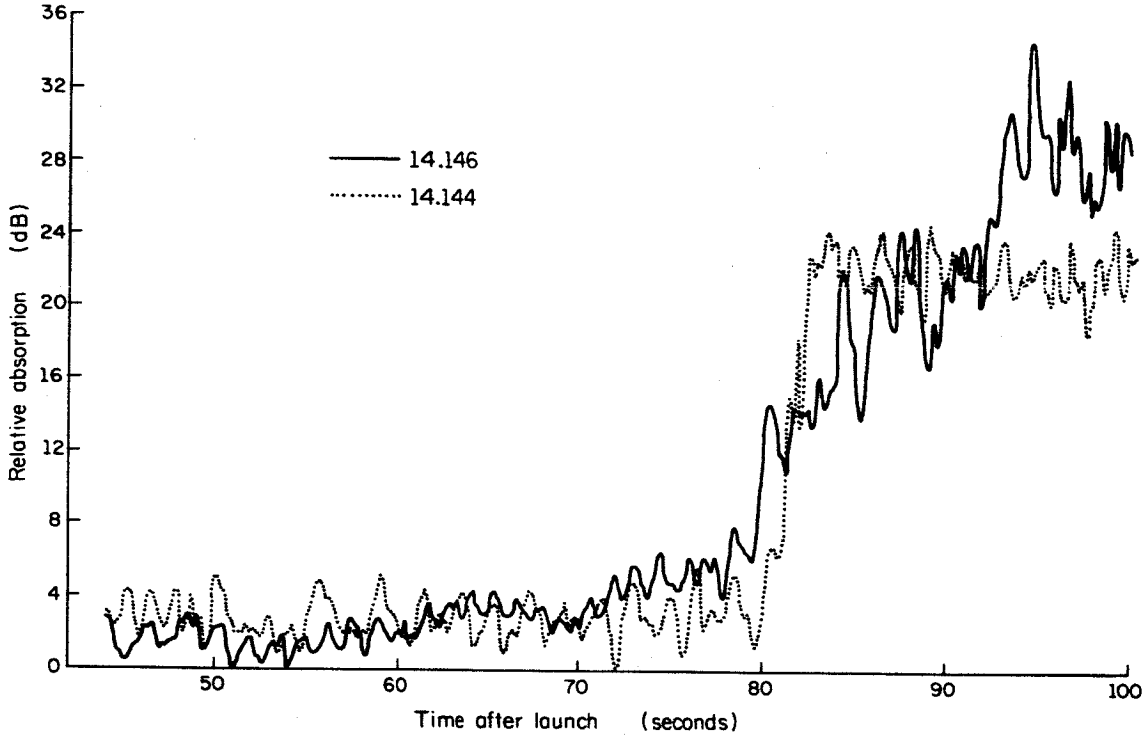

Figure 10

Differential Absorption vs Time
After Launch for Experiments 14.144 and 14.146

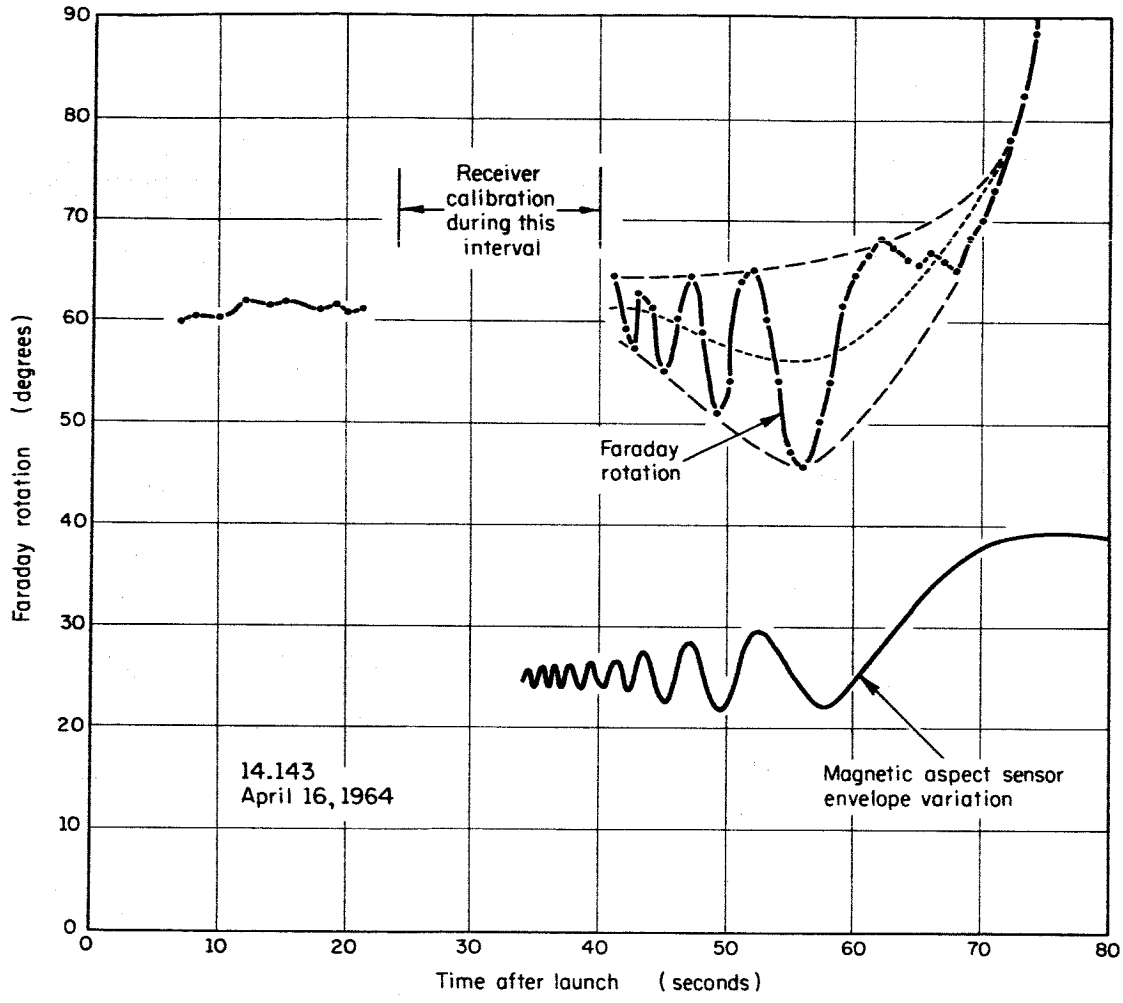

Figure 11

High Resolution Faraday Rotation vs Time After Launch for Experiment 14.143

III. Specific Description

A. Transmitters and Driver

This section describes the generation of both the ordinary and extraordinary transmitted waves by the system shown in block diagram in Fig. 12. In all 14 experiments the extraordinary wave was consistently maintained 500 cps higher than the ordinary. The exciters for both modes are electron-coupled crystal oscillators of the Pierce type in which one end of the parallel resonant crystal is grounded (see Fig. 13). A trimmer capacitor is shunted across each crystal for frequency pulling and is of small enough value to prevent cessation of oscillation at its maximum insertion. A range of 4-50μμf can pull the 2.225 mc crystal oscillator about 170 cycles. The circuit distributed capacitance and the oscillator excitation capacitors require that the crystals be cut to about 250 cps higher than the desired center frequency. For example, if an experiment is to be performed at 2,225.000 kc, then the required ordinary mode frequency is 2,224.750 kc and the required extraordinary mode frequency is 2,225.250 kc. If crystals of frequencies of 2,225.000 kc and 2,225.500 kc are used, the crystal oscillators will then be centered about the required frequencies.

The plate of the 6AU6 in Fig. 13 has a tuned circuit as a load, which feeds a 6BQ5 power amplifier. The power amplifier feeds the waveguide-beyond-cutoff attenuator, whose input consists of a 24 turn coil of 7/8" diameter, wound of # 16 wire and placed within a brass tube of 1.875" ID. This coil is resonated at the operating frequency by an appropriate variable capacitor. To keep the 6BQ5 output constant and to partially vary the output, a portion of the output is regeneratively fed back to the input via the IN611 diode and "rf output" variable potentiometer. An indication of the output power is provided by panel meters.

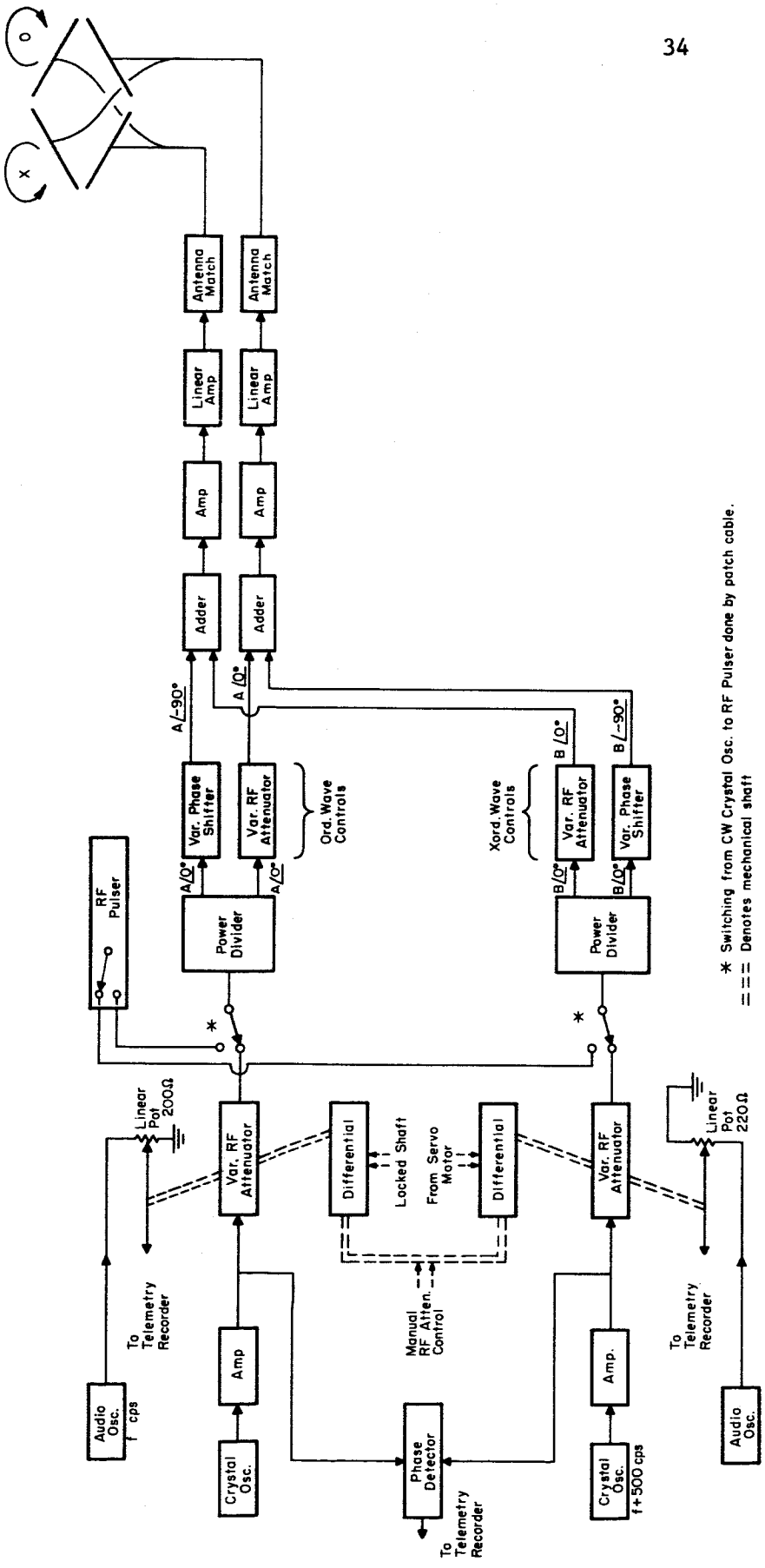

Figure 12
Block Diagram of the Rf System

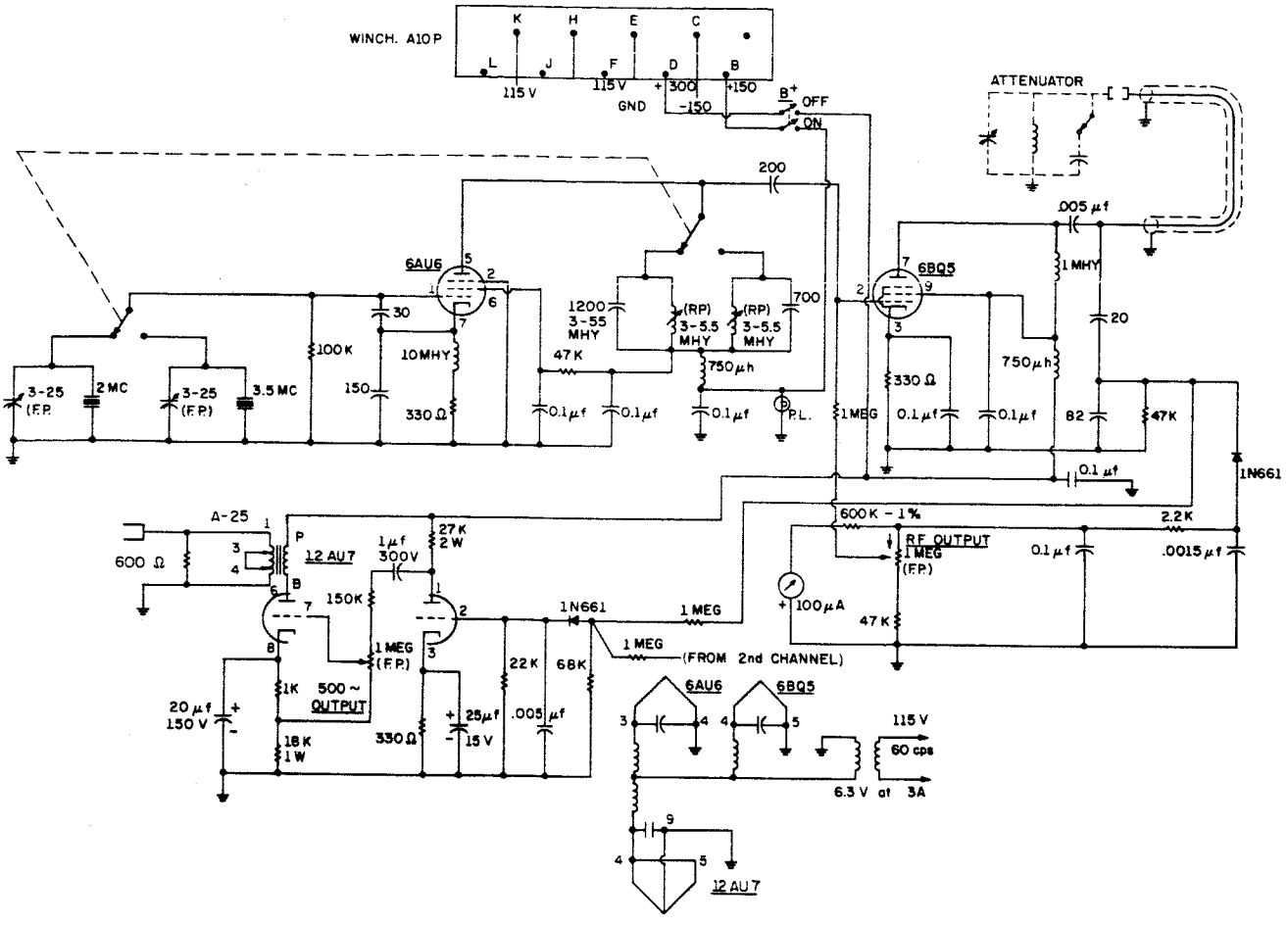

Figure 13

Transmitter Drivers Circuit Diagram

A portion of the outputs of the O and X oscillators is mixed and amplified by the 12AU7 to obtain the 500 cps reference signal. This is tranformer-coupled to the 600 ohm telemetry line for permanent recording.

The waveguide-beyond-cutoff rf attenuator consists of a fixed input coil described above and a movable output coil, both located with their axes parallel within a brass tube of 1.875" ID. The output coil is 1-5/16 in diameter and consists of four windings of # 16 wire. Construction details of the coils and tube are shown in Fig. 14.

Variable attenuation is obtained by using the $TE_{1,1}$ cutoff mode and moving the output coil with respect to the input. The attenuation in db is linearly related to the distance between coils for separations greater than the tube diameter according to the relation

$$\text{db per unit length} = \frac{54.58}{\lambda c} \sqrt{1 - \left(\frac{\lambda c}{\lambda}\right)^2}$$

where

$\lambda c = 3.41\ a$ for the $TE_{1,1}$ mode

λ = free space wavelength
a = radius of circular waveguide

For our attenuator dimensions and operating frequencies, $\left(\frac{\lambda c}{\lambda}\right)^2$ is negligibly small so that the attenuation per unit length is independent of frequency and is a function of the waveguide radius only. A simple calculation for a tube of 1.875" diameter gives one db per 0.585 inches for the attenuation per unit length, which accurately checks with the measured value. The attenuator has an insertion loss of about 25 db because of the minimum spacing requirement and has a constant phase shift for any attenuation.

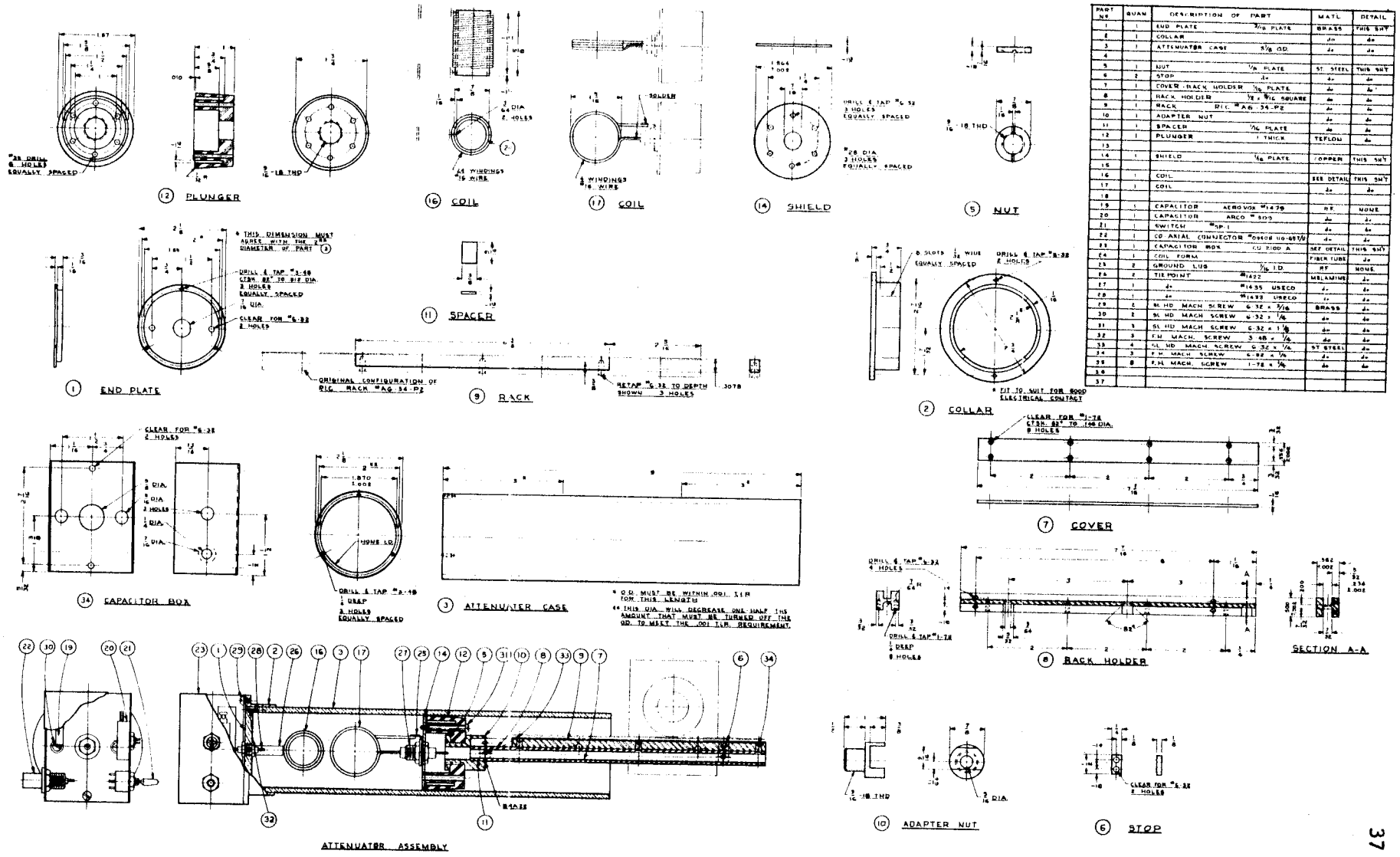

PART NO	QUAN	DESCRIPTION OF PART	MATL	DETAIL
1	1	END PLATE 3/16 PLATE	BRASS	THIS SHT
2	1	COLLAR	do	do
3	1	ATTENUATOR CASE 1 1/8 OD	do	do
4				
5	1	NUT 1/4 PLATE	ST. STEEL	THIS SHT
6	2	STOP	do	do
7	1	COVER - RACK HOLDER 1/16 PLATE	do	do
8	1	RACK HOLDER 1 3/8 x 3 1/16 SQUARE	do	do
9	1	RACK PIC "AG 34-P2	do	do
10	1	ADAPTER NUT	do	do
11	1	SPACER 1/16 PLATE	do	do
12	1	PLUNGER 1 THICK	TEFLON	do
13				
14	1	SHIELD 1/16 PLATE	COPPER	THIS SHT
15				
16	1	COIL	SEE DETAIL	THIS SHT
17	1	COIL	do	do
18				
19	1	CAPACITOR AEROVOX "1479	RF	NONE
20	1	CAPACITOR ARCO "509	do	do
21	1	SWITCH "SP-1	do	do
22	1	CO AXIAL CONJUCTOR "09608 110-6876	do	do
23	1	CAPACITOR BOX CU PLATE A	SEE DETAIL	THIS SHT
24	1	COIL FORM	FIBER TUBE	do
25	2	GROUND LUG 7/16 I.D.	RF	NONE
26	2	TIE POINT "1422	MELAMINE	do
27	1	do "1435 USECO	do	do
28	1	do "1433 USECO	do	do
29	2	84 HD MACH SCREW 6-32 x 5/16	BRASS	do
30	2	84 HD MACH SCREW 6-32 x 1/4	do	do
31	1	82 HD MACH SCREW 6-32 x 1 1/8	do	do
32	3	FH MACH SCREW 3-48 x 1/4	do	do
33	4	84 HD MACH SCREW 6-32 x 1/4	ST STEEL	do
34	3	F H MACH SCREW 6-32 x 1/4	do	do
35	8	F.H. MACH SCREW 1-72 x 1/4	do	do
36				
37				

Figure 14
Rf Attenuator Assembly

As shown in Figs. 1 and 12, one rf attenuator controls the ordinary wave transmitted power and the other the extraordinary wave transmitted power. In normal operation the ordinary attenuator is left in the 20 db position, (corresponding to 10 watts transmitted power) while the extraordinary wave is servo controlled. However, both attenuator settings can be manually changed while the servo maintains the same relative db difference. The method for doing this is described in section II B in connection with Fig. 2. In this figure the output shafts of the gear differentials control the positions of the rf attenuator output coils and thereby the degree of coupling. To each output shaft is connected a linear audio potentiometer for the purpose of monitoring the rf attenuation. Constructional details of the rf attenuators is shown in Figs. 14-17. The initial spacing between the attenuator coils, corresponding to zero db dial marking, can be adjusted by moving the circular waveguides with respect to their saddles. The input coil is wound and epoxied on a form and the secondary coil is potted in epoxy to eliminate effects of coil vibration.

The attenuator outputs are fed to a circuit which provides the proper polarizations for the ordinary and extraordinary waves. This circuit must compensate for the fact that in general the transmitting dipole antennas are not of the same impedance nor in perfect space quadrature. The requirements for circular polarization are that the two components which synthesize a circularly polarized transmitted wave be in time and space quadrature. For the early firings at Wallops Island special efforts were made to set the two dipole arrays symmetrical and at right angles to each other. The time quadrature was obtained by slightly detuning the transmitter's first amplifier tuning circuit. With the hybrid arrangement

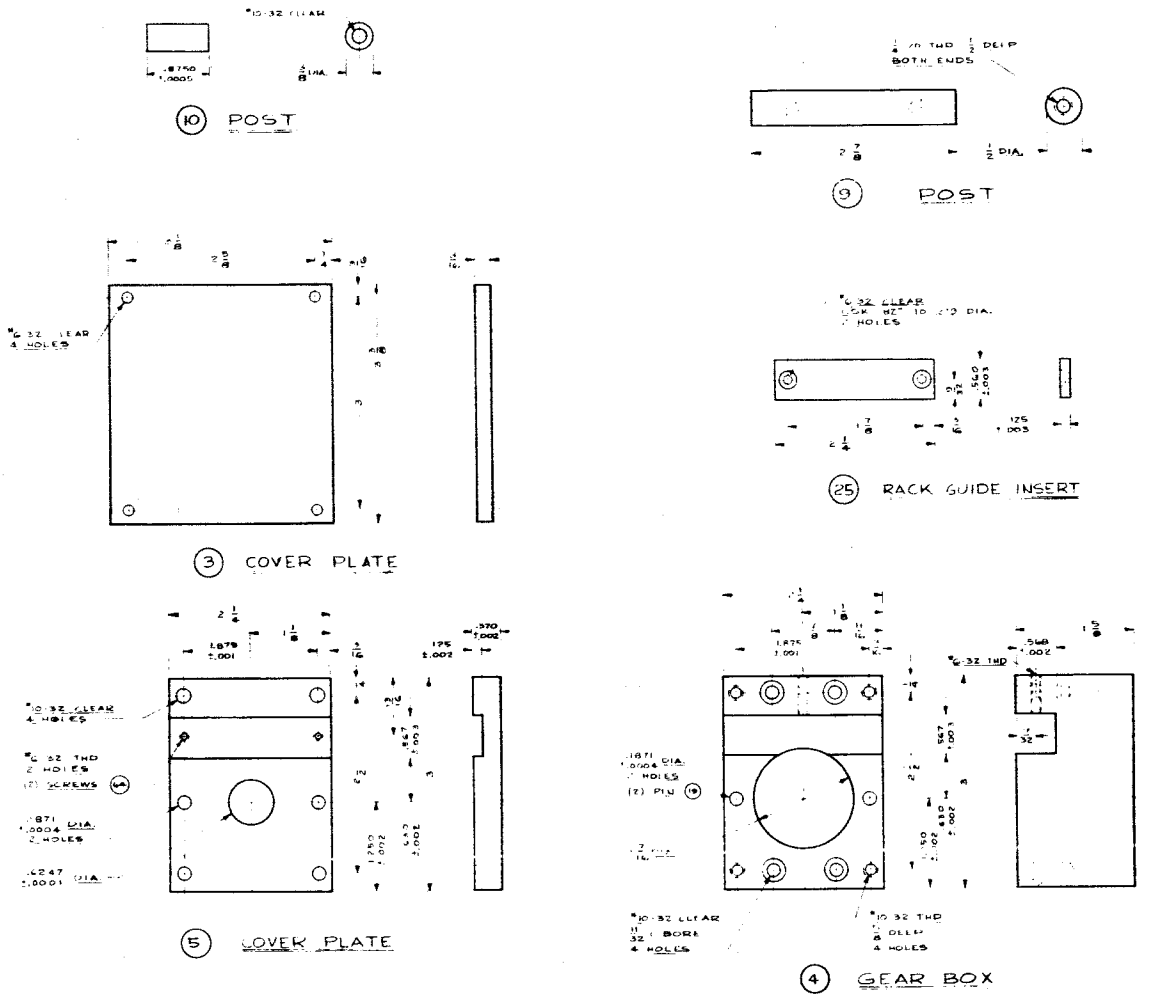

Figure 15

Rf Attenuator Driver Details

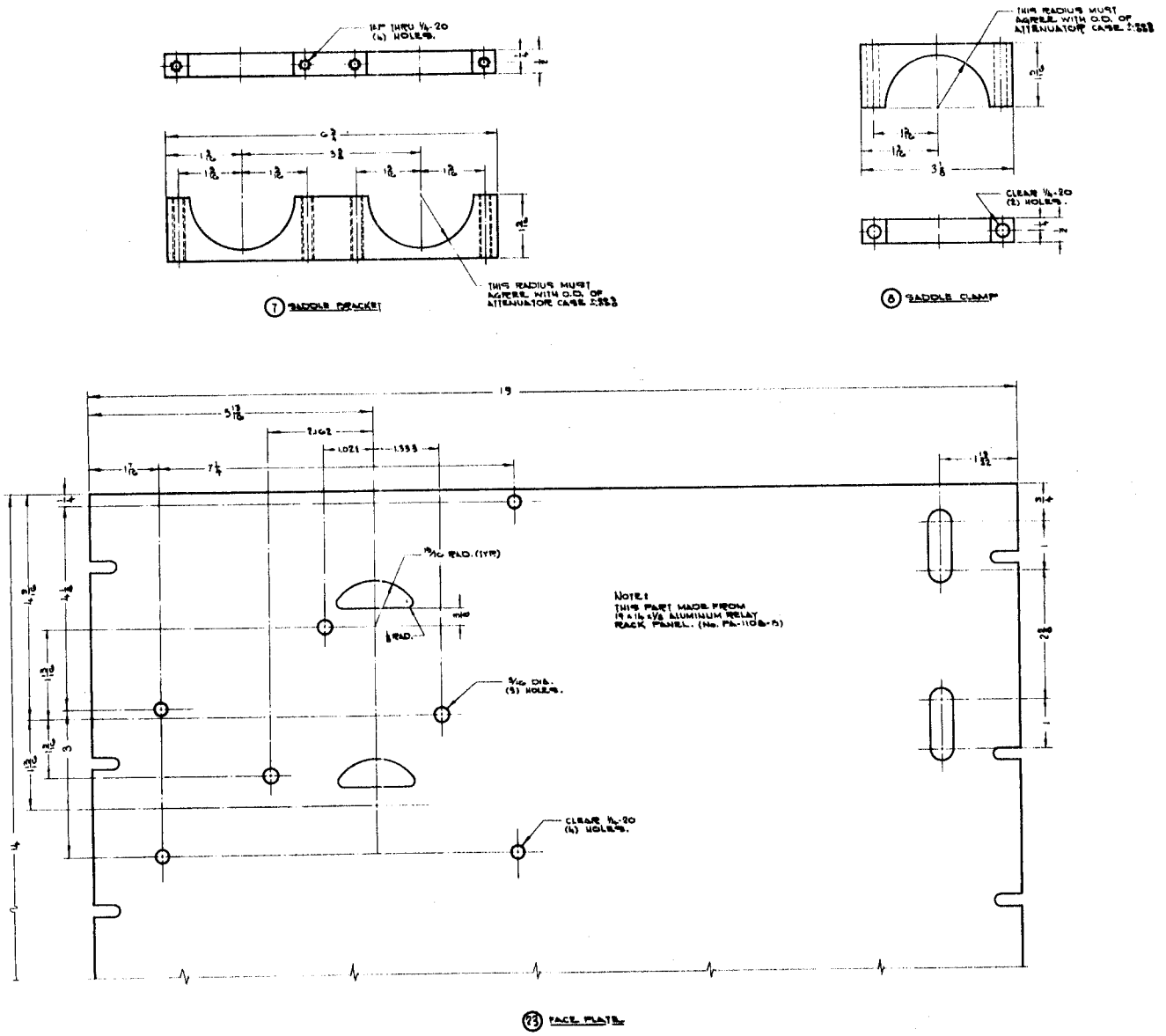

Figure 16
Rf Attenuator Face Plate and Saddle Details

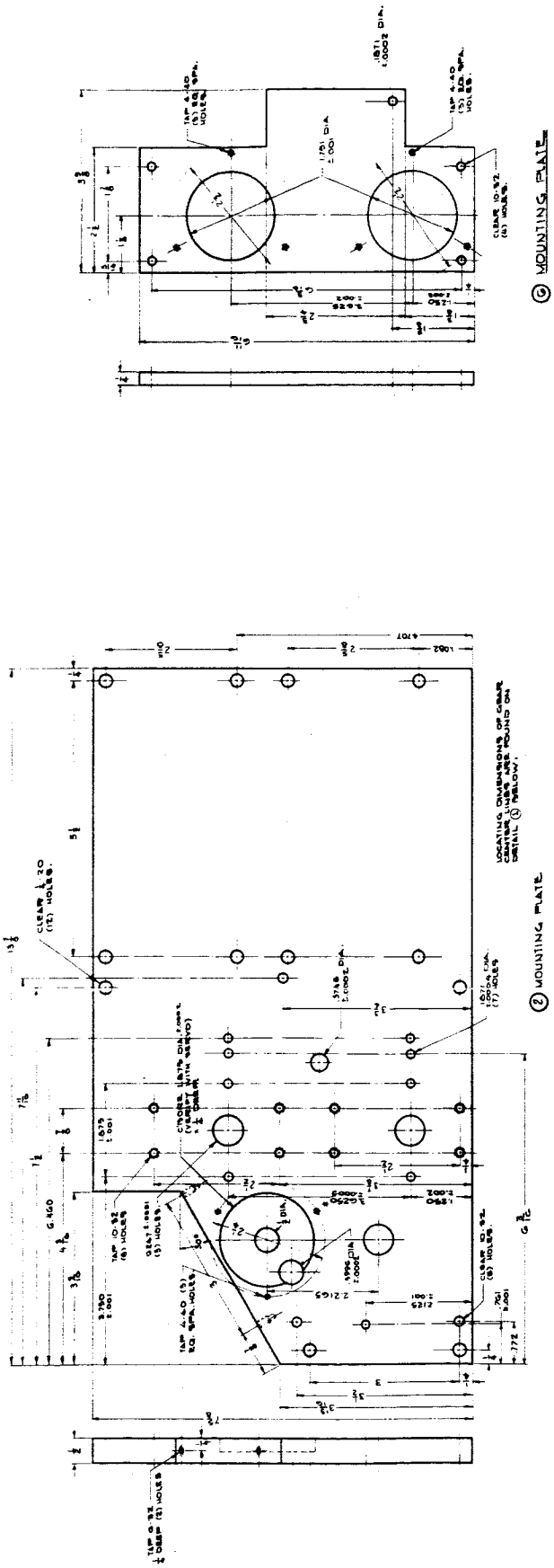

Figure 17
Rf Attenuator Driver Details.

shown in Fig. 1, if the extraordinary wave was adjusted for optimum circular polarization it was found that the ordinary wave was usually close to being optimally circularly polarized with opposite sense. However, only one wave could be adjusted with this scheme, relying on near perfect antenna array symmetry for the polarization of the other wave.

A much more satisfactory method for obtaining any polarization for any condition of the antennas was used in later firings and is shown in block diagram in Fig. 12 and in more detail in Fig. 18. If the antennas were perfect and at space quadrature, then, with the phase shifters set to -90° and the attenuators set to zero, two oppositely circularly polarized waves would be transmitted. With the phase shifters set to zero or multiples of half wavelength, two linearly polarized waves would be transmitted, the angle between the two planes of polarization being a function of the attenuator settings. Any imperfections in the antenna space quadrature or array symmetry can be compensated by suitable adjustments of the polarization circuit as described in section IV E.

The polarization circuit consists of two isolated channels, one which forms the extraordinary wave and the other the ordinary wave. Referring to Fig. 18, the input voltage to each channel is divided into two equal parts by PIC C-86 pulse transformers. One part goes to an adjustable phase shifter which is manufactured by General Radio and denoted as Variable Delay 314S86. This phase shifter has a maximum time delay of 0.5 microseconds; hence, the phase shift is 360° or greater for frequencies in the 2 mc and higher range. The characteristic impedance of the phase shifter is 200 ohms at frequencies up to 4.5 mc. The phase shifter output is fed to a linear amplifier through an adder fabricated by Adams-Russell and designated as ISO-T, TH75. The proper operation of this unit requires an output impedance of 75 ohms, in which case its input impedance is also

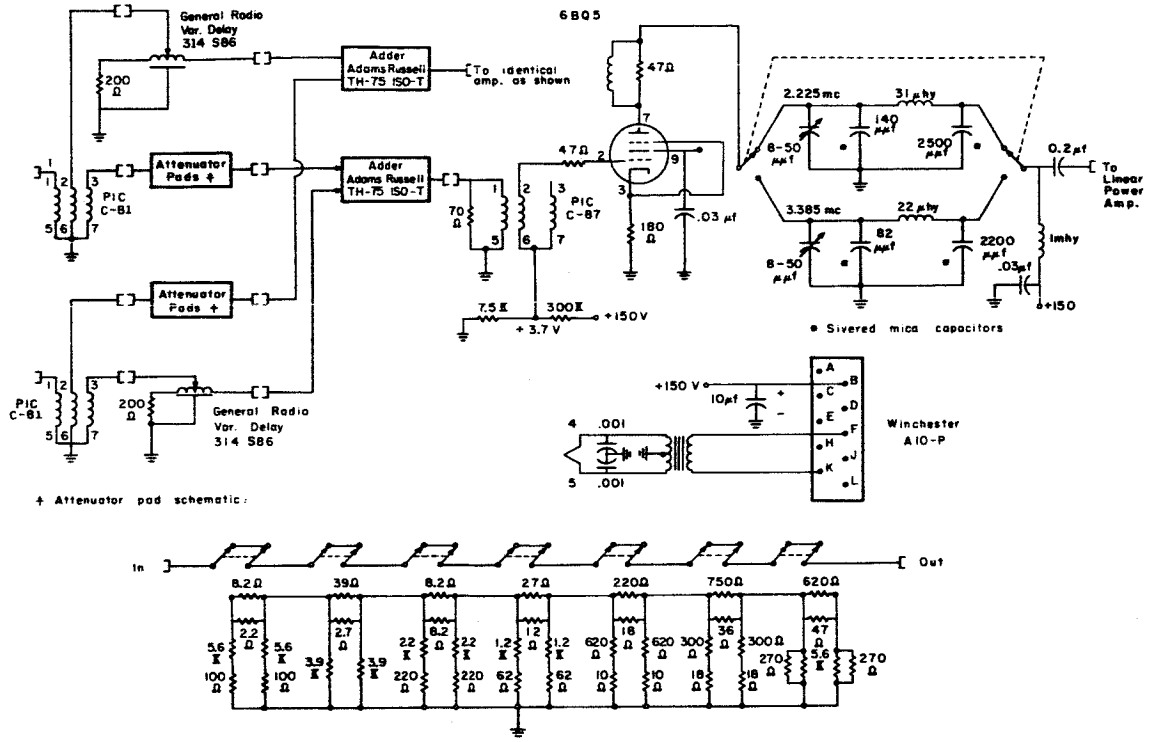

Figure 18.

Polarization Circuit Diagram.

75 ohms. Hence, there is a mismatch between the phase shifter and adder which causes an output amplitude variation with phase shift. This mismatch should be corrected in future refinements of the system. The other output of the pulse transformer is fed to an attenuator which is variable in steps as low as 0.2 db and which is used to compensate for any insertion loss through the phase shifter or to vary linearly polarized waves in azimuth. The attenuator output is also fed to a linear amplifier through an ISO-T adder.

Since the inputs to each adder are isolated by about 30 db, each channel, consisting of a variable phase shifter and attenuator, can be adjusted for a desired polarization without affecting the other. Also, since the amplifiers, baluns and antennas are linear, the X and O waves can be independently generated in this common system.

The two outputs of the polarization circuit are each amplified by a one stage 6BQ5 amplifier and fed to the two transmitters, which are 1 kw linear amplifiers built by the Technical Materiel Corporation. They were selected because of their ruggedness and use by the armed services, and are designated as Linear Power Amplifier PAL-1k(A) or AN/URA-36A. Each unit provides 1000 watts peak envelope power with a 100 mw input over the frequency range of 2 to 32 mc. Its input impedance is 72 ohms and it can be matched to any unbalanced load from 50 to 600 ohms at $\pm$ /45° by means of a panel controlled pi network. Each transmitter is divided into three sections: an rf section, a low voltage supply section, and a high voltage power supply section. The circuit diagrams are shown in Figs. 19, 20, and 21, respectively. A complete description of the PAL-1k(A) is given in the "Technical Manual for Linear Power Amplifier Model PAL-1k(A), (Amplifier Power Supply Group, AN/URA-36A)," which can be obtained from the Technical

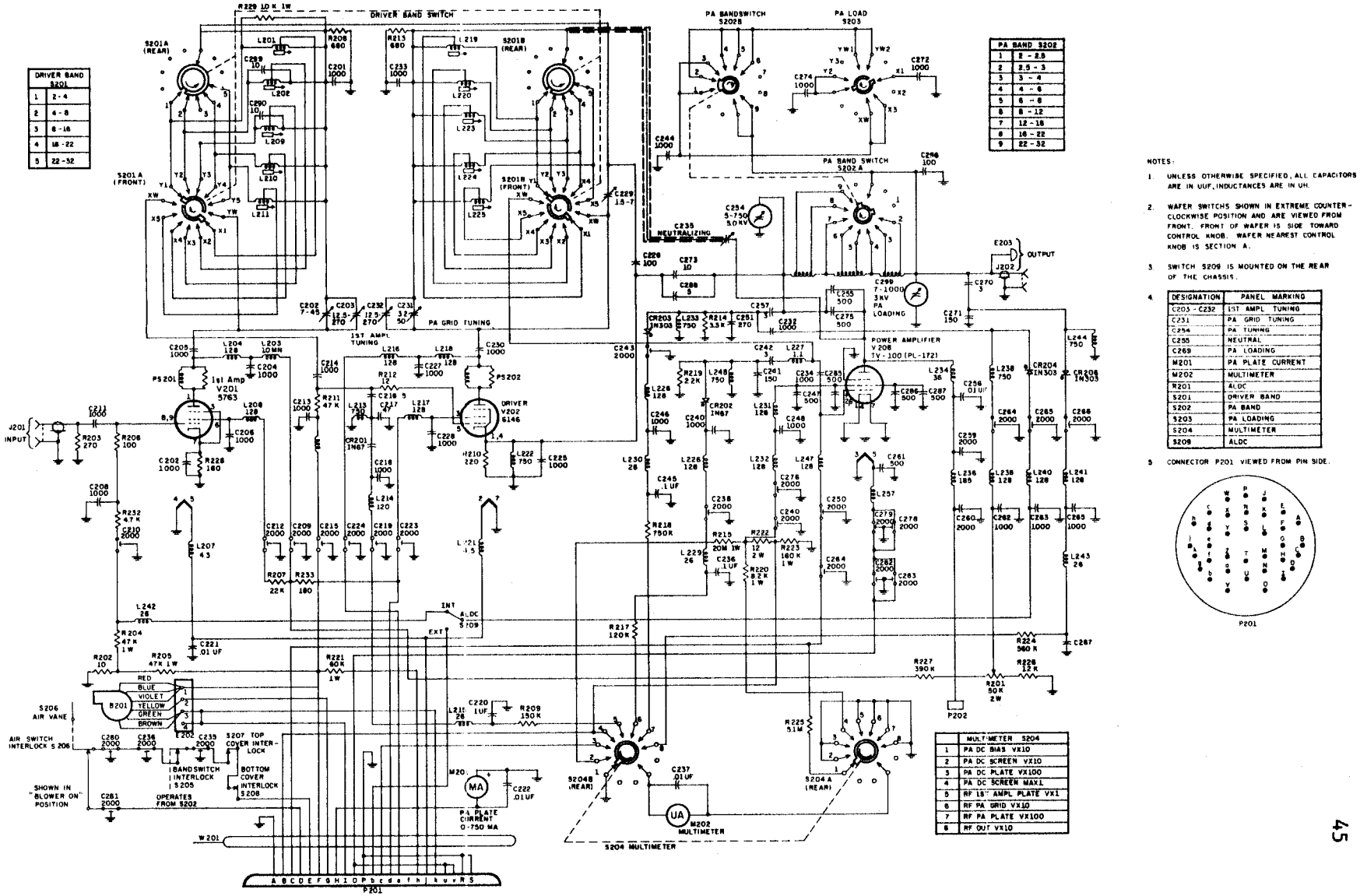

DRIVER BAND S201	
1	2 - 4
2	4 - 8
3	8 - 16
4	16 - 22
5	22 - 32

PA BAND S202	
1	2 - 2.5
2	2.5 - 3
3	3 - 4
4	4 - 6
5	6 - 8
6	8 - 12
7	12 - 18
8	18 - 22
9	22 - 32

MULTIMETER S204	
1	PA DC BIAS VX10
2	PA DC SCREEN VX10
3	PA DC PLATE VX100
4	PA DC SCREEN MAX1
5	RF 1ST AMPL PLATE VX1
6	RF PA GRID VX10
7	RF PA PLATE VX100
8	RF OUT VX10

NOTES:

1. UNLESS OTHERWISE SPECIFIED, ALL CAPACITORS ARE IN UUF, INDUCTANCES ARE IN UH.
2. WAFER SWITCHS SHOWN IN EXTREME COUNTER-CLOCKWISE POSITION AND ARE VIEWED FROM FRONT. FRONT OF WAFER IS SIDE TOWARD CONTROL KNOB. WAFER NEAREST CONTROL KNOB IS SECTION A.
3. SWITCH S209 IS MOUNTED ON THE REAR OF THE CHASSIS.
4.

DESIGNATION	PANEL MARKING
C203 - C232	1ST AMPL TUNING
C231	PA GRID TUNING
C254	PA TUNING
C255	NEUTRAL
C269	PA LOADING
M201	PA PLATE CURRENT
M202	MULTIMETER
R201	ALDC
S201	DRIVER BAND
S202	PA BAND
S203	PA LOADING
S204	MULTIMETER
S209	ALDC

5. CONNECTOR P201 VIEWED FROM PIN SIDE.

Figure 19
TMC Linear Amplifier PAL-1K(A) Rf Circuit Diagram

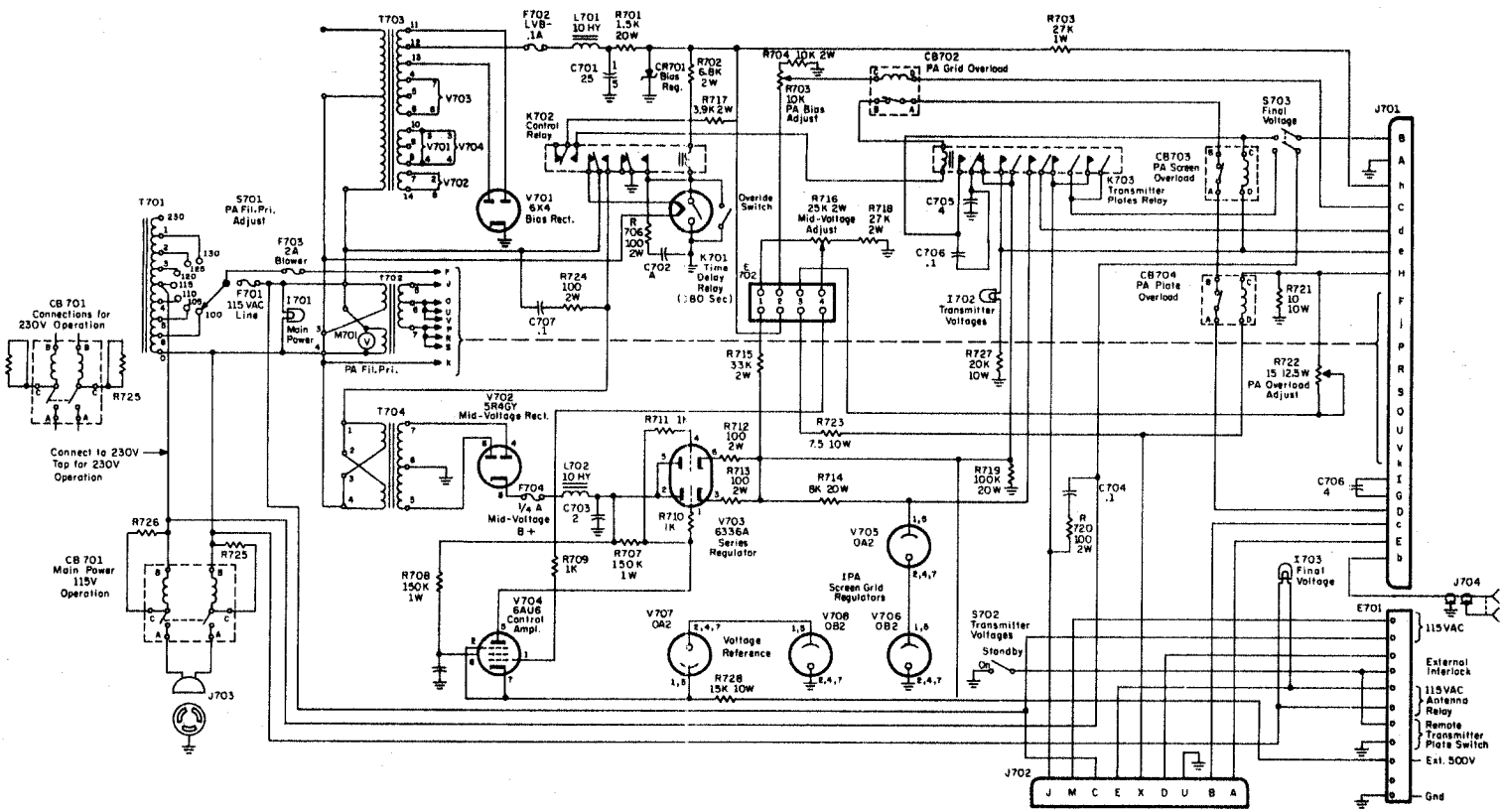

Notes:

1. Unless otherwise specified, all resistances are in ohms. All capacitors are in UF.
2.

Designation	Panel Marking
CB701	Main Power
CB702	PA Overload Cont Grid
CB703	PA Overload Scrn Grid
CB704	PA Overload Plate
F701	Line 5A
F702	L.V.B. - 1/10 A
F703	Blower 2A
F704	M.V.B. + 1/4 A
I701	Main Power
I702	Transmitter Voltages
I703	Final Voltages
M701	PA Fil Pri
S701	PA Fil Pri Adjust
S702	Transmitter Voltages
S703	Final Voltages

3. Switch S701 shown in extreme counterclockwise position as viewed from the front. Front of S701 is side towards control knob.
4. Receptacles viewed from mating side.

Figure 20
TMC Linear Amplifier PAL-1K(A) Low Voltage
Power Supply Circuit Diagram

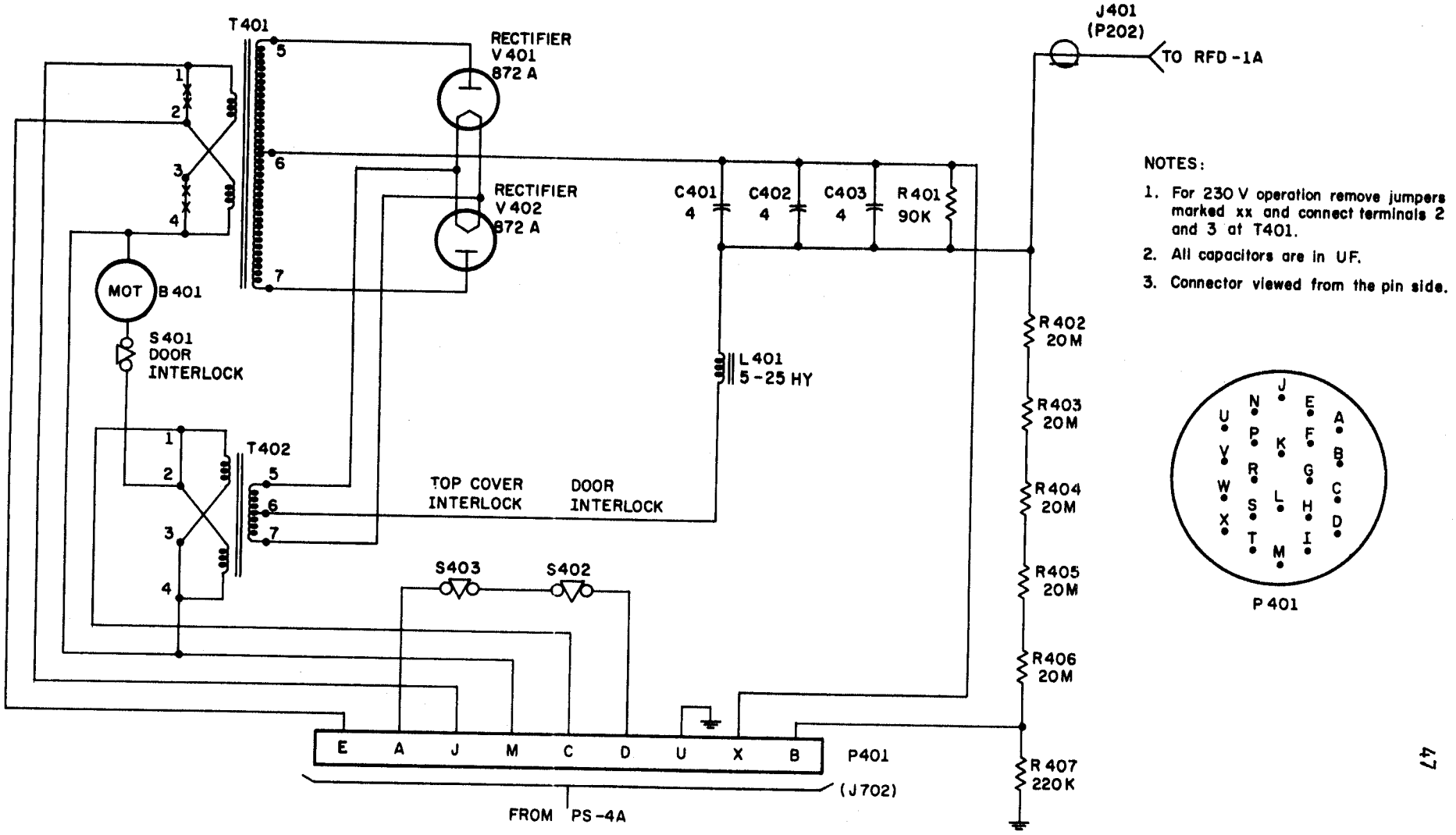

Figure 21
TMC Linear Amplifier PAL-1K(A) High Voltage
Power Supply Circuit Diagram

Materiel Corporation, Mamaroneck, New York. The outputs of the linear power amplifiers are fed to the antenna baluns and matching sections, described in section III B.

The transmitter exciters were designed with sufficient output to drive the transmitters at the kilowatt level. This required sufficient drive to overcome the large insertion losses of the piston attenuators and antenna polarization network. For the mobile launch firings, large values of attenuation were required, resulting in a need for more amplification in the system. For this reason, a one stage rf amplifier was designed and inserted in the system ahead of the linear power amplifier.

The amplifier is a single stage 6BQ5 with two switchable pi-section networks in the output. The pi-section networks provide impedance matching between the 6BQ5 and the 70 ohm input of the T.M.C. linear amplifiers at 2.225 mc or 3.385 mc selectable by switch. The input transformer has a dual winding secondary with turns ratios such that the overall gain is either two or four, approximately, depending upon the winding connected. A gain of two is sufficient for the present system. A schematic diagram of the amplifier is shown in Fig. 18.

B. Antennas

Both the circularly and linearly polarized O and X waves are radiated from an antenna array which is described in this section. A simple array providing this consists of two horizontal crossed dipoles in a turnstile type antenna. This array was used on a mobile rocket launching expedition aboard the escort aircraft carrier USNS Croatan, where almost unlimited impact areas allowed launchings in near vertical trajectories. Also, a center supported, center loaded turnstile of two 0.24 wavelength

elements was erected atop the CSL building at Urbana, and used to test a phase and amplitude adjusting system by pulsed sounding.

The ground antenna used for a majority of shots was erected on the south end of NASA Wallops launch range. A typical trajectory of these launches placed the rocket apogee about 27° off the vertical axis of the antenna array. A more ideal circularly polarized wave is provided at the rocket in these launches by using a square array of 4 dipoles, where each arm is replaced by two parallel, half-wave spaced, dipoles. The arrays used are shown in Figs. 22 and 23. A pattern null exists at the horizon off the ends of a dipole, and by feeding the parallel dipoles in phase, a matching null is produced broad-side to the dipoles. Equal contribution from each pair of parallel dipoles is required to produce a circularly polarized wave. Thus by making the spacial pattern of each pair of parallel dipoles symmetrical about the vertical axis of the array, circular polarization is maintained over a large region about the vertical axis.

Feed System

Each dipole driving point impedance can be calculated using the 73 ohm free space resistance modified by a mutual impedance of $-33\underline{/70°}$ due to the parallel dipole,[1] and by the mutual impedances due to asymmetry of the square[2] and to the ground image. However, these mutuals have a weak effect on the dipole impedances. The most suitable balanced line available appeared to be Amphenol 214-023, which is a heavy-duty twin line with two # 12 conductors in brown polyethelene. It is rated at 1 kw for use below

---

[1] Terman "Radio Engr. Handbook" 1st Ed., p. 777

[2] D. R. Capps and D. L. Waidelich "The Mutual Impedance of Perpendicular Half-Wave Antennas" Proc. N.E.C. 15 (1959) P. 986.

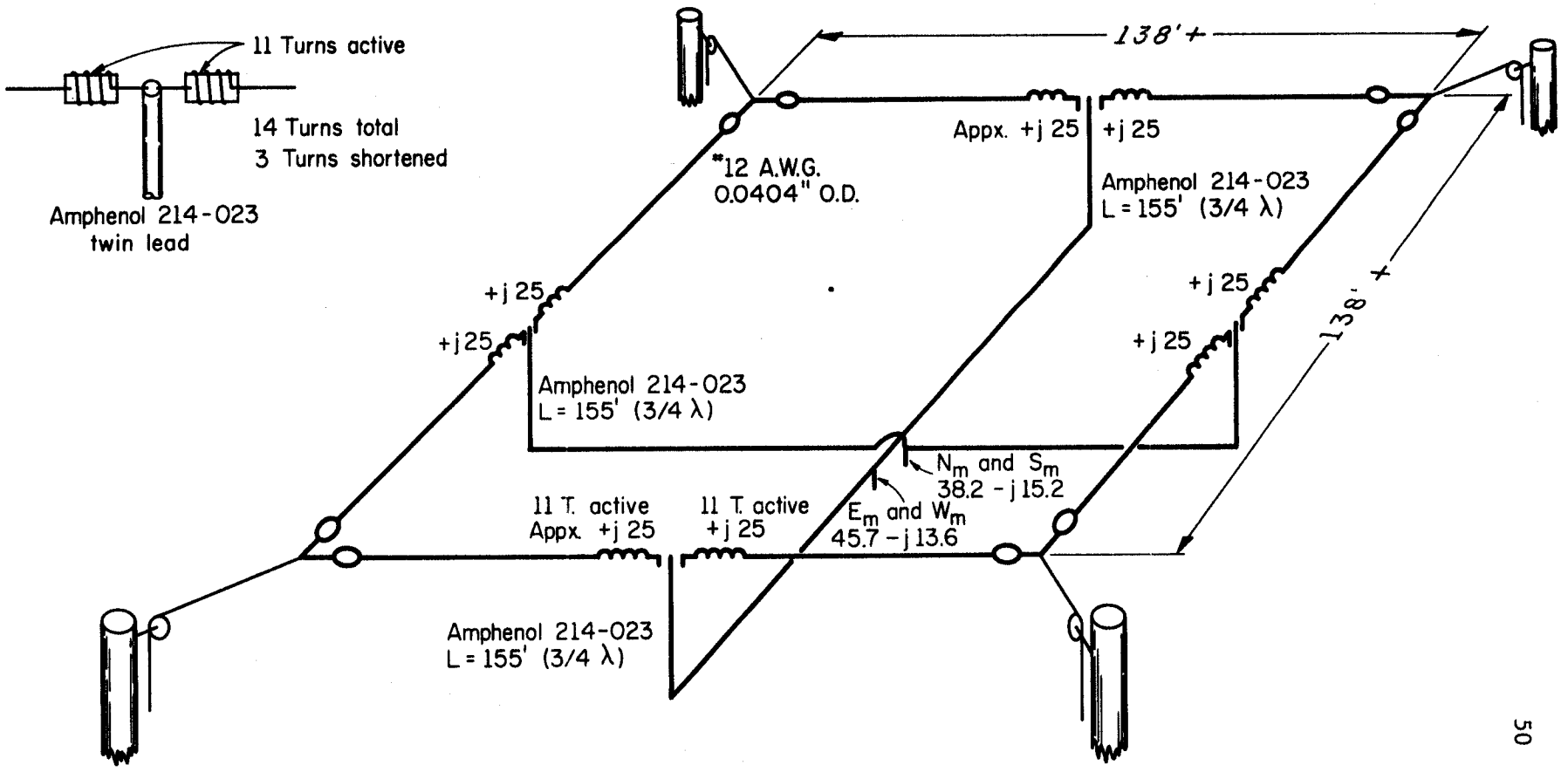

Note: cut antennas 138 ft. long.

Figure 22
Schematic of 3.385 mc Transmitting Antenna Array

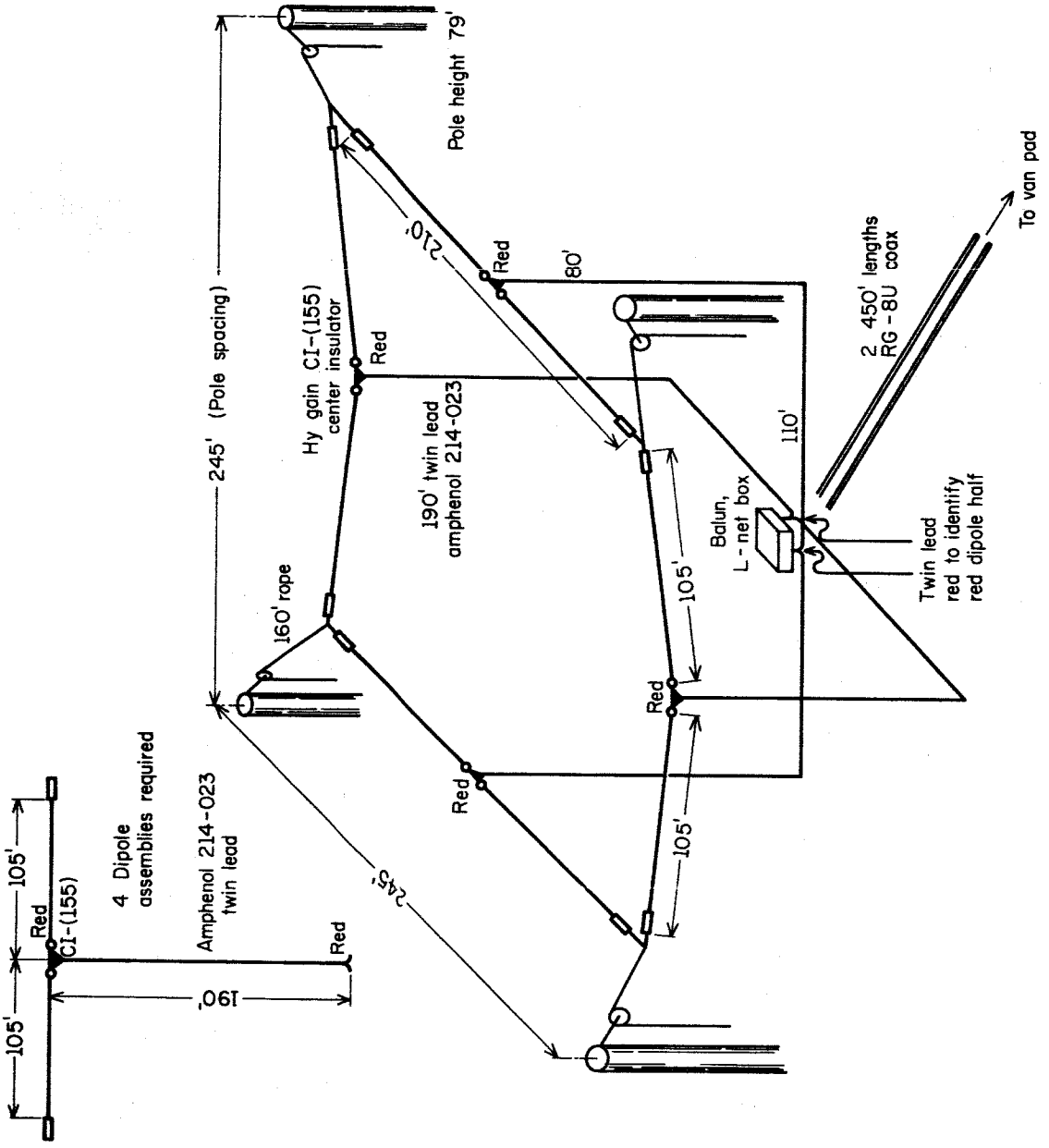

Figure 23
Schematic of 2.285 mc Transmitting Antenna Array

30 mc, has a velocity factor of 0.71, and at 3 mc has a flat line loss of about 0.3 db per 100 ft. With a characteristic impedance of 75 ohms it operated at a low V.S.W.R. when attached to the dipole centers. Matched lengths from the dipole centers to a weather-proof box located at ground center of the array were used to feed the parallel dipole pairs in phase. These twin lines were each 3/4 electrical wavelengths long and assisted in decoupling common mode currents from the dipoles.

Separate propagation measurements were made on 2.087 mc and 3.385 mc. Antenna supports (wooden poles) for each experiment were made available by Wallops Station and were sited for the two frequencies in squares 140 and 240 feet on a side. Existing pole supports were used for the higher frequency, and because they were slightly less than half-wavelength spaced, small, 11 turn loading coils were inserted on the dipole center insulators, as shown in Fig. 22, to cancel the capacitive reactance at the short dipole driving points.

Baluns

At the ground center of the square array, twin lines from parallel dipoles are connected to feed the parallel dipoles in phase. To convert these balanced-to-ground feed lines to unbalanced coaxial cables, balun coils were provided. These are wound on 6-inch diameter forms and connected to the paralleled 75 ohm twin transmission lines. To cause an impedance discontinuity as small as possible, the balun coils were made of bifilar windings of paralleled, side by side, 214-023 twin line. On a 6-inch form, 28 turns gave a common mode inductive reactance greater than 10 times the nominal 75 ohm impedance at the lower frequency. Small diameter ferrite cores could possibly be used to reduce balun size, but further development work

would be required at rf levels of kw range.[3] These baluns isolated and maintained balance in the system on the dipole side of the balun box, and were sufficiently broad-band to use at both transmitting frequencies. The balun coils appeared to have a characteristic impedance near 27 ohms resistive. To match the balun coil impedance to the lengths of 50 ohm RG-8/U leading to the transmitter van, an L-type network was used. By placing this network between the balun coils and coax cable, an unbalanced network could be used. Since this network is a one frequency device, separate networks were built for the two frequencies and switched when transmitting frequencies were changed. The antenna matching system used is shown in Fig. 24.

A large burden of the antenna array design and adjustment, which is to provide correct 90° phased currents of equal magnitude in the perpendicular elements, is avoided by having separate feed lines, from separate transmitting amplifiers, to each pair of parallel dipoles. The currents are adjustable independently in the two "arms" of the square as described in sections III A and III E. The rocket attitude remains nearly constant throughout the useful trajectory and results in the ground transmitting antenna being in a direction off axis of the rocket receiving antenna. This results in approximately 1.5 db loss in gain when the rocket is at apogee, corresponding to an inclination of 27° with the antenna array azimuth.

The higher powered of the two ground transmitters is used to transmit the ordinary wave (the circular polarized component suffering least absorption). Attenuation of this component, due to absorption in transmission

---

[3] A. I. Talkin and J. V. Cuneo, "Wide-Band Balun Transformer" R.S.I., 28. no. 10, October 1957, p. 808.

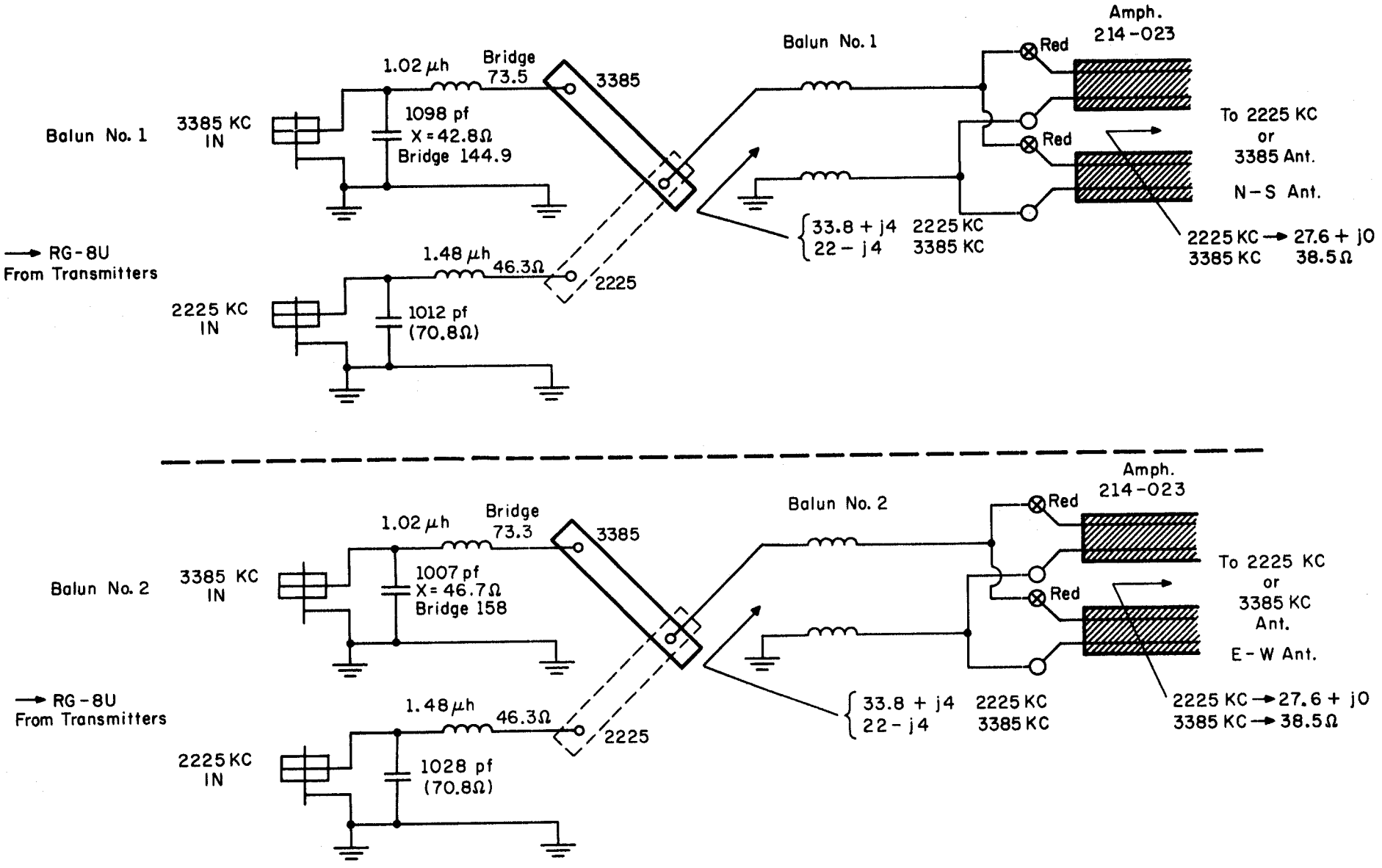

Figure 24
Antenna Matching Circuit Diagram

through the ionosphere, is estimated to be 10 db at the proposed frequency.

Field Intensity at Rocket Apogee

In free space, a dipole radiating 0.1 watt will produce a field strength of 16μ volts/meter at a distance of 100 miles.[4] This value of free space field intensity is modified by the following factors:

1.	Ground antenna gain as previously described	+ 6 db
2.	Loss due to apogee off axis of major lobe of ground transmitting antenna	- 1.5 db
3.	Loss due to rocket attitude at apogee resulting in receiving antenna not pointed toward ground transmitter	- 1.5 db
4.	Ionospheric absorption occurring in transmission of ordinary wave	- 10 db
	TOTAL	- 7 db

This 7 db loss decreases the 16μ volt-free space field intensity by a factor of 0.44 and yields a predicted equivalent intensity of 7μ volts at the rocket, for the assumed power of 0.1 watt.

C. Servo

The function of the servo system is to maintain a fixed ratio (10 db) between the ordinary and extraordinary waves at the rocket receiving antenna by controlling the amount of transmitted extraordinary power during the period of differential absorption. The rocket receiver output signal consists of a nominal 500 cps component and a dc component, the ratio of the two depending upon the ratio of extraordinary to ordinary power at the

---

[4] F. T. R. Handbook, "Reference Data for Radio Engineers" 3rd Edition, p. 375

rocket antenna. Fig. 25 (a) shows the receiver signal for four conditions: the first segment represents no ordinary or extraordinary signal, the second represents ordinary signal only, the third is for the extraordinary signal 10 db down from the ordinary, and the fourth represents equal ordinary and extraordinary signals. The servo system develops its error signal by comparing the difference between the ac and dc component of the telemetered signal. For this reason the telemetered rocket receiver signal must preserve the dc component up to the point where it is measured and compared.

The receiver calibration signal corresponds to zero volts into the receiver detector, which provides the lower band edge signal to the telemetry discriminator. The discriminator translates the receiver band center from +2.5 volts to zero volts, at the same time applying any desired gain to the signal [Fig. 25 (b)]. The resulting telemetered signal to the van corresponding to that shown in Fig. 25 (a) is fed to a balanced, inverting amplifier whose output is shown in Fig. 25 (c). The discriminator gains are set so that upper and lower band edges are at +4V and -4V, respectively. If this resulting signal were used, then during in-flight rocket receiver calibration there would be a large dc component and no ac component of the signal, which would generate a large servo error signal. Consequently, an offset voltage is applied to bring the lower band edge signal to zero volts dc, as shown in Fig. 25 (d).

The telemetered signal to the van, after being inverted and amplified, is fed into the percent modulation servo chassis whose circuit diagram is shown in Fig. 26. The ac and dc components are separated by bypass filters and blocking capacitors. An adjustable offset voltage is applied to the dc portion and the resultant potential applied to one terminal of a balanced modulator. The ac portion is amplified by one-half of a 12AU7

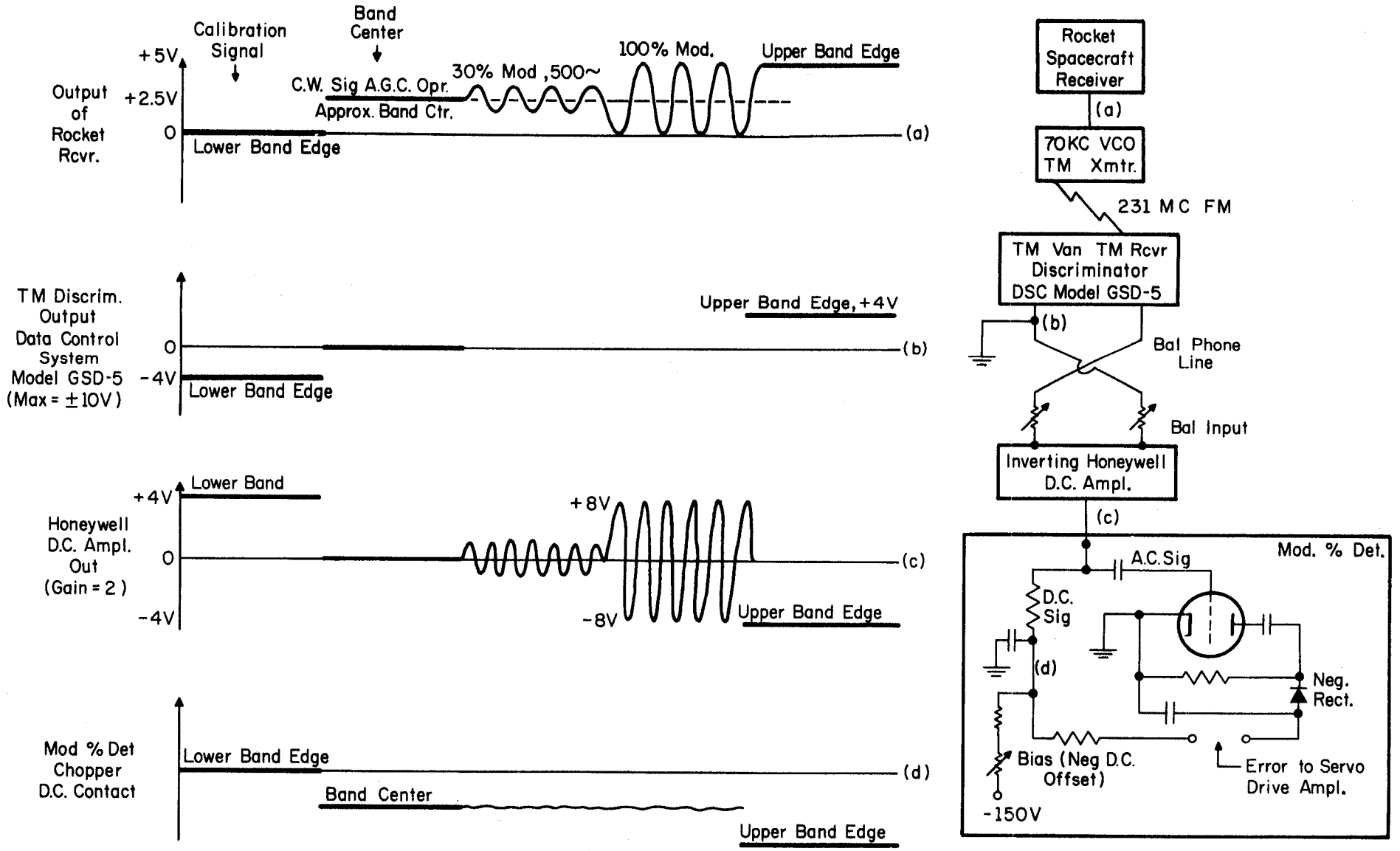

Figure 25
Rocket Receiver Signal at Various Points in the System

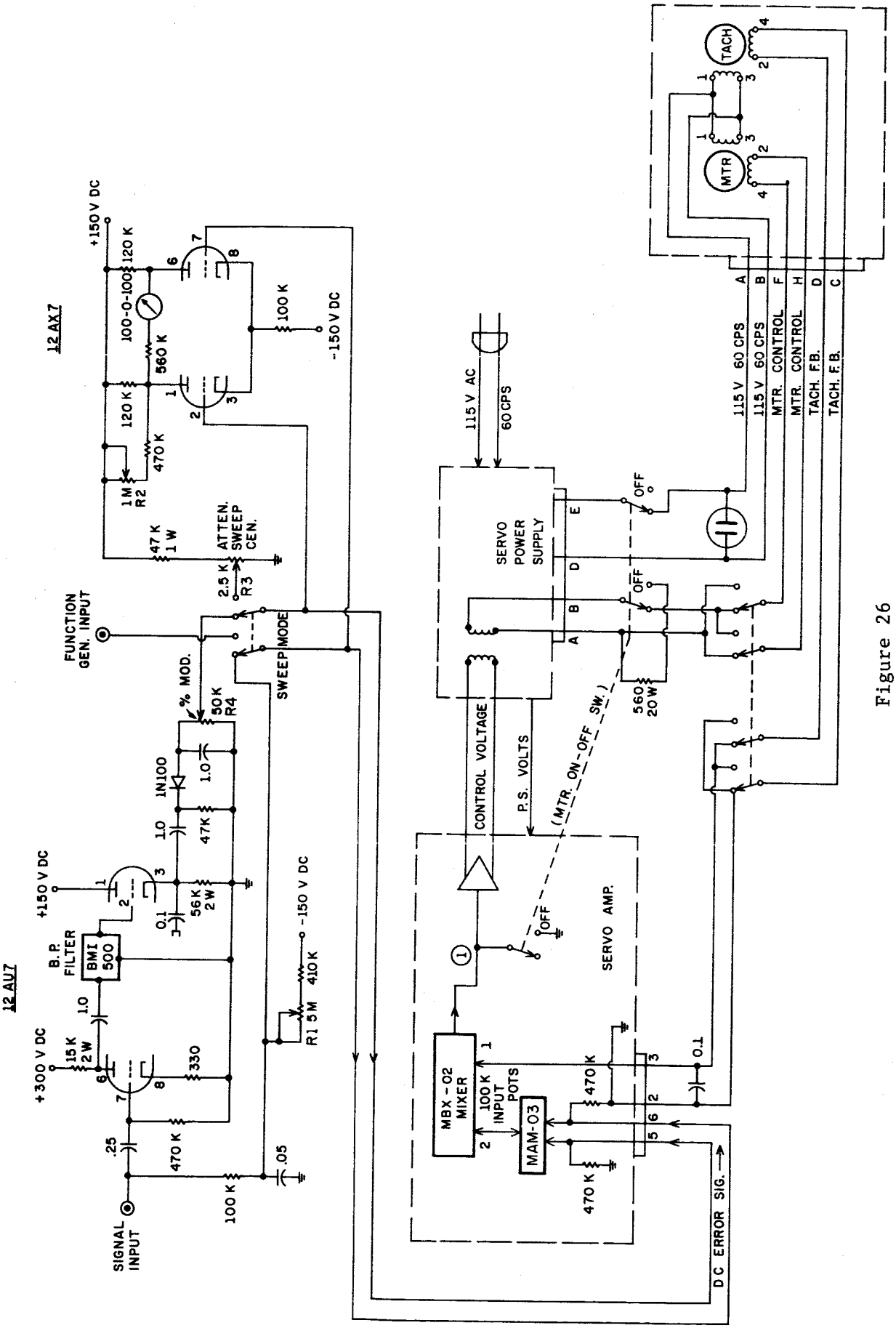

Figure 26
Percent Modulation Detector Circuit Diagram

and passed through band pass filter BMI500 (UTC) which has a center frequency of 500 cycles and a 3 db pass band of 20 cycles. This is another place where an improvement can be made by increasing the pass band so that high rates of Faraday rotation do not affect the amplitude of the filter output. The ac component is then rectified and a portion fed to the other terminal of the balanced modulator. The input to the balanced modulator is the servo error signal, and, for any relative value of dc and ac components (so-called "percent modulation") can be set to zero by adjustment of R4. This error signal is also amplified by a 12AX7 and visually displayed by a 100-0-100 ma panel meter. The balanced modulator MAM-03 (Fig. 27) converts the dc error to 60 cps and feeds this to potentiometer input no. 2 of mixer MBX-02 (Fig. 28). Both these units are manufactured by Diehl Manufacturing Company of Sommerville, New Jersey, and are described in their "Application Bulletin 605A." The tachometer output is fed to potentiometer input no. 1 of the mixer. Thus, the gain and feedback of the servo loop is adjusted by potentiometers no. 2 and 1, respectively, of the mixer. The mixer also has a carrier phase shift control for adjusting the two-phase servo motor control and reference signals 90° apart in phase in order to get full output torque.

The mixer output is fed to the Diehl VA075-OA-301 servo amplifier, described in Diehl's "Application Bulletin 603A." This 75-watt amplifier has an adjustable feedback loop for greater stability. It has a separate power supply, Diehl VP3-100. Circuit diagrams for amplifier and power supply are shown in Figs. 29 and 30, respectively. The amplifier feeds the 60 cps error signal and a reference signal to the two-phase servo-tachometer Diehl FPE25L-105-1T. The servomotor is rated at 5 watts. Panel switches are provided on the servo control chassis to reverse the servo

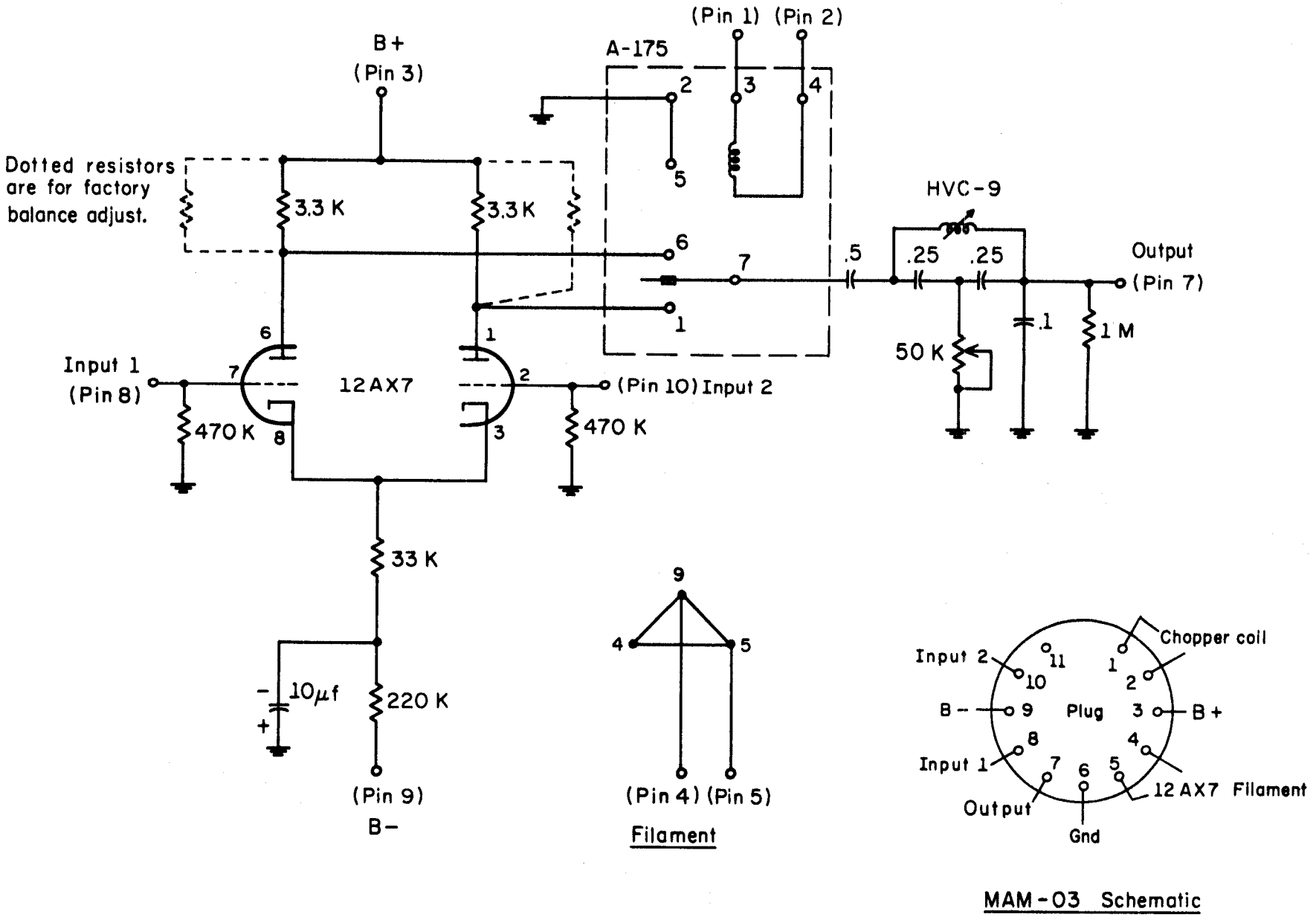

Figure 27
Diehl MAM-03 Balanced Modulator Circuit Diagram.

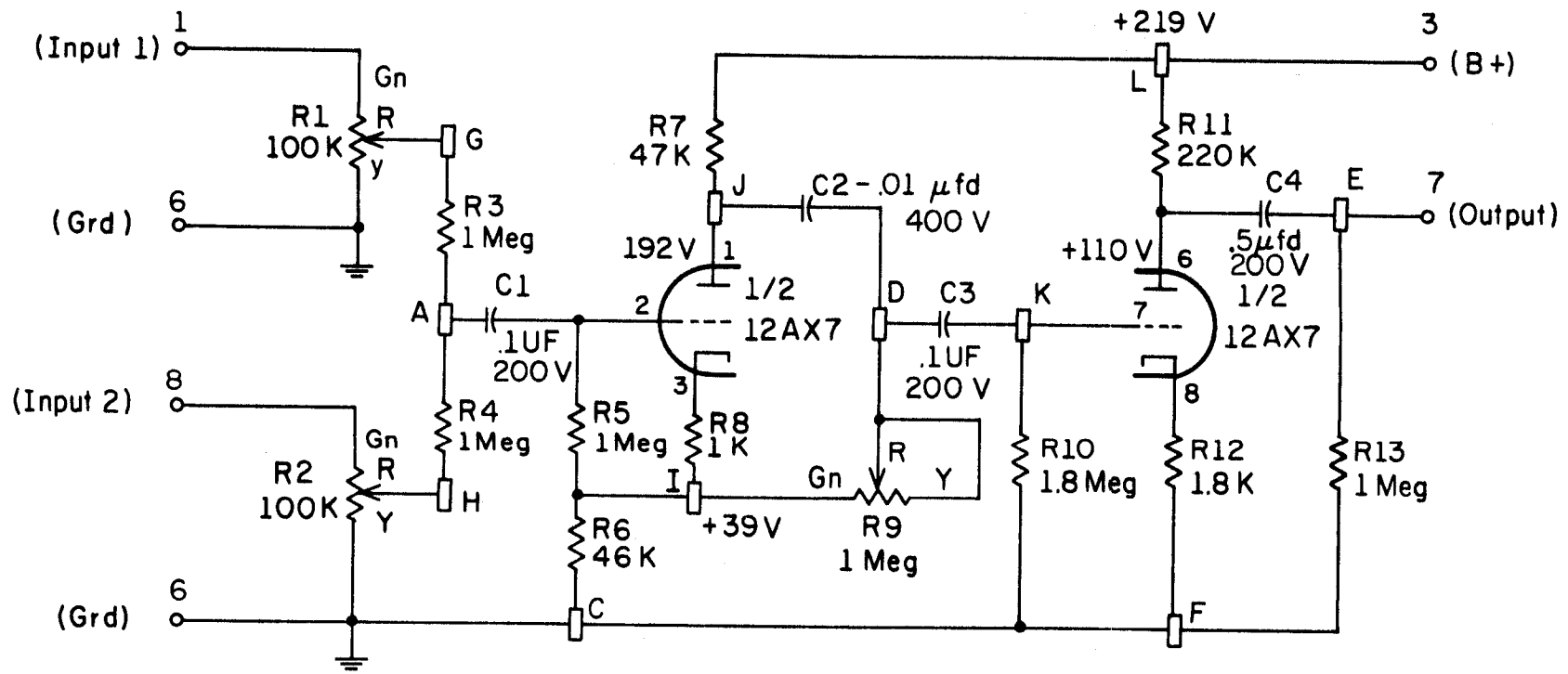

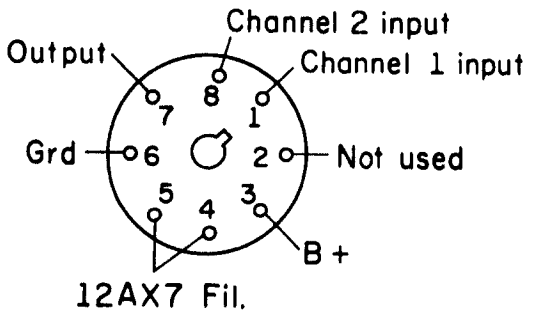

Socket

Note : D.C. voltages measured with inputs grounded.

All resistors are 1/2 watt ± 10%.

"o" denotes vector plug terminals.

"[]" denotes turret terminals.

Figure 28
Diehl MBX-02 Mixer Circuit Diagram.

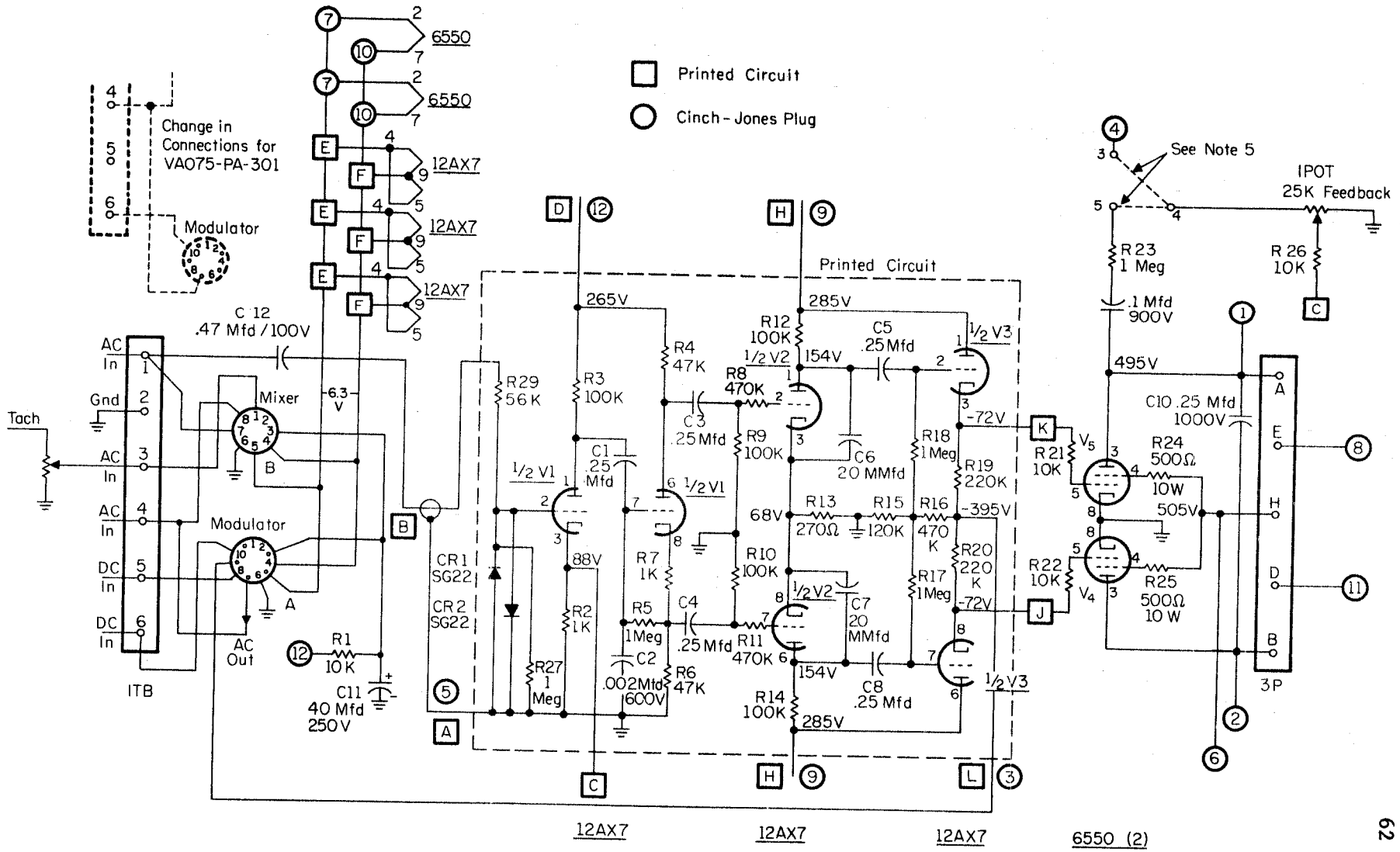

Figure 29
Diehl VA075-OA-301 Servo Amplifier Circuit Diagram.

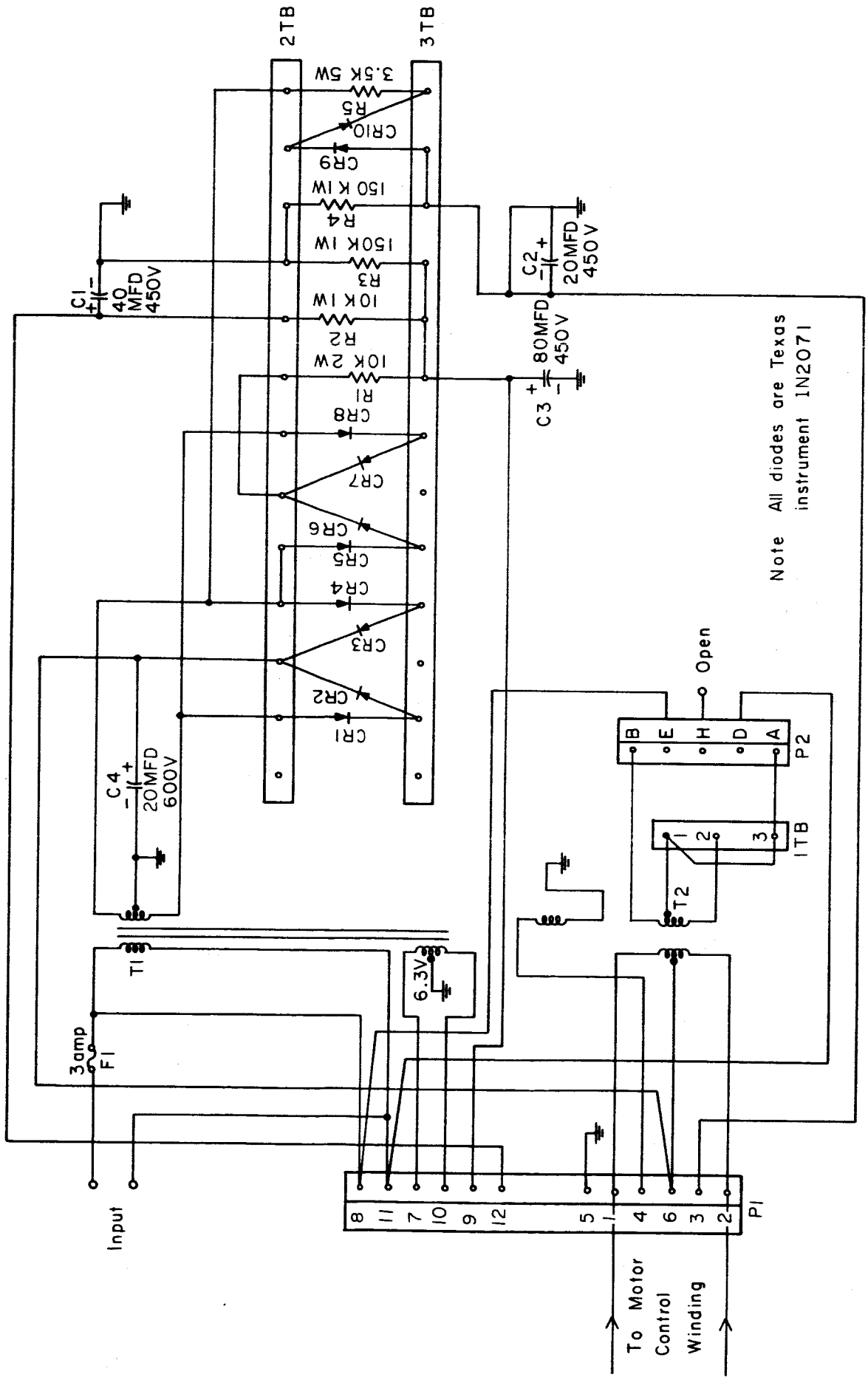

Figure 30
Diehl VA075-)A-301 Power Supply Circuit Diagram.

motor direction and to disconnect the servo motor while its amplifier is still operating and suitably loaded.

Provision is made to test the servo preamplifiers, amplifier, motor and tachometer system by injecting synthesized signals. By throwing the panel switch to "Sweep Mode" (see Fig. 26) the rectified ac component is obtained from the +150 V power supply via potentiometer R3, and the dc component is fed via a potentiometer mounted on the X attenuator shaft by a function generator which provides either sine wave, square wave, or sawtooth wave varying at one cycle per second. In this way, the servo motor cyclically operates the rf attenuator, thereby enabling the servo system to be checked in a closed loop operation. The block diagram for this operation is shown in Fig. 31.

The servo system closed loop response has its 3 db point at about 1 cycle per second.

D. Rocket Antenna and Receiver

Receiver

The payload receiver (see Fig. 6) was manufactured by Space Craft, Incorporated, of Huntsville, Alabama, to meet the following specifications:

1. Operating Frequency. 2.225 mc or 3.385 mc
2. Type of Signals to be Received. Two carriers spaced 500 cps apart, 250 cps on each side of the above frequency
3. Sensitivity. -120 dbm or better for 10 db $\frac{S+N}{N}$ at 90% 500 cps modulation
4. Dynamic Range. From threshold to -60 dbm with no more than 6 db change in output level

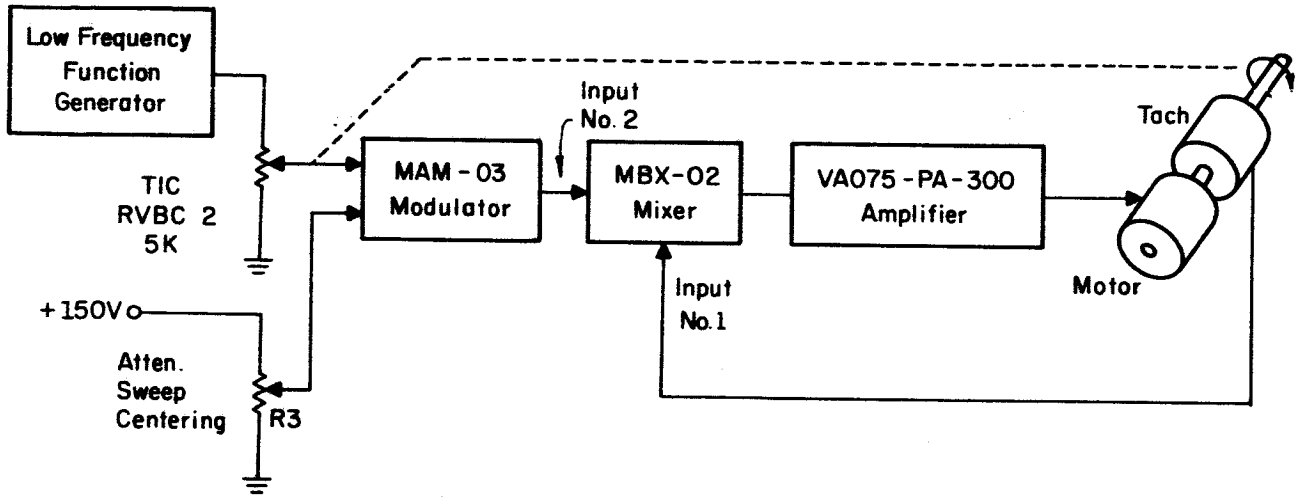

Figure 31

Servo Test Circuit Block Diagram

5. Output. Output of a "linear" detector to be dc-coupled at a level suitable for feeding a standard telemetry subcarrier oscillator. Outputs of interest are the dc level and the 500 cps difference signal level. Later versions of the receiver had the AGC brought out to feed a telemetry subcarrier oscillator.
6. Operating Frequency Versatility. A crystal-controlled super-heterodyne receiver with replaceable crystal for changing operating frequency approximately $\pm$ 1 kc without a major retuning of receiver circuits. In practice, the receivers were encapsulated in foam with the local oscillator crystal and series filter crystal installed fixing the center frequency.
7. Receiver Bandwidth. Approximately 2 kc. The first receivers had about 800 cps bandwidth.
8. Noise Figure. Lowest practical noise figure consistent with current state-of-the-art using transistors, but not to exceed 4 db.
9. Mechanical Configuration. To fit available space in the Apache missile with a maximum length not to exceed 4 inches. Outside diameter approximately 5 inches, giving room for connectors.

10. Connectors. Type DAM-7W 2P-NMB-2
11. Supply Voltage. +28 volts dc not to exceed 40 volts
12. Rf Input Impedance. 500 ohms
13. In-Flight Calibration. Provision for biasing off the detector by an external signal to give a zero set.
14. Ambient Temperature Range. 0-150°F
15. Shock and Vibration. Must survive Nike-Apache launch; i.e., approximately 40 g linear acceleration. (The receiver operated before, during, and after both Nike and Apache burning with no evidence of microphonics or deterioration.

The receiver schematic is shown in Fig. 32. There are two rf stages Q1 and Q2 followed by a series crystal filter Y1 which determines the selectivity of the receiver. The rf signal and the output of the crystal-controlled local oscillator Q7 are combined in a balanced mixer CR1 and CR2. The 600 kc if is amplified by three broadly tuned stages, Q3, Q4, and Q5. The detected dc plus 500 cps is taken from the emitter of Q6 at an impedance of 1 K. Q6 with Q9 serves to amplify the AGC signal which is applied to the second rf stage and the first two if stages. Q8 serves as a voltage regulator maintaining approximately 18 volts in the receiver with supply voltages from less than 24 volts to as high as 40 volts. Typical output vs input characteristics are shown in Fig. 33. Outline drawings of the receiver are shown in Fig. 34.

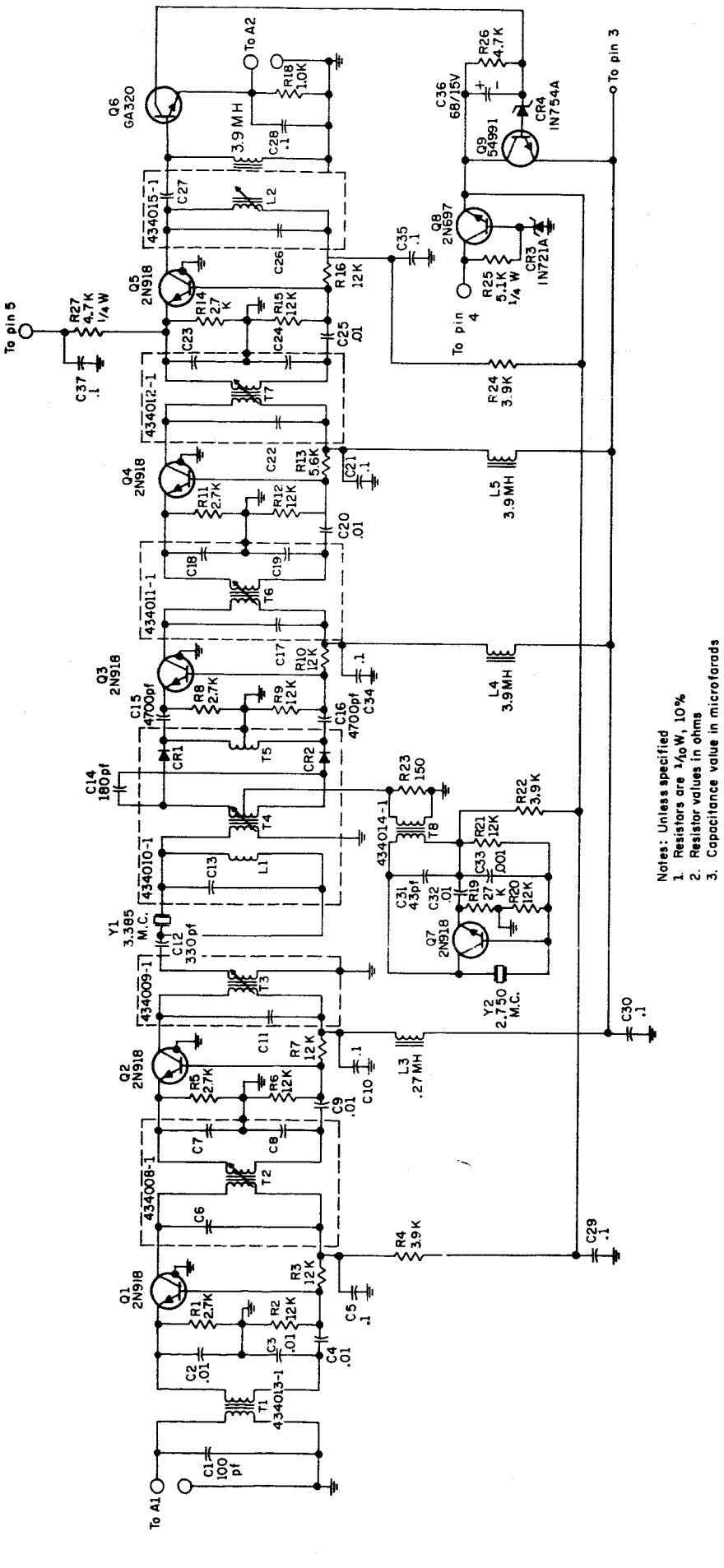

Notes: Unless specified
1. Resistors are 1/10 W, 10%
2. Resistor values in ohms
3. Capacitance value in microfarads

Figure 32
Space Craft Rocket Receiver Block Diagram

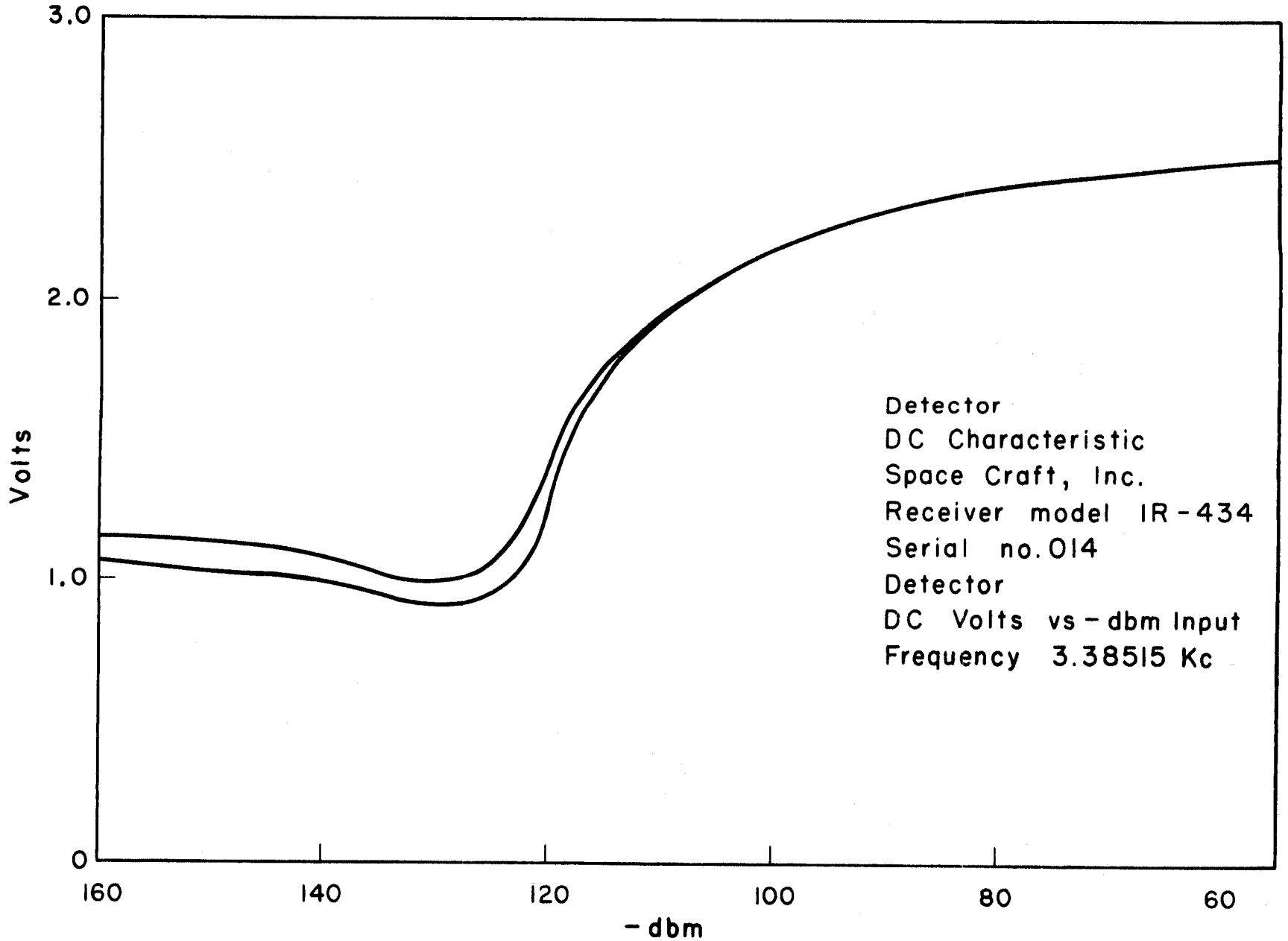

Figure 33
Rocket Receiver Output vs dbm Input Characteristics

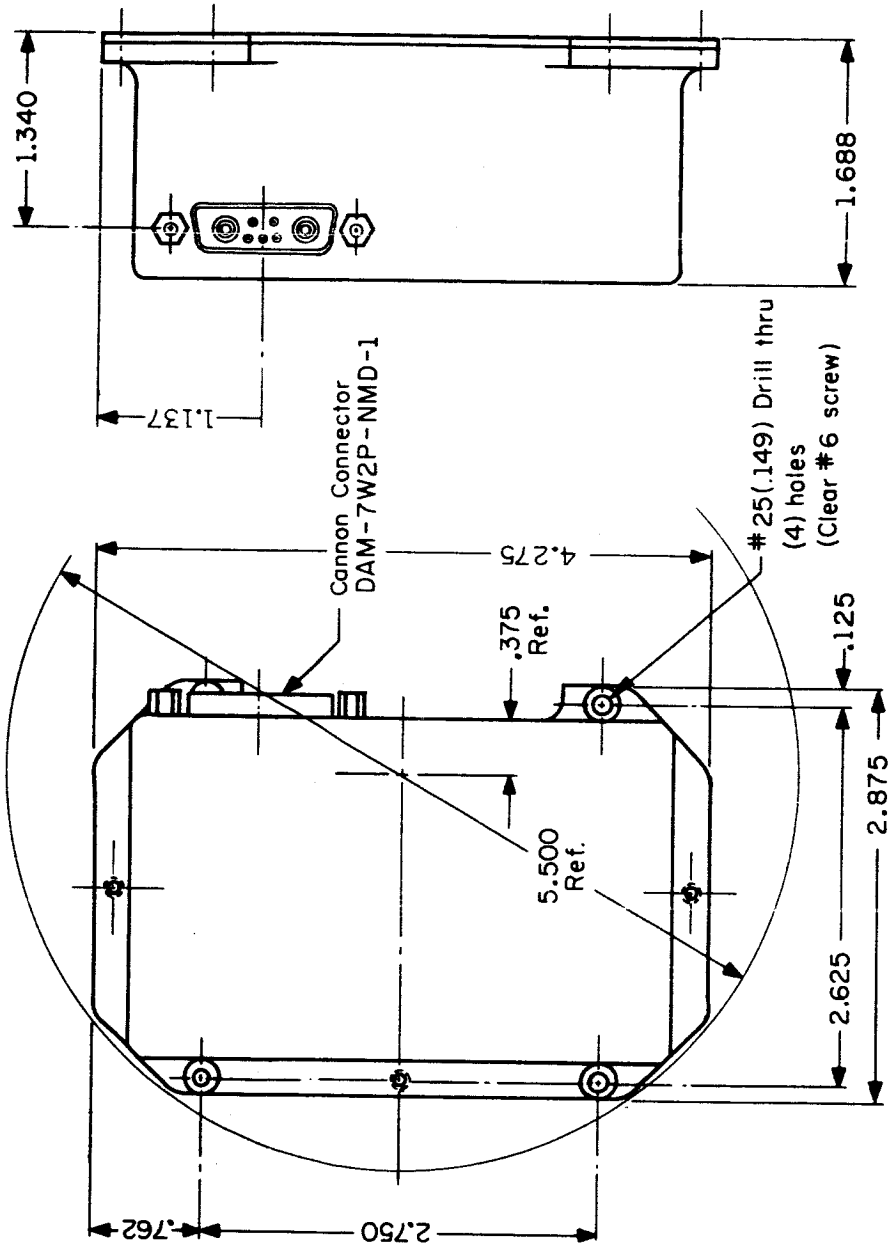

Figure 34
Space Craft Rocket Receiver Outline Drawing

The payload antenna for the radio propagation experiment is a ferrite loop antenna, Fig. 5, oriented perpendicular to the longitudinal axis of the rocket. The antenna is located inside a fiberglass section of the payload skin, Fig. 35. The metal-to-metal length of this fiberglass section was made approximately equal to the diameter of the payload shell (6-5/8 inches) after tests of longer and shorter insulating sections.

Other instrumentation in the nose of the payload required that several conductors pass through the section allocated for the antenna. To obtain good nulls in the antenna pattern it was necessary to maintain electrical symmetry as much as possible. This is the reason for the configuration using two parallel rods with a space between, as shown in Fig. 36. An aluminum wiring channel passes between the rods at each end. Only one of the channels is used for the wiring, the other merely maintaining electrical symmetry. The channels are electrically bonded to the antenna section, top and bottom decks. The bottom deck is rigidly attached to the payload shell. A rf gasket forms a good electrical bond between the upper deck and the upper portion of the payload shell. The ferrite rods are made as long as possible within the fiberglass shell.

The antenna of 18 or 26 turns for 3.385 mc or 2.225 mc, respectively, is wound with 24 gauge nylon-jacketed polyethylene insulated wire. The winding is distributed over the length of the rods between the support structure to achieve a higher "Q". The unloaded "Q" of the antennas is from 250 to 300. The coil is resonated by a total capacity of approximately 50 pico-farad. This capacitance is made up of the temperature compensating capacitors and a hermetically sealed trimmer capacitor. The trimmer permits final tuning of the antenna after the payload is assembled.

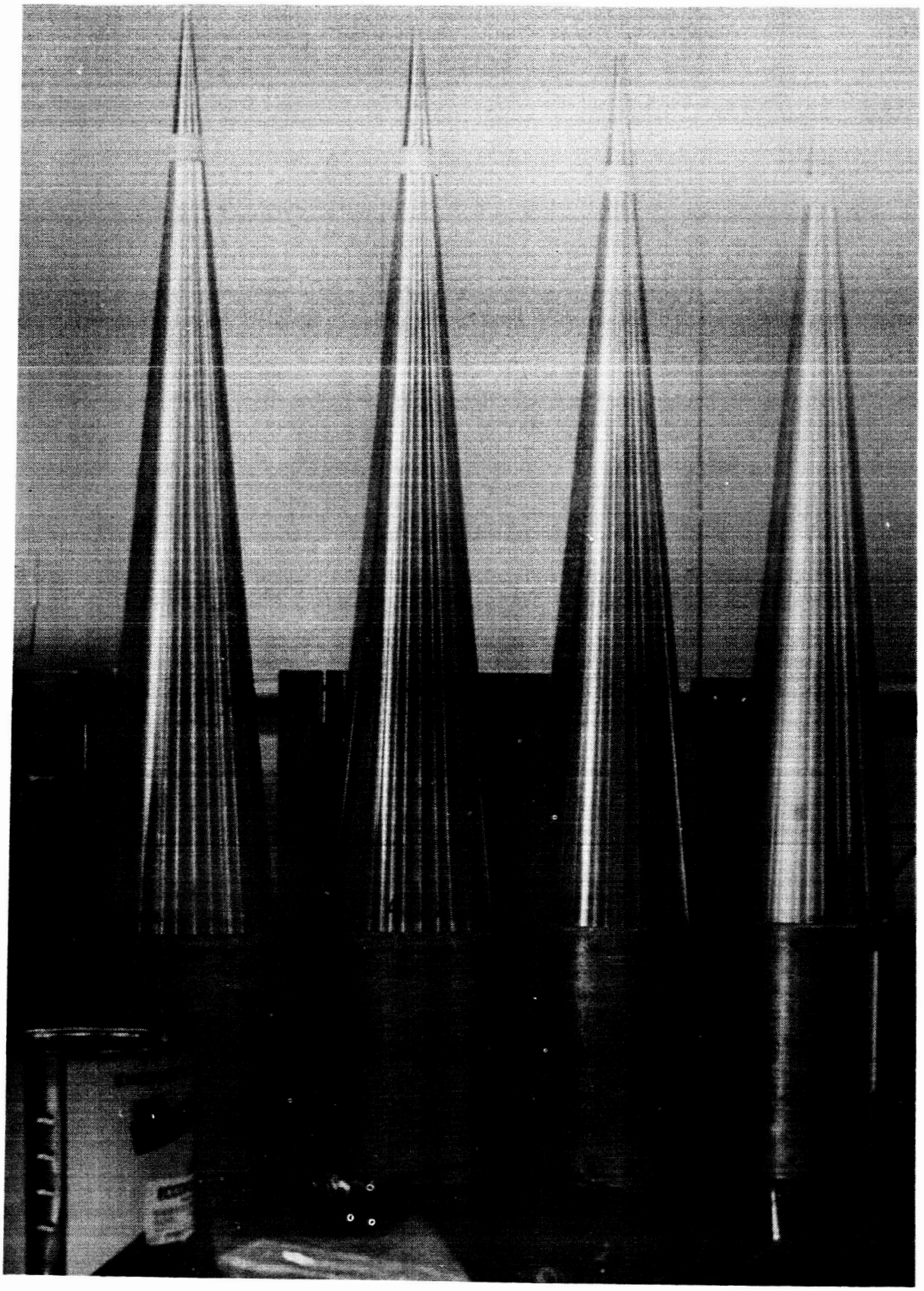

Figure 35

Fiberglass Section of the Apache Stage

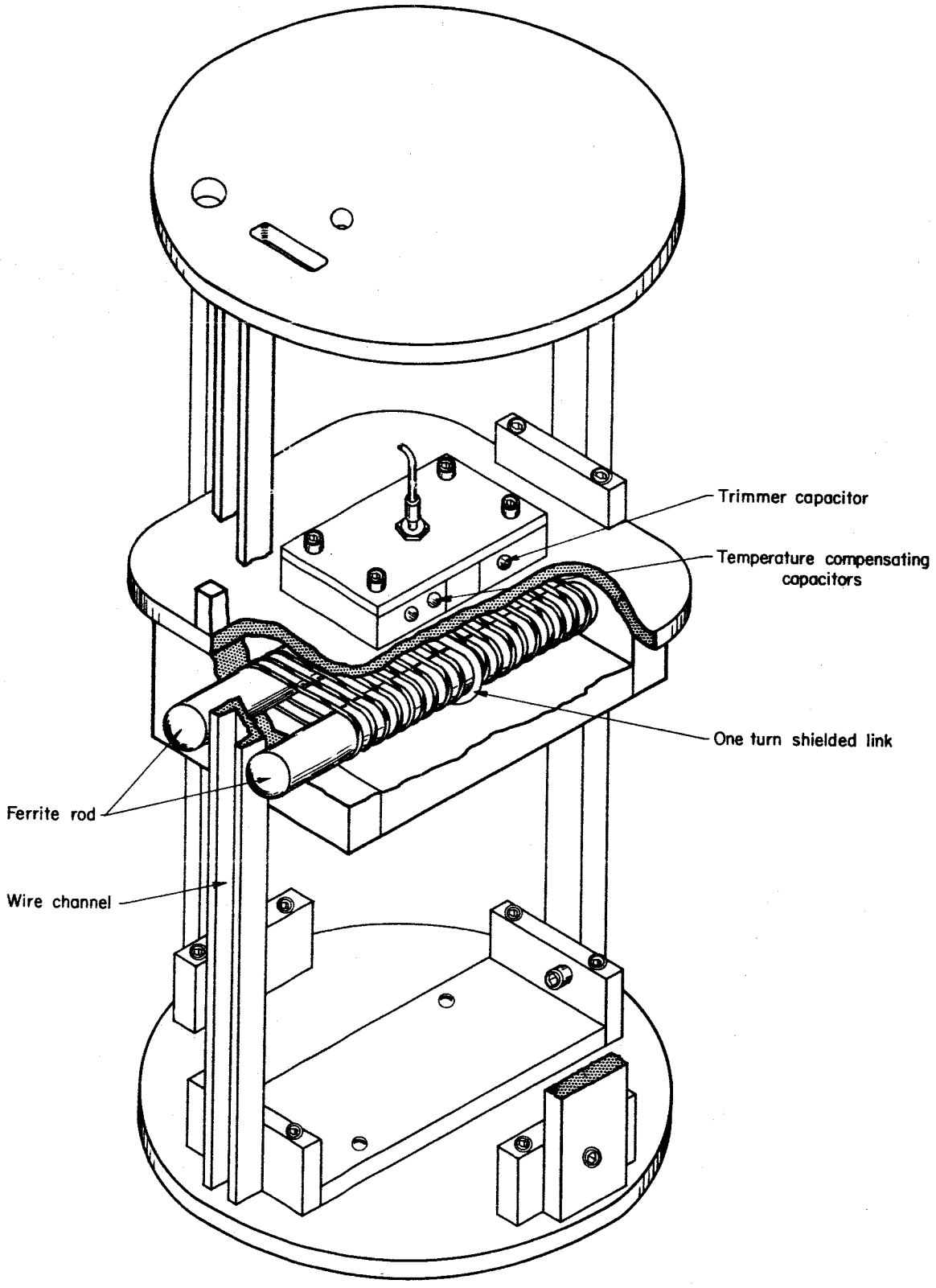

Figure 36

Schematic of the Circularly Polarized Rocket Receiving Antenna

A one-turn shielded link is used to couple the antenna to the receiver. The shield of the link is connected to the center of the antenna winding, again maintaining symmetry to eliminate vertical pick up. The one-turn link has an impedance of the order of 500 ohms. The receiver input circuit was designed to work with this impedance. Field tests of the antenna in a dummy payload indicate that the nulls were better than 35 db.

The central portion of the antenna was encapsulated in foam to provide additional support for the ferrite rods. In later payloads, foam was also placed between the antenna deck and the bottom of the antenna section for more support.

For the firings at the magnetic equator, a circularly polarized payload antenna, Fig. 37, was required by the nature of the experiment. In this case two ferrite loop antennas similar to the linearly polarized version were mounted perpendicular to each other as shown in Fig. 38. The aluminum conduit through the center of the antennas was used for the wires to the upper section of the payload. The link outputs of the two antennas were coupled to the receiver by a hybrid junction circuit.[5] The antennas were then tuned off resonance, one above and the other below, to give a circularly polarized pattern.

E. Polarization Test Equipment

One method of testing the transmitting antenna array for purity of polarization involves transmitting short pulses of rf with the system set up for extraordinary polarization. A sensitive receiver is tuned to the frequency transmitted, with the output of the receiver displayed on an

---

[5] R. S. Berg and B. Howland, "RF Component Development for the Decon System," Technical Report No. 275, Lincoln Laboratory, August 3, 1962.

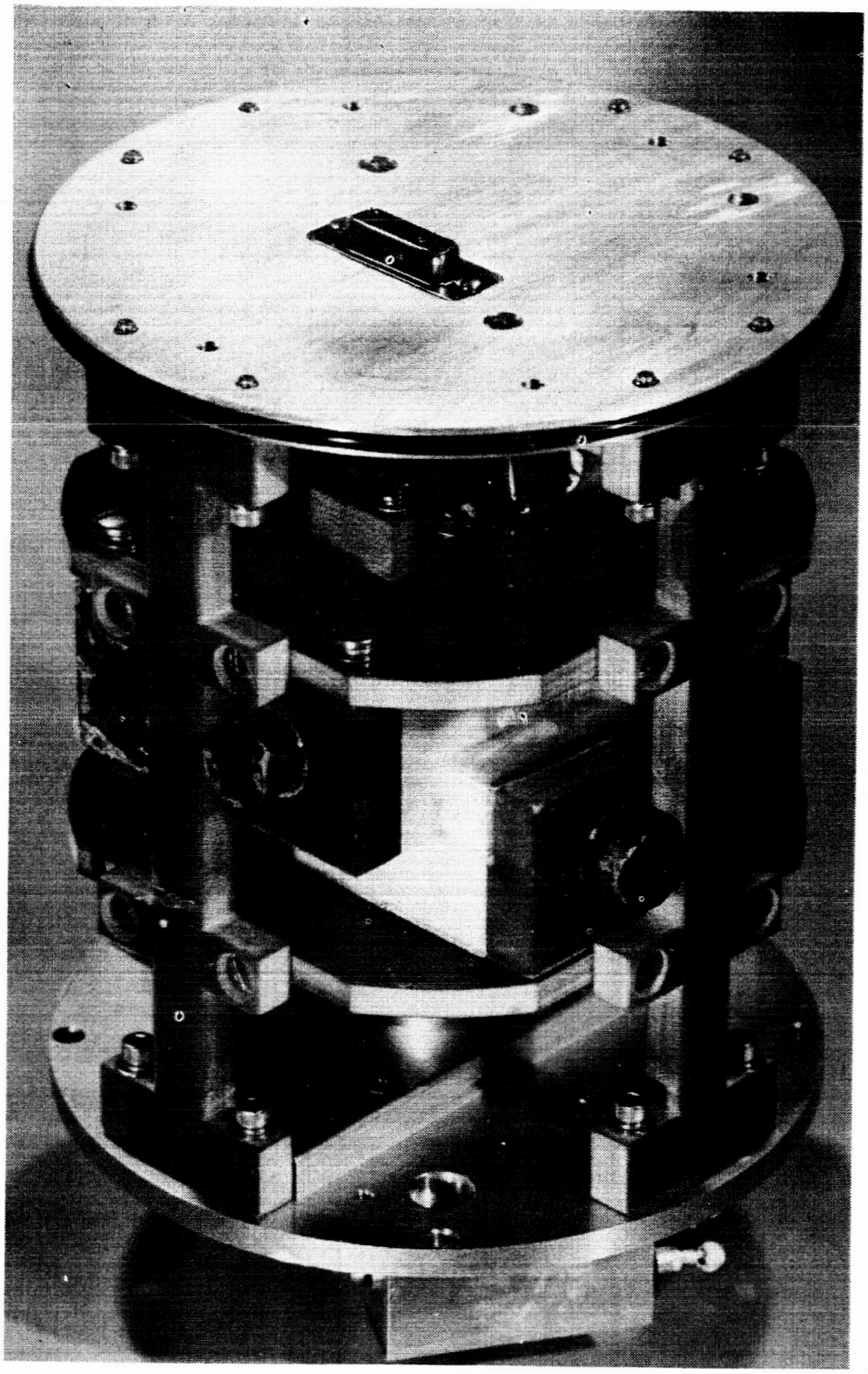

Figure 37

The Linearly Polarized Rocket Receiving Antenna

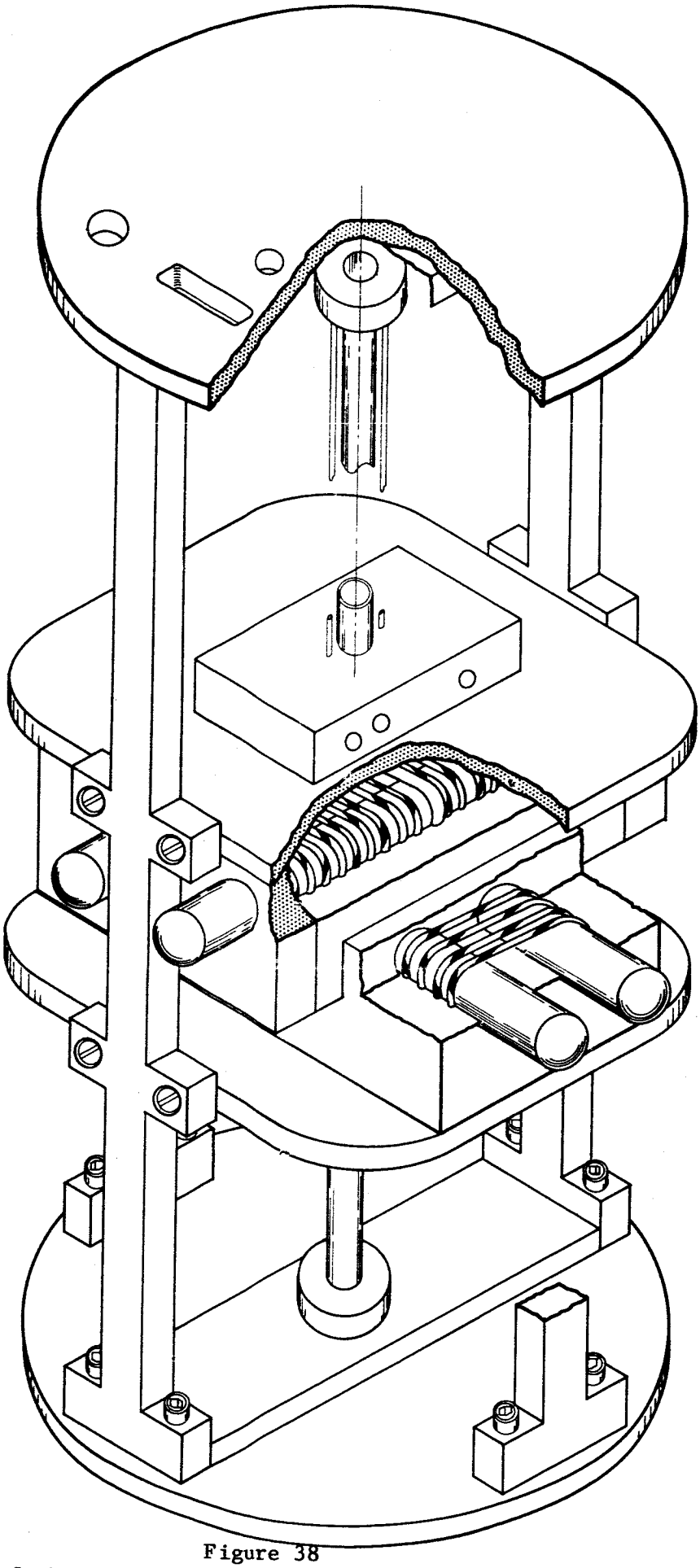

Figure 38
Schematic of the Linearly Polarized Rocket Receiving Antenna.

oscilloscope. Any return pulses from the ionosphere, observed on the oscilloscope, are indications that the polarization is not purely extraordinary, as during the daylight hours, extraordinary polarization is so highly attenuated by the D layer that any reflected energy would be too small to be detectable. Therefore any echos observed indicate that energy is being transmitted in other than the extraordinary mode and adjustments should be made to minimize this return energy. Conversely, it is possible to transmit in the ordinary mode of polarization and adjust for maximum return echos as the ordinary mode is less attenuated by the D layer. This, however, is not a precision adjustment as the maximum return is a broad function as compared to adjusting for a minimum return which is sharply defined.

For convenience it is desirable to have the pulse receiver located at the transmitter site. This means that the transmitter, which is on for the duration of the pulse (approx. 100 microseconds), must be off as completely as possible until the next pulse so that any return echos will not be obscured by energy being received directly from the transmitter. To accomplish this, a gated amplifier was designed to supply pulses of rf from the transmitter exciters to the power amplifiers (see Fig. 39).

The amplifier was designed using type 6AS6 sharp-cutoff pentodes that can be gated on the suppressor grid. By using these tubes in push-pull pairs, the large step voltage generated by the gating is cancelled in the transformer output while the rf signal is reinforced. Capacitive feed-thru of the exciter was objectionably high with one push-pull stage. Addition of a second push-pull stage plus a 6BQ5 driver stage reduced the feed-

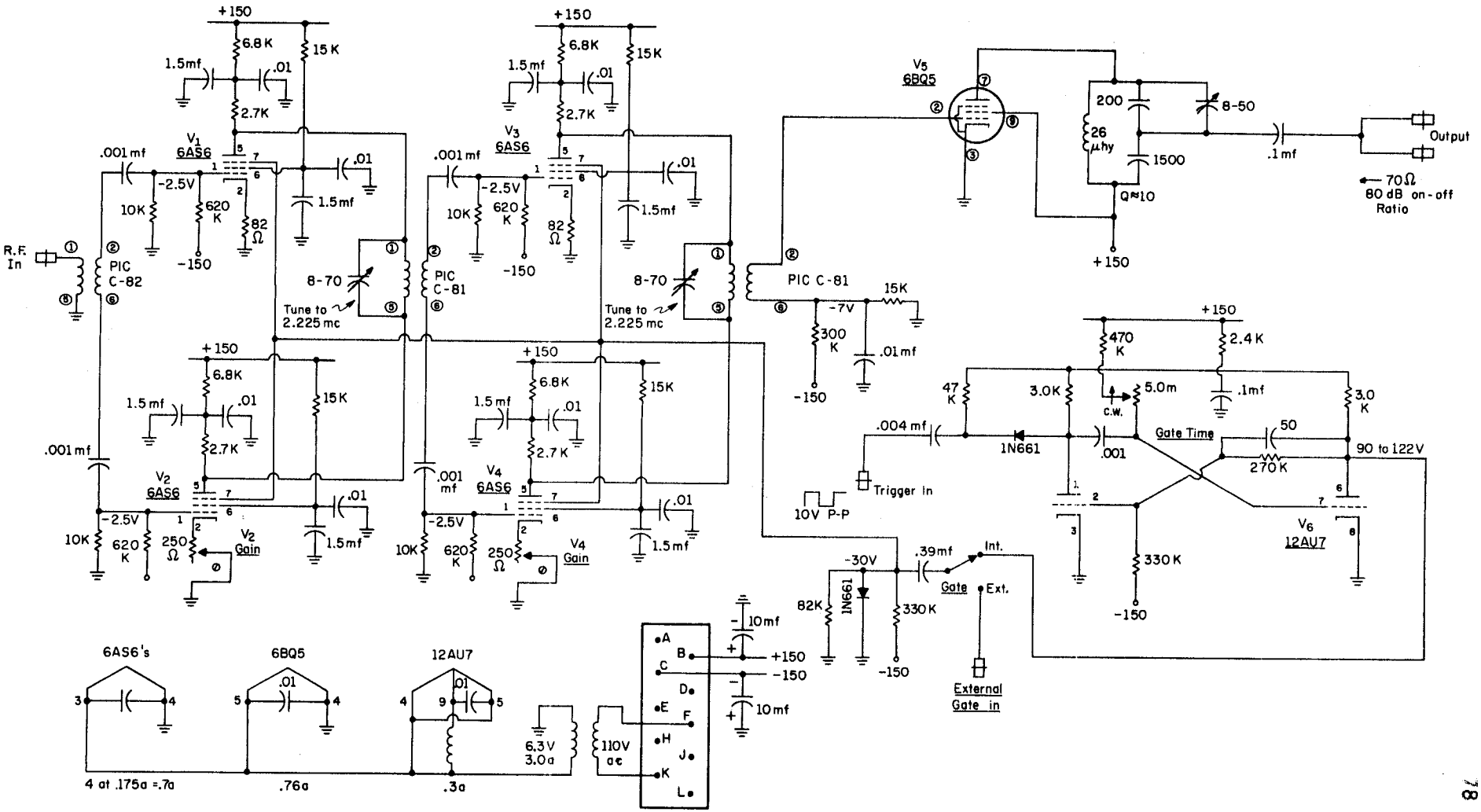

Figure 39
Rf Pulse Generator Circuit Diagram, Early Version

thru so that an on-off ratio of 80 db was obtained. The 6BQ5 stage was designed to furnish 0.1 watt into the 70 ohm input impedance of the linear amplifier.

A monostable multivibrator was incorporated to produce the gate voltage for the 6AS6 tubes. The multivibrator period and hence the transmitter pulse length is adjustable. An external square wave trigger of approximately 10 volts peak to peak is required to trigger the multivibrator.

This scheme worked successfully with some two miles separation of transmitting and receiving antennas. The receiving antenna being a loop, further discrimination against the ground wave was obtained by pointing the null of the loop toward the transmitting antennas. This was necessary even though the exciter output was down by 80 db during the off-time of the pulse. The transmitter gain is also 80 db; therefore, the antennas were receiving roughly the power output of the exciters. However the discrimination against the ground wave by both the receiving and transmitting antennas (the transmitting antennas also have nulls off their sides) made the system usable.

A better heterodyne system was developed which allows the receiver to be located alongside the transmitters. The block diagram is shown in Fig. 40. A gated heterodyne mixer is used to mix oscillator frequencies of 2680 kc, and 455 kc to obtain an output of 2225 kc, when the mixer is gated on. This avoids fast pulsing of a crystal oscillator and also avoids any energy being generated at the 2225 kc frequency during the period of listening for echos from the ionosphere. A receiver for use in ionosphere sounding was built and is shown in Fig. 41. The design incorporated low

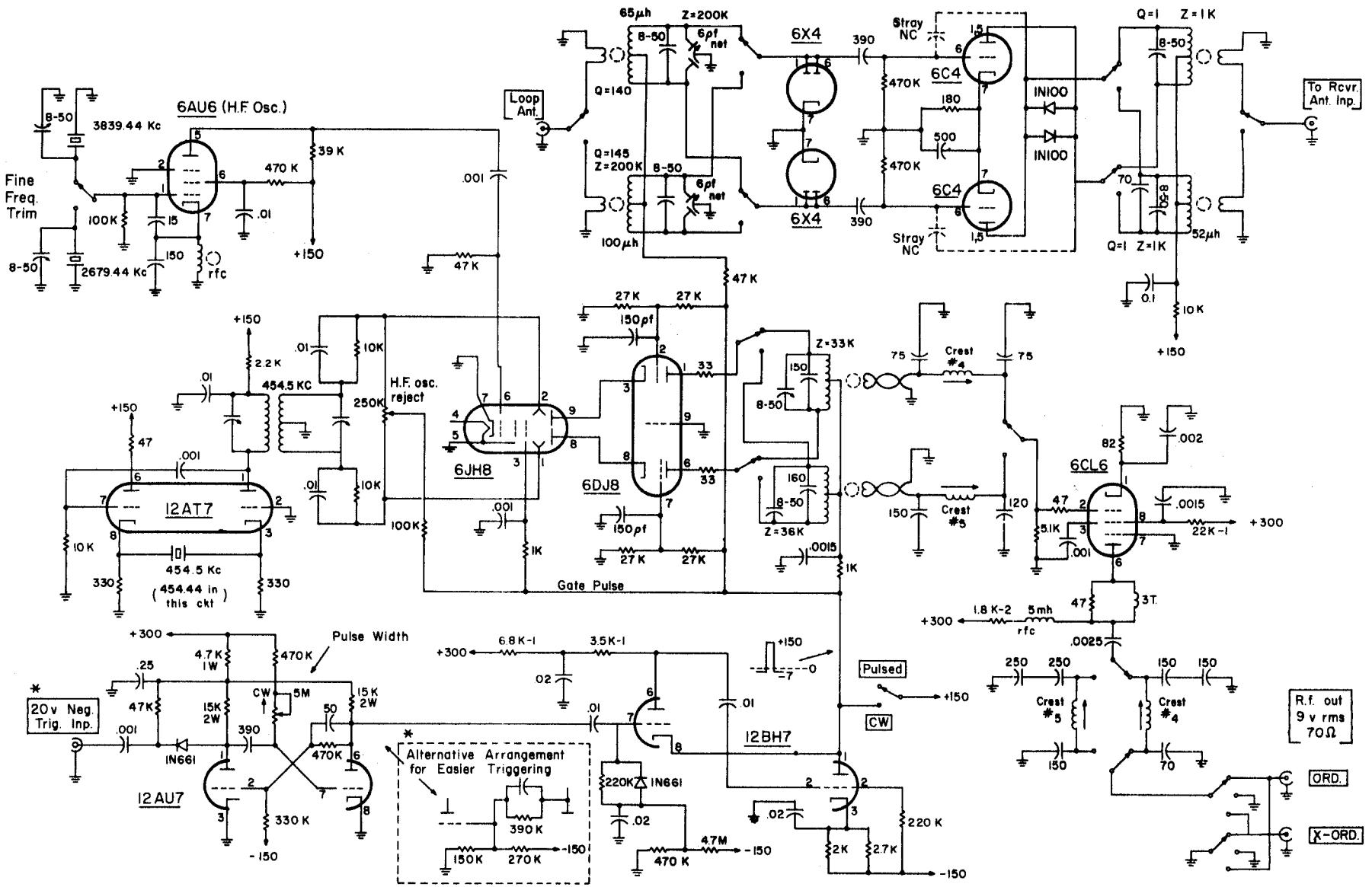

Figure 40
Rf Pulse Generator Circuit Diagram, Present Version

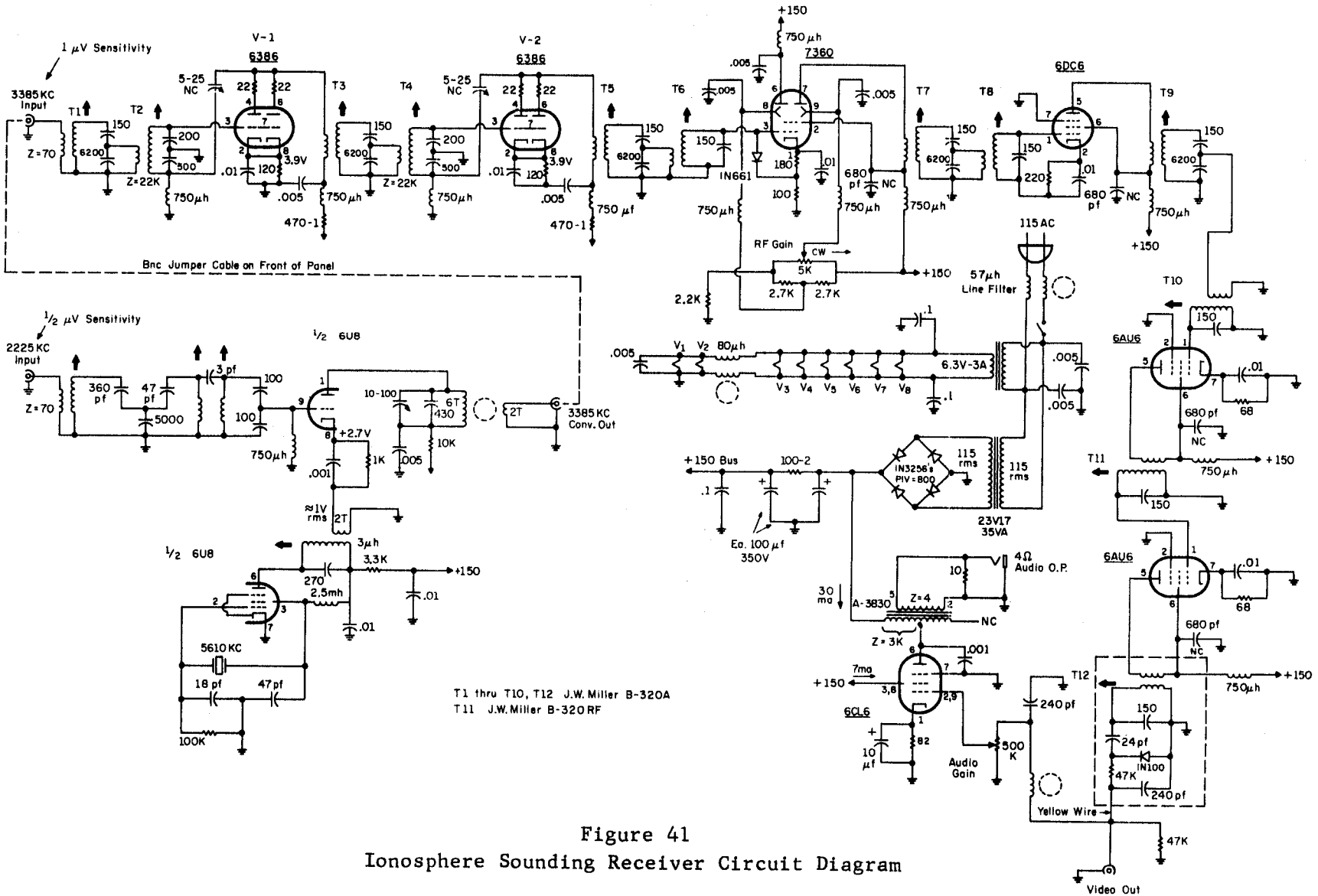

Figure 41
Ionosphere Sounding Receiver Circuit Diagram

impedances in grid return lines, short decoupling time constants in supply voltage lines, and used 12 cascaded, medium Q selective circuits. This provided fast recovery following the overload of a transmitted pulse and good pulse shape of the received pulses, while at the same time giving good skirt selectivity to protect against adjacent channel interference. The receiver was used as a 3385 kc straight through amplifier with 100 db gain and had 12 tuned circuits on 3385 kc. For operation on 2225 kc a converter was used to change this frequency to 3385 kc. Its output was fed to the above-described receiver.

Another method of testing the transmitting antenna array for polarization purity is by use of a horizontal ferrite rod antenna placed at the center of the array and rotating at 600 rpm. An antenna section identical to that used in the payload is mounted on a motor drive unit as shown in Fig. 42. The one-turn link output of the antenna is brought through rf slip rings and a coaxial line to an oscilloscope in the transmitter van. A synch pulse for the oscilloscope is also generated by the rotating antenna. Two triggering methods were tried, neither of which were completely satisfactory. One was a mechanical contact and the other a permanent magnet and pick-up coil. The mechanical contact was very noisy and subject to wear. The only pick-up coil available at the time gave a very small output pulse. Perhaps a permanent magnet and reed switch would be a better solution. The use of this rotating antenna is described in section IV E.

F. Telemetry

The CSL portion of the payload experiments called, in general, for three telemetry channels. These are as follows:

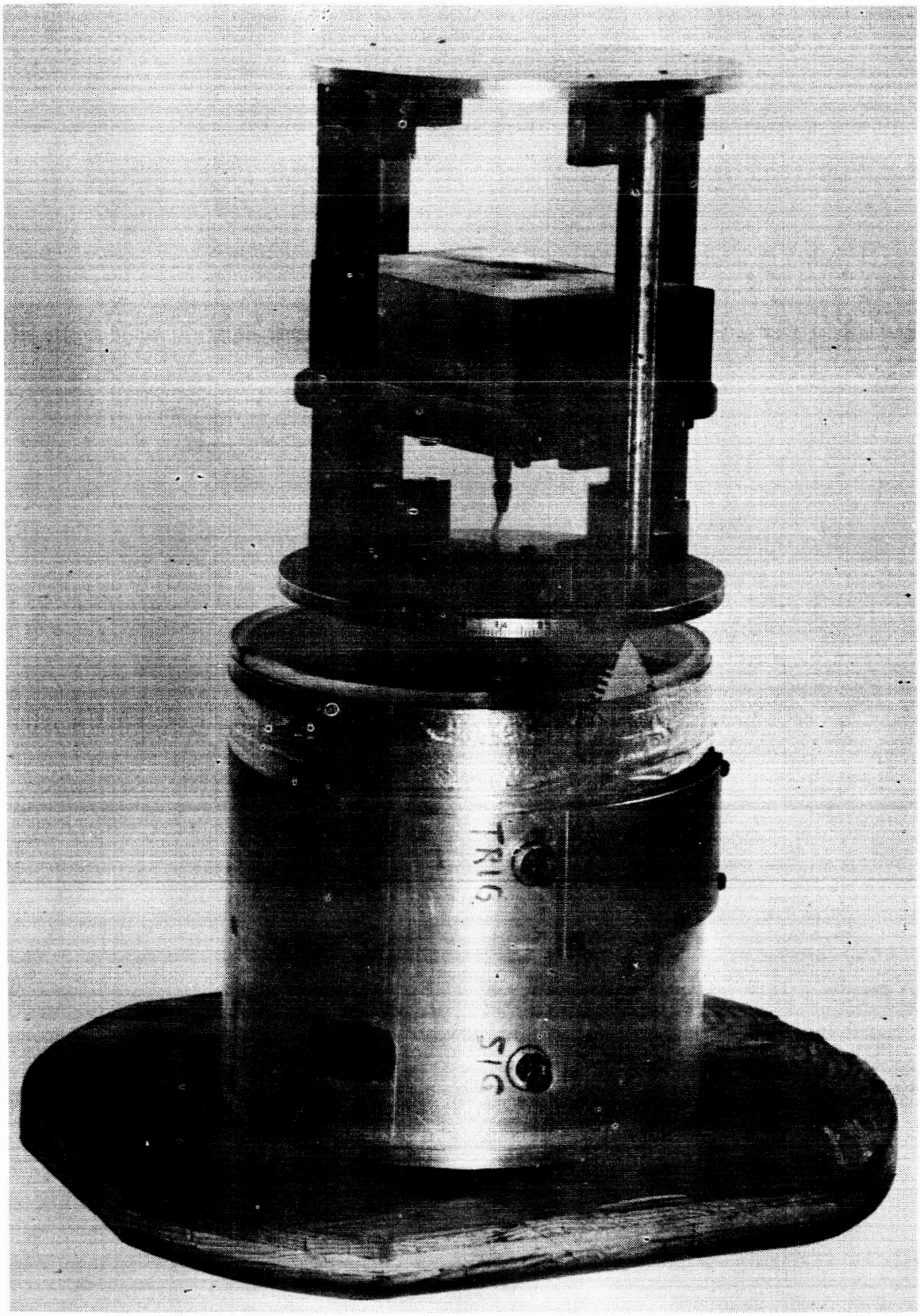

Figure 42

Rotating Ferrite Rod Antenna
for Testing the Transmitting Array Polarization

T.M. Band	Subcarrier Freq.	Information
E	70 kc	Output of Rocket Receiver
10	5.4 kc	AGC from Rocket Receiver
9	3.9 kc	Magnetic Aspect Sensor

The above channels are used with the type "A" payload. Two of the rocket flights contained an additional experiment in the payload, and was designated as a type "B" payload. The telemetry channels for the type "B" payload are as follows:

T.M. Band	Subcarrier Freq.	Information
E	70 kc	Output of Rocket Receiver
6	1.7 kc	Magnetic Aspect Sensor
4	0.96 kc	AGC from Rocket Receiver

The information from these telemetry channels are recorded by NASA on magnetic tapes and graphically on chart paper. The outputs from the discriminators of these subcarriers are also fed, by way of the telephone lines, to the CSL ground transmitting station where they are also recorded on the Minneapolis-Honeywell tape 8100 portable magnetic tape recorder. (The mobile launch flights were an exception to this as the Honeywell tape recorder was not taken on that expedition.) In addition, the channel E output is fed to the percent modulation detector to form the closed loop system described earlier.

The data lines carrying the 500 cps reference, extraordinary power level, and ordinary power level from the transmitting van to the telemetry stations are balanced to avoid excessive ac hum pickup. They are driven by transformers from the sending end as described below. A transformer termination is also used at the receiving end. An exception to this is at Goddard

Station, a telemetry station. This station is near enough to the transmitter van that balancing at one end is sufficient. Figures 43 and 44 are schematic diagrams of the terminations used at the Wallops Island Readout Station (main base) and on the mobile launch telemetry van, respectively. Potentiometer outputs are provided on the Wallops Island readout termination for ease in adjusting for the proper drive for the chart and tape recorders. This would be a desirable feature for the mobile launch termination also.

The data line junction box performs the following functions: (1) It provides, by means of transformers, a balanced-to-ground signal for the data lines which carry the 500 cps reference, extraordinary power level, and ordinary power level signals to the two telemetry stations. This is necessary in order to keep the ac hum pick-up level low on the long data lines. (2) It allows a means of connecting the balanced-to-ground data lines, that carry the rocket receiver output, the rocket receiver AGC, and magnetic aspect sensor data, to the inputs of the Honeywell differential input amplifiers. This data is transmitted from the telemetry stations to the transmitter van. (3) It furnishes all inter-connections necessary between data lines, transmitter servo-control circuits, and Honeywell tape recorder. (4) It provides a monitoring output that can sample any of the incoming or outgoing data. Figure 45 is a schematic diagram of the junction box.

G. Transmitting Station Van

The ground transmitting stations are housed in semi-trailer vans provided by NASA for this project. The vans are equipped with 16 tons of air conditioning which is adequate for keeping the inside temperature at a comfortable level with the two, one kilowatt transmitters and all

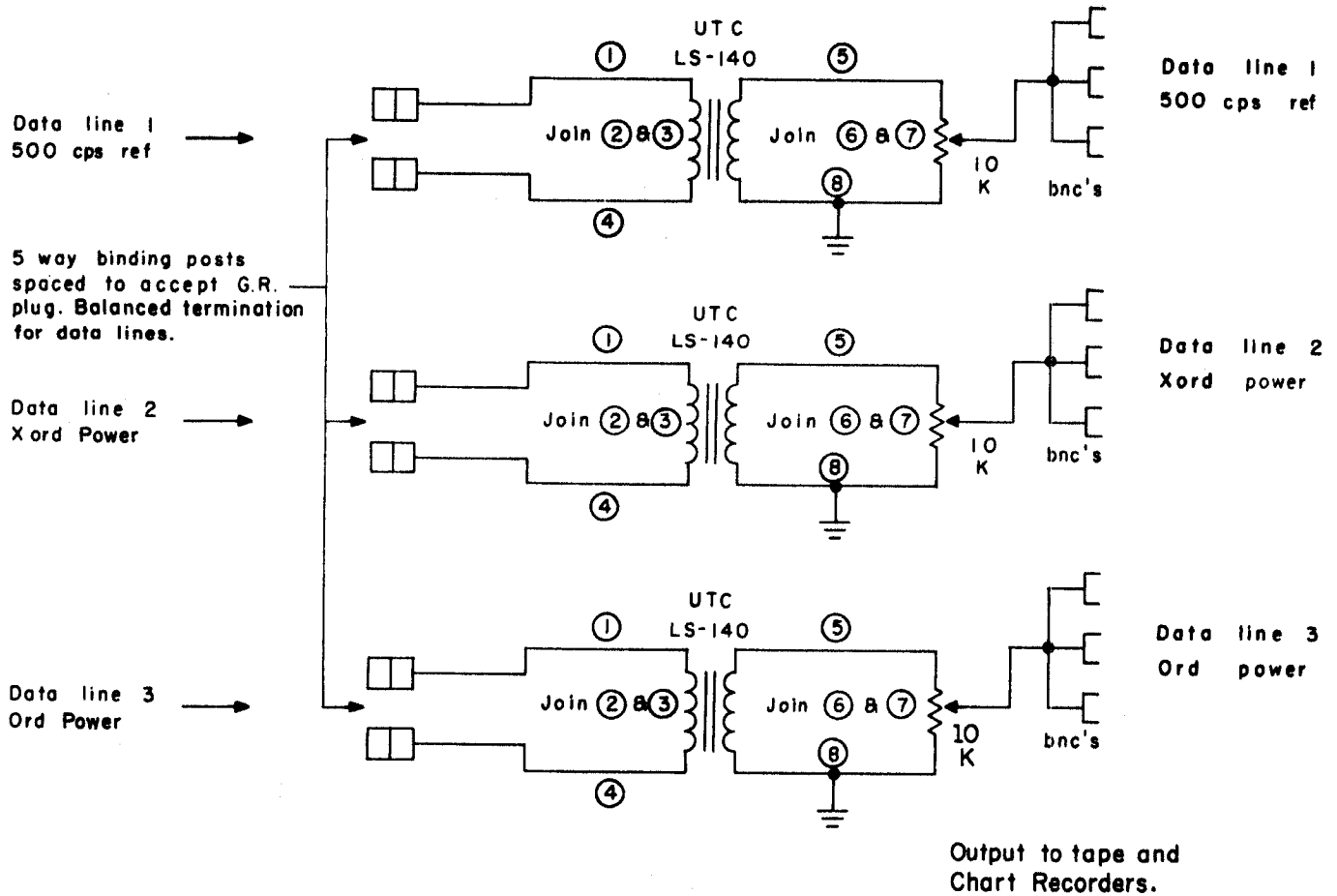

Figure 43
Circuit Diagram of Data Line Termination
Used at Wallops Island Readout Station

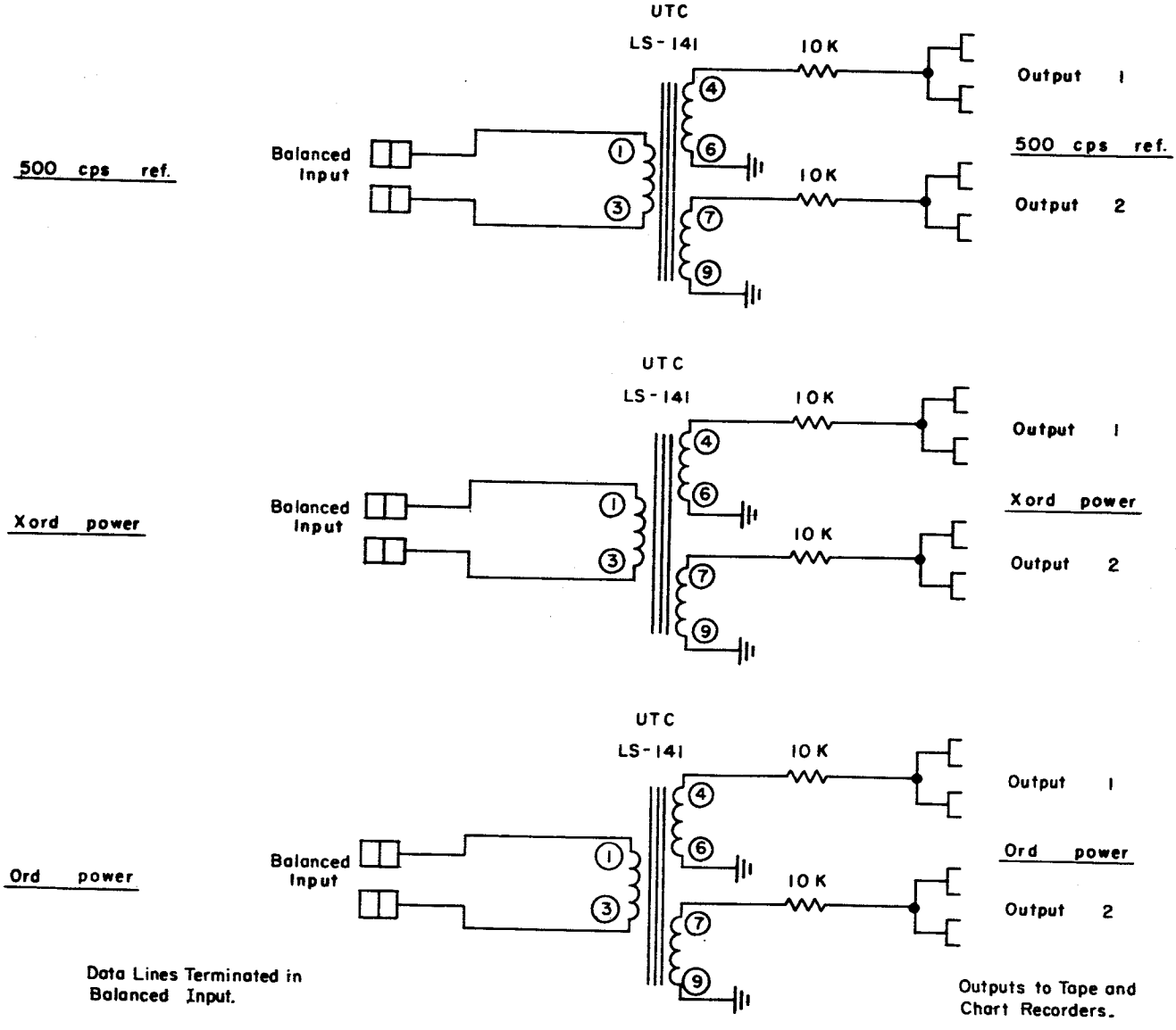

Figure 44

Circuit Diagram of Data Line Termination
Used on the Mobile Launch Telemetry Van

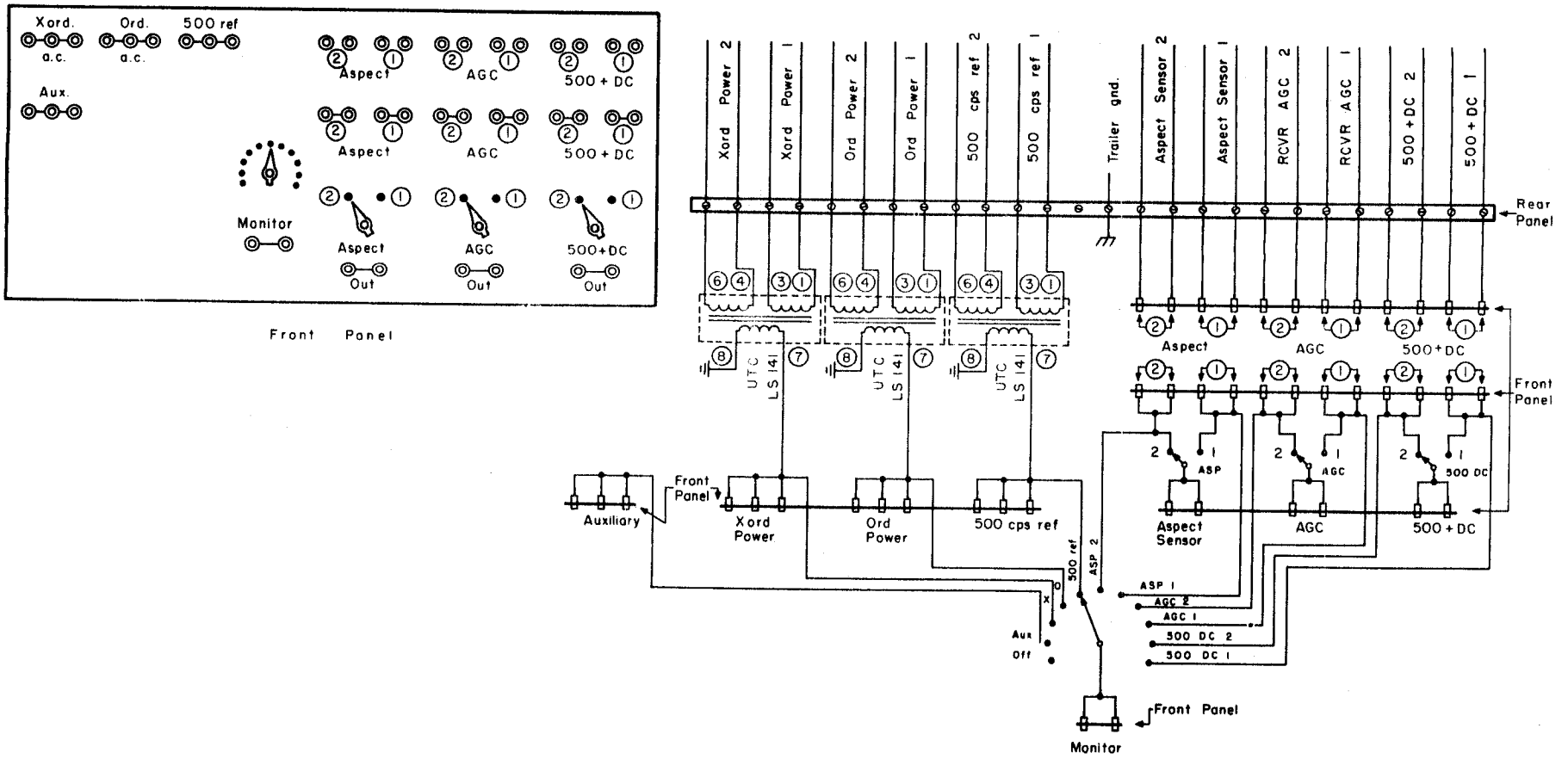

Figure 45
Data Line Junction Box Circuit Diagram

associated electronic equipment operating. Along one side of the vans, five standard 19 inch by 66 inch relay racks are shock mounted and contain all the electronic equipment. A separate shock mount is provided for the Minneapolis-Honeywell magnetic tape recorder in the forward end of the van. Figure 46 is a diagram of the relay racks indicating the components that are contained in each. In the remaining space inside the van, adequate storage cabinet and work bench area was installed. Antenna feed lines and other test leads entered the van through small ports near the transmitters.

The van, as received from NASA, was equipped to receive 220 volts, three phase power from the Wallops Island power system through a four conductor "Umbilical" cord. 220 volt outlets are provided inside the van through a three phase fuse and switch box. One circuit of 110 volt, single phase power is taken from each of the phases of the three phase power and distributed through appropriate fuses and switches to outlets along the side of the van.

Many of the electronic chassis associated with the transmitting equipment did not have self-contained dc power supplies, particularly those units designed and constructed at CSL. It was also necessary to provide ac power for filaments for these units. Three electronically regulated dc power supplies, with outputs adjusted for + 150 volts, + 300 volts, and - 150 volts, respectively, were mounted in one of the shock mounted relay racks in the van. A 500 volt-ampere line voltage regulator was also mounted near the power supplies and its output used to provide regulated voltage for the filament transformers.

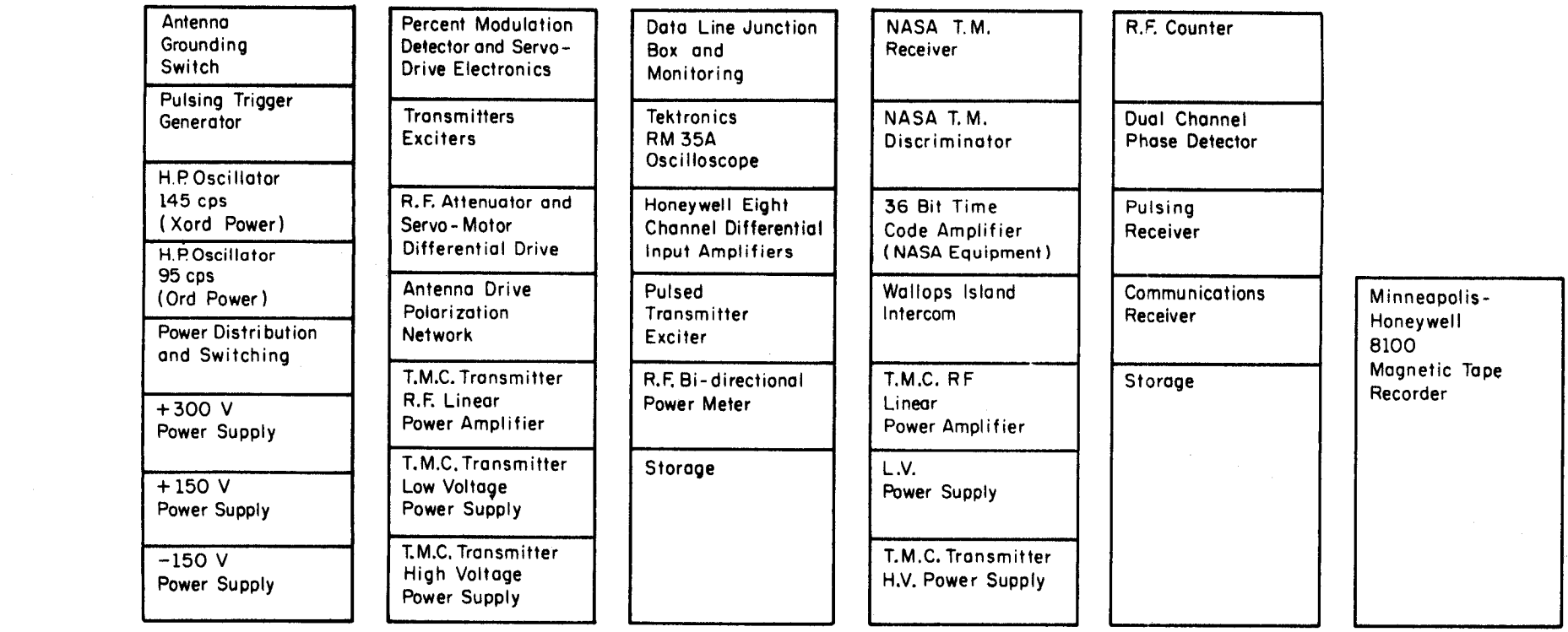

Figure 46
Transmitting Van Relay Rack Components Schematic

Figure 47 is a diagram of the power distribution and switching box which makes dc and ac power available to any chassis by way of Winchester type A-10 connectors. Switches on the front panel switch the power on or off simultaneously to all connectors. The dc power supplies and line voltage regulator obtain their ac power through the distribution box by way of the "unregulated ac" switch. Fig. 47 shows the power distribution connector voltages.

H. Auxilliary Test Units

To determine the center of the bandpass of the rocket receiver in its environment on the launch pad, a two frequency, tunable signal generator is used. This allows bracketing of the somewhat triangular shaped bandpass of the receiver by two signals equally down on the skirts. These frequencies are determined by a counter, and used to set the transmitter exciter frequencies.

A tunable signal generator is shown in Fig. 48. Two frequencies are generated at precisely 500 cps apart. Either frequency output can be selected by a switch. The tuning range of the two frequencies is approximately 10 kc, centered on the experiment frequency. A tuning fork oscillator at 500 cps is used to modulate a 454.5 kc crystal oscillator, producing frequencies of 454 and 455 kc. A narrow filter selects the 455 kc signal in one channel, and the 454.5 kc signal is used in the other channel. These two frequencies are heterodyned in separate mixers, against a common oscillator tunable from 2675 to 2685 kc. The outputs of the two mixers are signals tunable from approximately 2220 kc to 2230 kc, individually selectable at the output, and always 500 cps apart as specified by the tuning fork oscillator. The 2675 to 2685 kc, tunable heterodyning oscillator has a

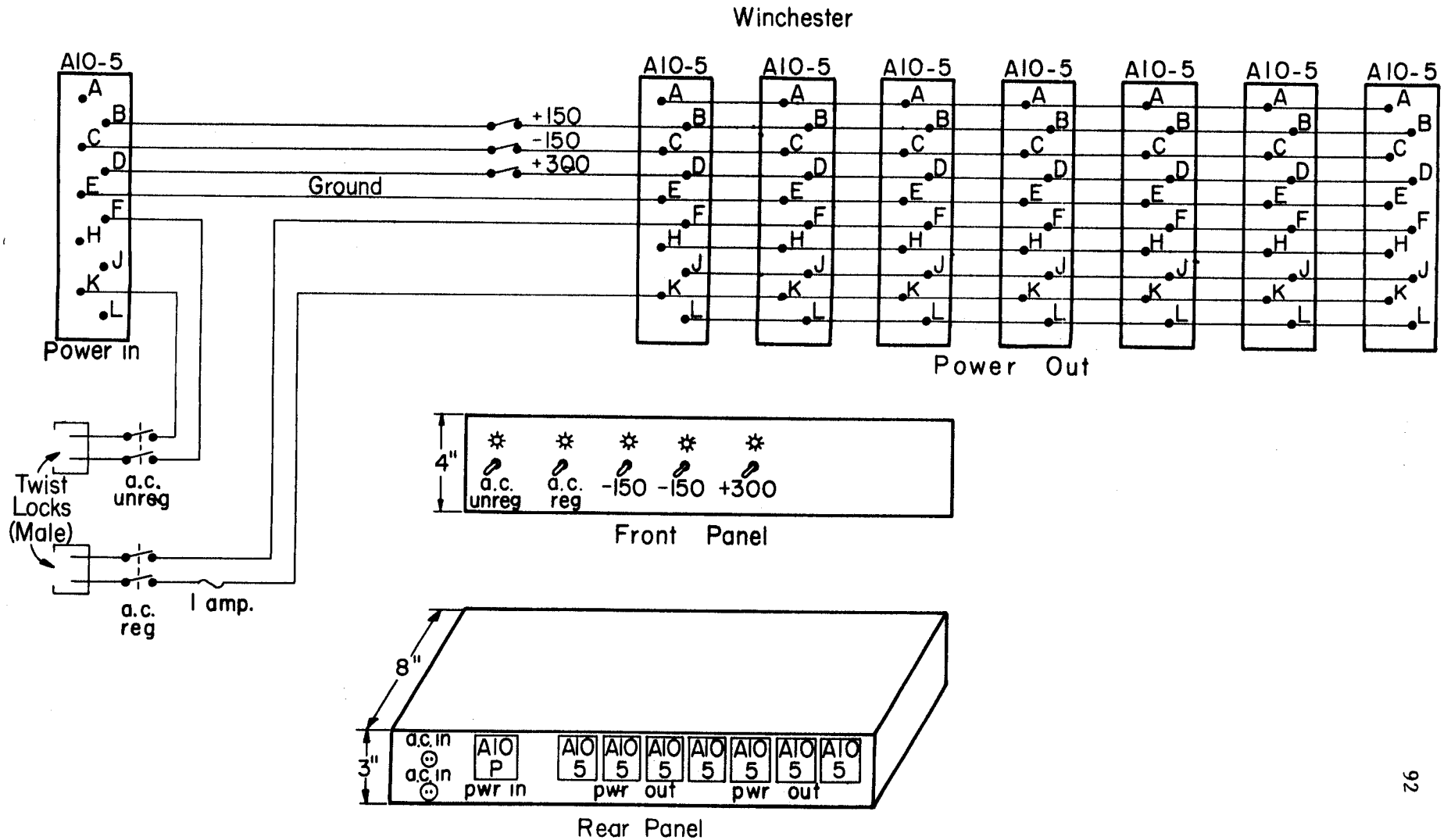

Figure 47
Power Distribution Network for Transmitting Van.

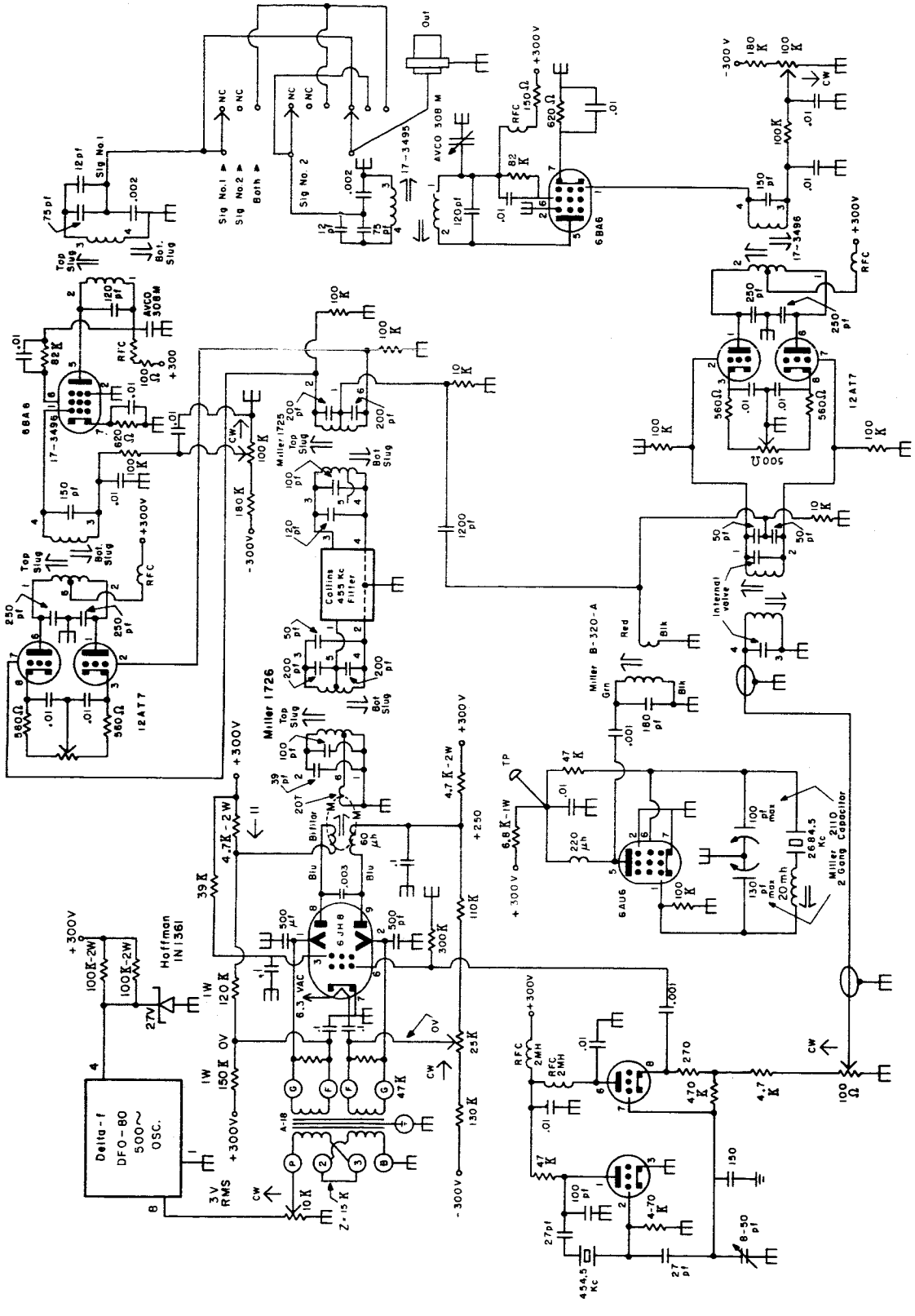

Figure 48
Circuit Diagram of Tunable Signal Generator for
Testing Rocket Receiver Bandpass Center.

stability of a few cycles per hour, and a large band-spread. A variable crystal oscillator is used to achieve this.

For the experiment on 3385 kc, a similar unit was built using a separate heterodyning oscillator.

The receiver shown in Fig. 49 was used in early experimental tests where the rocket pay-load was transported aboard a CSL station wagon, and suspended below a helicopter rented from the University of Illinois Institute of Aeronautics. The receiver uses seven type 8056, and one 7587 nuvistors in cascade connection to furnish four stages of gain at 3385 kc. Selectivity was furnished by a band-pass crystal filter using two half-lattice sections. Operation was from 24 volts, furnished by four lantern batteries in the dummy payload.

Power required was 370 ma at 24 volts for plates and heaters. Care was taken in the design of the AGC circuit, and an input-output characteristic shown in Fig. 50 was obtained. A 3900 ohm resistor is placed across the input grid circuit to avoid overload in tests where flights were made in close proximity to the transmitting array. This type design was discarded in favor of an all transistor purchased unit having lower power requirements, high sensitivity, and very high AGC loop gain.

The transistorized 3.385 mc receiver shown in Fig. 51 was constructed as a model to use in preliminary system tests of the transmitting antenna array. It was installed in a dummy rocket housing and suspended on a swivel below a helicopter. The housing also contained a 231 mc FM telemetry transmitter and was fitted with pin-wheel vanes to rotate the housing. A low receiver gain was used to avoid saturation during close-in, low altitude helicopter operation.

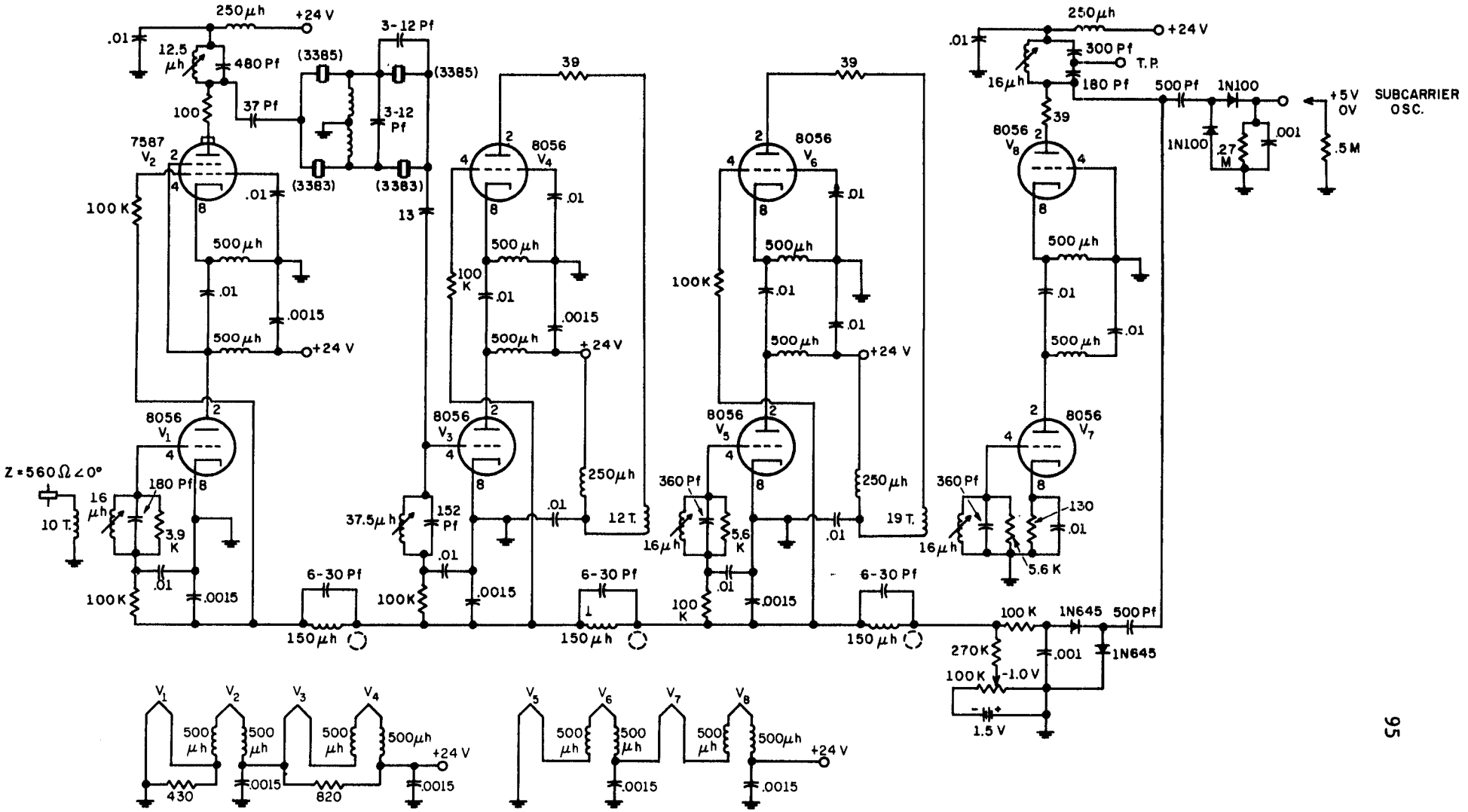

Figure 49
Circuit Diagram of Early Dummy Payload Receiver

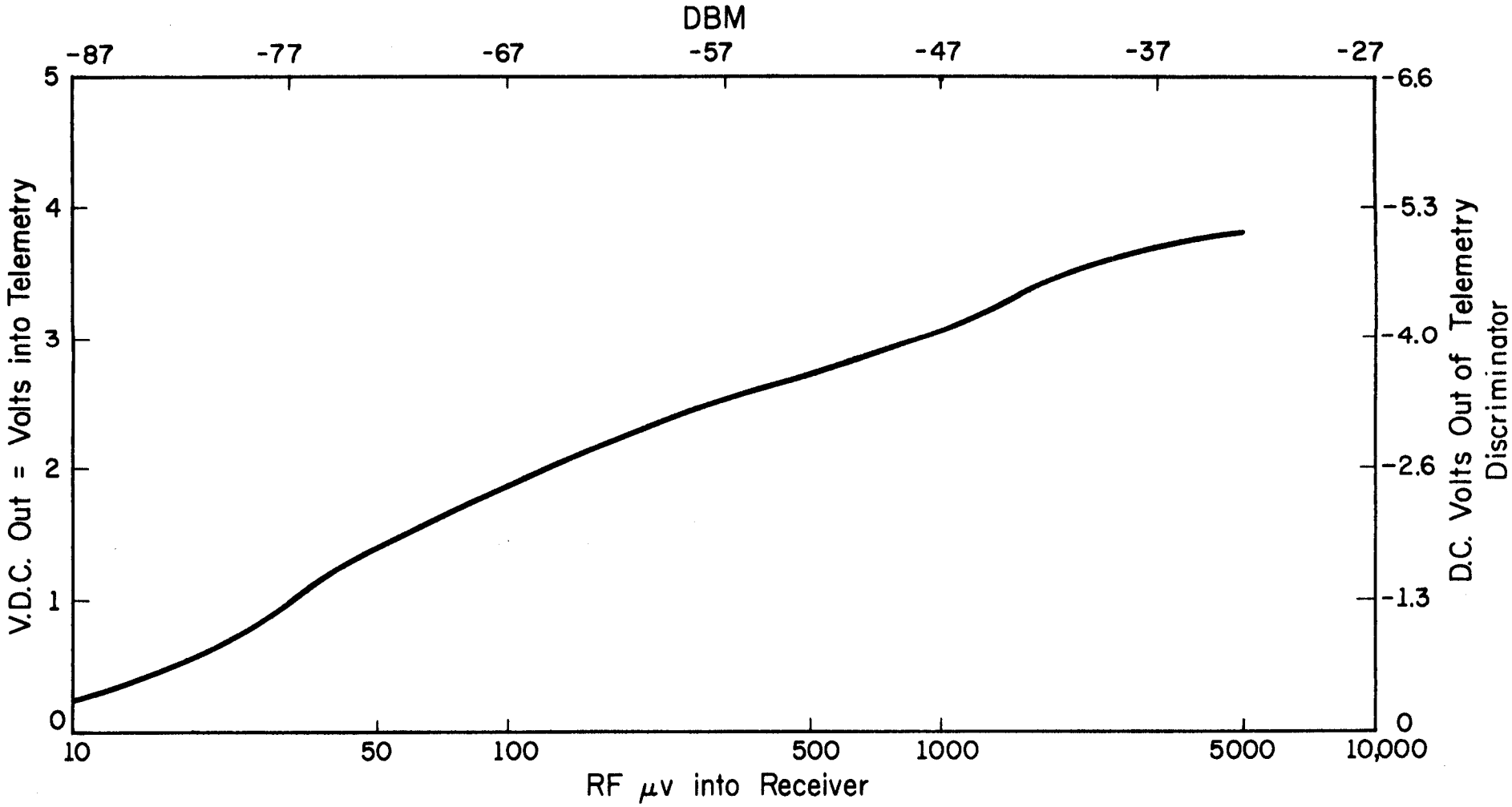

Figure 50
Input-Output Characteristics of the
Early Dummy Payload Receiver

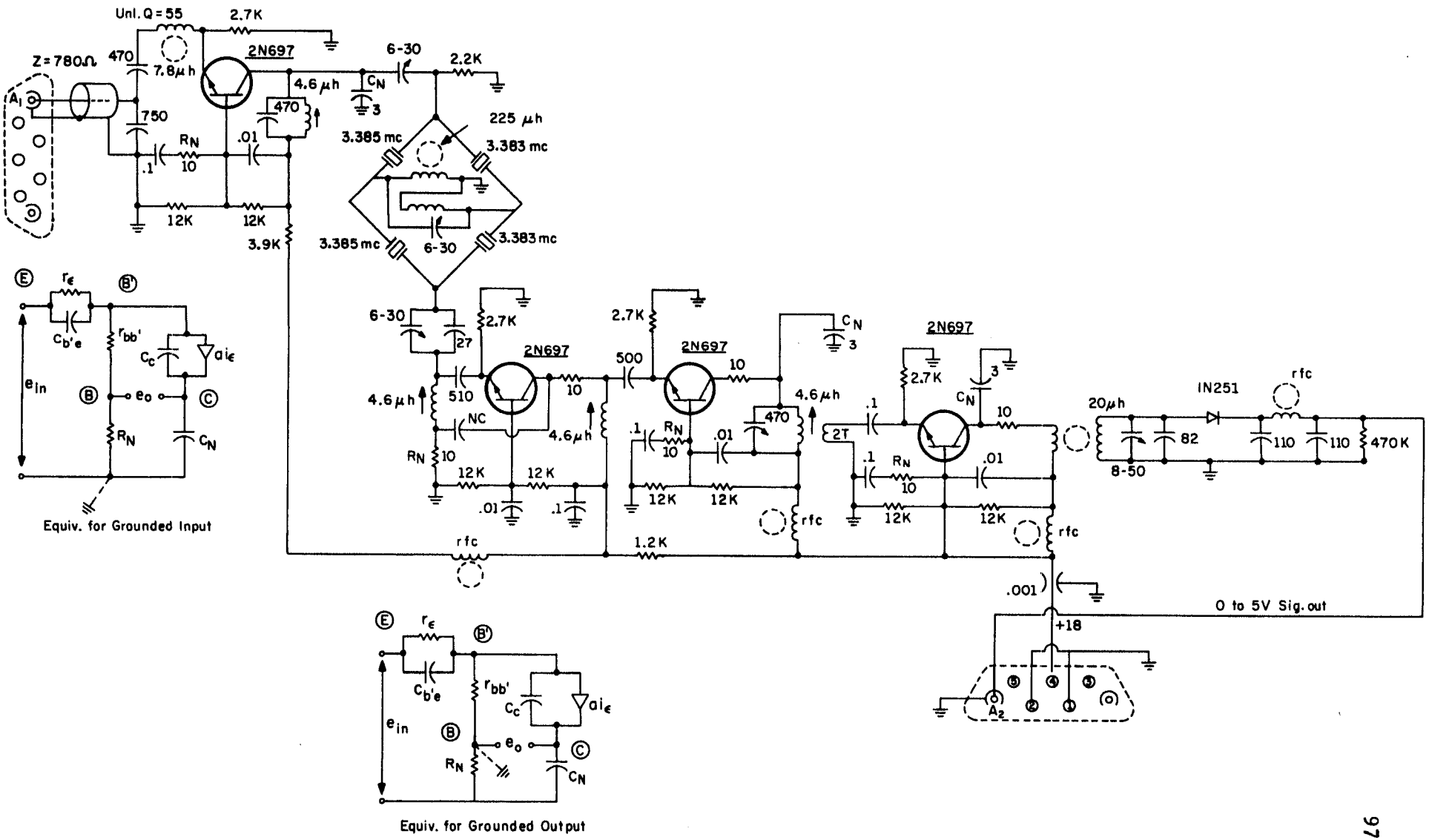

Figure 51
Circuit Diagram of Transistorized Dummy Payload Receiver

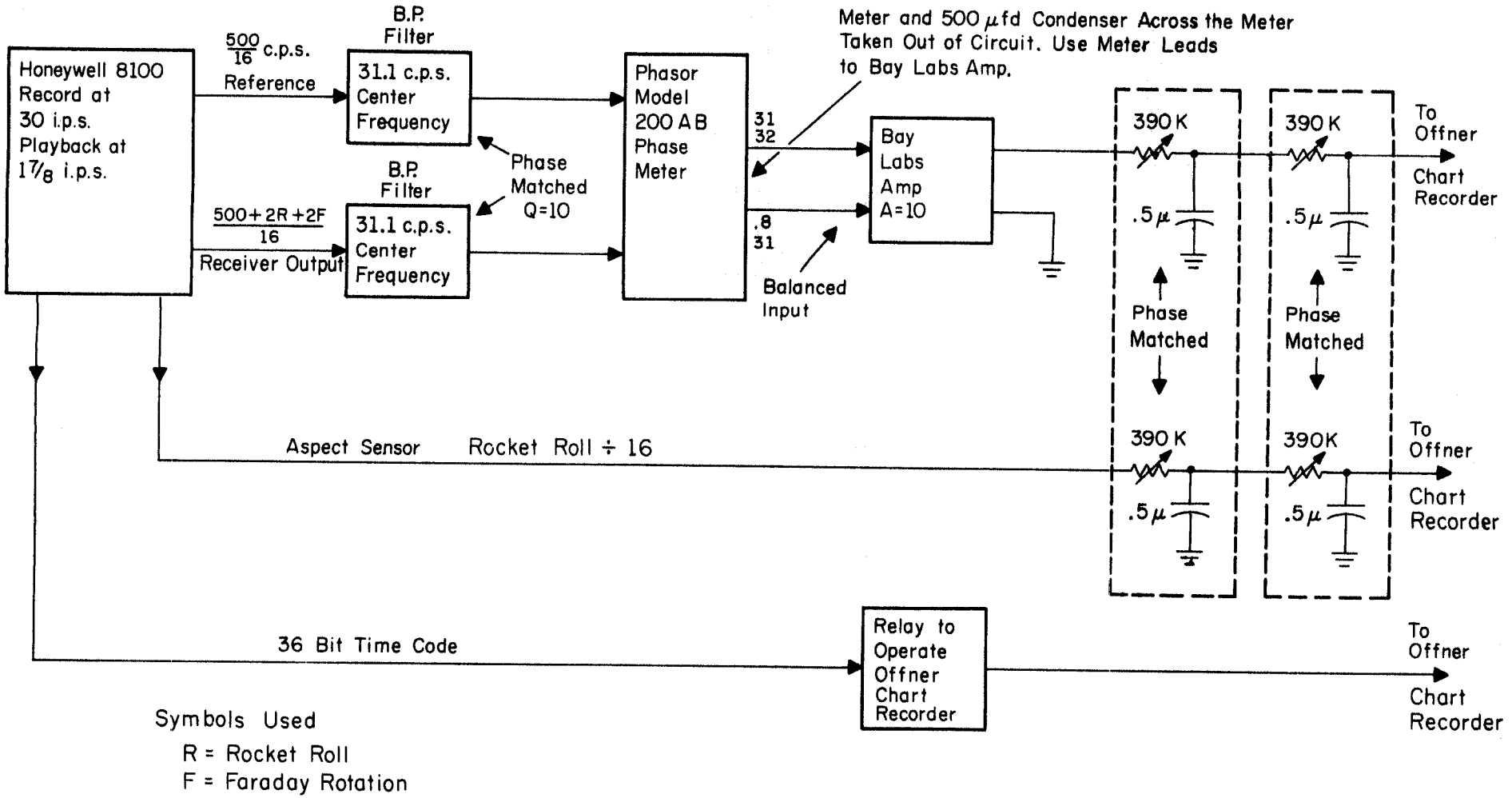

Figure 52
Block Diagram of High Resolution
Faraday Rotation Data Extraction System

reference frequency, the magnetic aspect sensor output, the rocket receiver output, and a 36 bit time code. The rocket receiver output contains a 500 cps component, corresponding to the frequency of the transmitted wave, a component corresponding to two times the rocket roll frequency ($\pm 2f_s$), and a component equal to twice the Faraday rotation frequency ($\pm 2f_F$). The frequency of the receiver output waveform is the sum of these three frequencies.

After filtering by phase matched, band pass filters, the reference and the receiver output channels are fed to the inputs of a phase meter built by Phasor and designated as model 200 AB. This instrument is essentially a two channel amplifier, the outputs of which drive a Hall effect (or similar) multiplier. The output is taken from the multiplier with the instruments' meter and integration circuits disconnected. Two output components appear at frequencies equal to the sum and difference of the two input signals. After amplification, the output is passed through a low pass filter, to remove the sum frequency component, to one channel of a three channel pen recorder. The information contained on this channel is thus $(500 \pm 2f_s \pm 2f_F) - 500$ or $(\pm 2f_s \pm 2f_F)$. The magnetic aspect sensor output from the magnetic tape, $\pm f_s$, is fed by way of a low pass filter to a second channel of the pen recorder. This low pass filter is very carefully phase matched to the filter on the multiplier output, so that phase errors due to filtering are kept to a minimum. On a third channel of the pen recorder, the 36 bit time code is recorded. The paper speed used is 125 mm/sec. so that one cycle of the rocket roll, for example, occupies 10 to 11 inches of chart length. The periods of the waveforms on the chart are accurately determined and compared. In the absence of any Faraday rotation, the periods of the two waveforms differ by a factor of two. Any deviation from this factor of two represents Faraday rotation. The time code is taken from the third channel of the recorder and a plot made of Faraday rotation vs time.

Another method for extracting Faraday rotation data is by the use of a dual phase detector, shown in Fig. 53. Each channel uses a Hall effect multiplier[6] to give the instantaneous product of the ground phase reference and the rocket receiver voltages. The sum frequency is discarded, while the difference frequency is recorded on the telemetry paper and tape records. A comparison of this record to twice the rocket roll frequency yields Faraday rotation data more quickly, since fewer cycles (of lower frequencies) have to be counted and compared.

Duplicate channels are provided in the unit. The 500 cps transmitter phase reference is split into two channels, one channel is phase shifted 90°, and difference frequencies taken in two separate mixers. Two outputs of frequency ($\pm 2f_s \pm 2f_F$) and differing by 90° in phase are produced. The phase sequence of these two channels indicates that the rocket receiver telemetered signal is higher or lower in frequency than the ground transmitter phase reference. This information establishes that transmitted circular polarization, rocket roll, and Faraday rotation are in the proper circular rotation sense.

This unit is used at either the CSL van or at the telemetry station. The two required input signals are available at both locations. Two additional data lines are required to the TM station recorders if the dual phase detector is installed at the transmitter van.

The highest performance chassis is shown in Fig. 53, although useful output has been obtained from earlier models shown in Figs. 54 and 55, which require no ac line power.

---

[6]Used were Type HM-3031, Manufactured by F. W. Bell, Columbus, Ohio

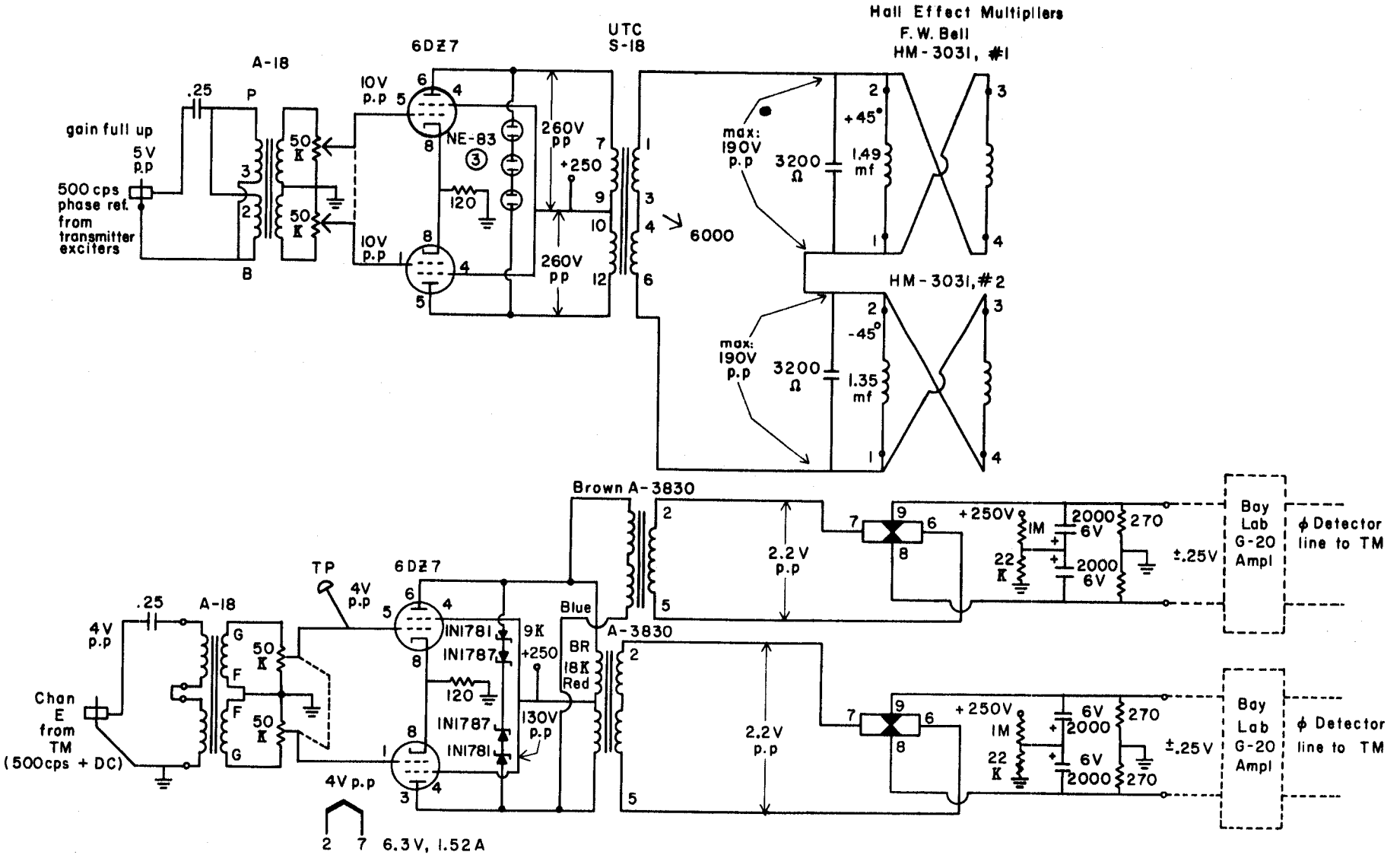

Figure 53
Circuit Diagram of System to Extract Low Resolution Faraday Rotation

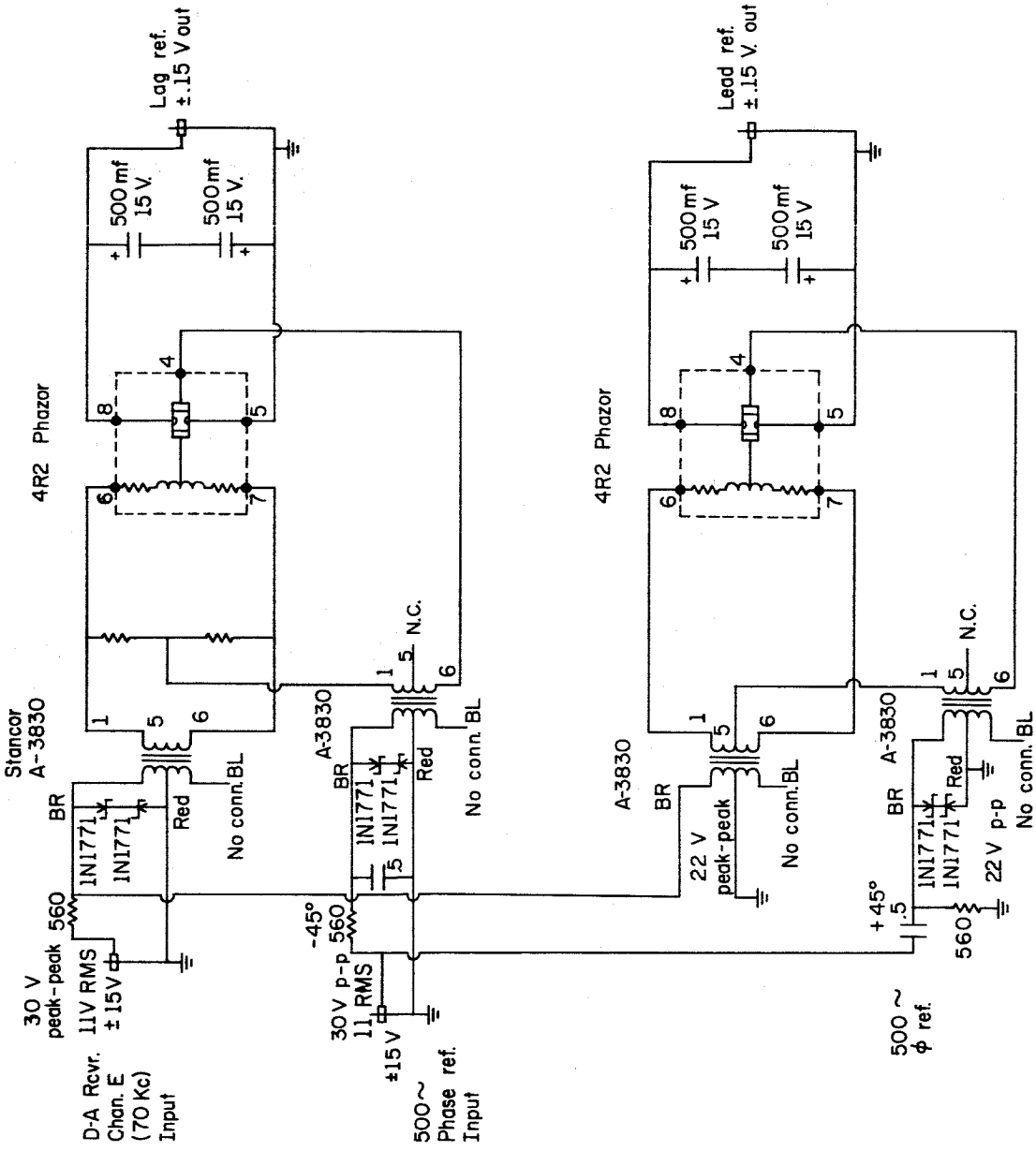

Figure 54
Circuit Diagram of Earlier System Used to Extract Low Resolution Faraday Rotation.

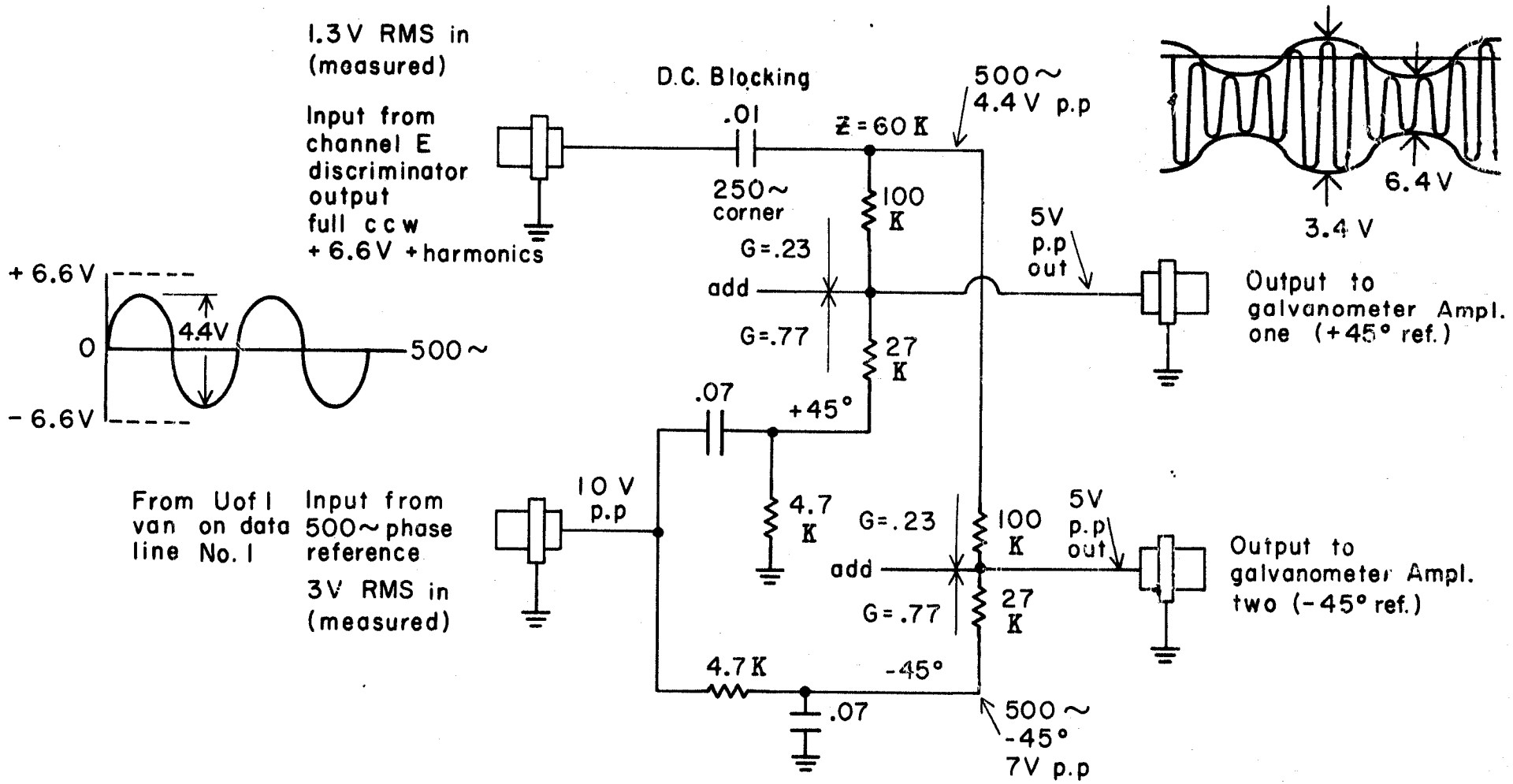

Figure 55
Circuit Diagram of Earlier System
Used to Extract Low Resolution Faraday Rotation

IV. Operational Procedure

A. Transmitters and Drivers

The tuning and operational procedure of the linear amplifiers are completely covered in the "Technical Manual for Linear Power Amplifier Model PAL-1K(A)" issued by the manufacturer, Technical Materiel Corporation. These units were tested by CSL for output amplitude stability over long periods of operation to our satisfaction. CSL has made one small modification in the transmitter's power supply time delay relay for the following reason. If, during an experiment, primary power were momentarily lost, the time delay relay would open and require three minutes to close again, thereby causing a complete experimental failure. Therefore, a pushbutton switch was added at a readily accessible place in the rear of the transmitter low-voltage power supply for over-riding the time delay relay. This should be used for emergencies only. The modification was made by putting a shorting type switch across terminals 5 and 7 of K701 time delay relay in Fig. 8-2 of the technical manual (see Fig. 20).

A constant source of trouble in the linear amplifiers was the frequent failure of the final power amplifier V203 (PL-172). This has been attributed to long periods of inactive use, thereby leading to tube outgassing, and to excessive vibration during van transportation. It is recommended that these tubes be removed from the transmitters during transportation, and that a simple circuit be built in which the tubes can be operated under standby conditions during long intervals between experiments.

The crystal-controlled transmitter drivers can be adjusted by front panel control. Either of two pre-tuned frequencies is selected by a ganged switch on the front panel of the driver chassis, by a toggle switch

on each of the two rf attenuator input boxes and by a switch on the polarization chassis. Tuning is accomplished by first adjusting the inductance in the plate of the 6AU6 (Fig. 13) and the capacitor in the plate circuit of the 6BQ5, observing the rf output meter for a maximum indication. The remaining adjustments are covered in Section IV E, Polarization Tests.

B. Transmitting Antennas

In order to produce pure polarizations, the antenna array should be kept as symmetric as possible with a square geometry. This avoids mutual coupling of the perpendicular pairs of elements. Neglect of this can lead to large power from one transmitter being fed back down the transmission line to the other transmitter where plate modulation could occur and cause non-linearity of the power amplifier. Symmetric location of feed-lines also aids in keeping the near-radiated field in correspondence with the far field, so that a radiated field sampling device such as the rotating dipole at the ground center of the array gives a valid indication of polarization purity. Care should also be used in connecting feed-lines together from parallel elements to insure in-phase operation.

The driving point impedance of the array was found to increase by approximately 20% when moved from central Illinois to Wallops Island, Virginia, beach. This was believed due to the location of the effective ground plane or the dielectric constant of the ground. Also, in many locations some form of lightning protection is necessary. Satisfactory results have been had from both an antenna grounding switch and from an effective lightning arrester.[7]

---

[7] Used were Hy-Gain Type LA-1, manufactured by Hy-Gain Antenna Products Corp., Lincoln, Nebraska.

C. Servo

This section describes the procedure for adjusting the servo system, the percent modulation, and the telemetry offset voltage. The pre-flight servo tests are also outlined.

The servo amplifier is adjusted with maximum possible feedback, and thereby lowest gain, since there is enough gain in the system with the servo preamplifier. The feedback control potentiometer R26 is located on top of the amplifier chassis (Fig. 29). The relative phase between the servo motor control and reference signals must be adjusted to 90°. This is done by observing these signals on a dual trace or Lissajou scope while varying the carrier phase shift control on mixer MBX-02. As a check, the servo motor output torque should be a maximum, and can be qualitatively checked by noting the torque on the extraordinary rf attenuator manual control knob. The 180° phase relationship between the error signal and tachometer output signal is obtained by shunting the tachometer output winding by 0.1 μf. The phase relationship can also be checked by an oscilloscope.

The servo gain and feedback controls and percent modulation setting are checked and adjusted under actual experimental conditions, usually during the horizontal check. After the polarization and telemetry tests and adjustments have been completed, usually several days before the experiment, one of the transmitters is turned on, the servo motor is turned off, and the rf X and O attenuators are set 10 db apart. This produces an rf signal modulated by a 500 cps signal at 31.7%. The servo chassis is switched to receive the telemetered rocket receiver signal and the percent modulation potentiometer R4 of Fig. 26 is adjusted to produce a zero error signal displayed by the panel meter. The servo motor is then turned on and

should be "locked in;" i.e., the X rf attenuator should track the O rf attenuator while the latter is moved by its manual control knob. With about one volt peak to peak ac component of the 500 cps modulated rocket receiver output signal the gain adjust (input no. 2 of Fig. 28) of servo mixer MBX-02 should be adjusted until the desired torque is obtained on the X attenuator manual control knob. The tachometer feedback gain adjust (input no. 1) should be adjusted so that when the X attenuator manual control knob is given an angular displacement and released, it moves to its equilibrium position with just one overshoot.

The proper dc offset voltage is then applied to the input servo signal by adjusting the channel E telemetry discriminator upper and lower band edges to +4V and -4V, respectively, by means of dual pots preceding the balanced dc amplifiers on the van's telemetry control panel. At some interval during the vertical and horizontal payload checks a receiver calibration signal is requested and, with the servo motor alternately turned off and on, potentiometer R1 on the servo chassis (Fig. 26) is adjusted until the servo error voltage is zero and the X manual control knob stops rotating. The servo is now set so that the X attenuator setting will not drift during the two automatic receiver calibration intervals of the rocket flight.

The servo components can be tested at any time by switching the servo chassis to "Sweep Mode" and applying a function generator signal of about 0.6 cps through the linear potentiometer mounted on the X rf attenuator shaft and to the "function generator" input (see block diagram in Fig. 31). For example, by applying a square or sine wave signal the X rf attenuator will move in and out at the applied frequency and at a displacement proportional to the applied voltage.

D. Rocket Antenna and Receiver

The following procedure is based on the IRE Standards on Radio Receivers: Method of Testing Receivers Employing Ferrite Core Loop Antennas, 1955.[8]

The standard loop produces a magnetic field which varies as the cube root of distance. The equivalent electric radiation field which would accompany a magnetic field of this magnitude is given by the following formula:

$$E = \frac{30\pi\, n_1\, a_1^2}{x^3}\, I_1$$

Where

E = equivalent electric field intensity in volts per meter at the receiving loop antenna

n_1 = number of turns of radiating loop

a_1 = radius of radiating loop in meters

x = distance in meters between center of radiating loop and the axis of the ferrite rod receiving antenna

I_1 = current in the radiating loop in amperes

Using the General Radio type 1000-P10 test loop at a distance of 49 inches as shown in Fig, 56 this equation reduces to $E = 1/165\ E_m$ where E_m is the measured rf voltage at the loop input.

---

[8] Proceedings of the IRE September 1955, Vol. 43, No. 9, pp. 1086-1088

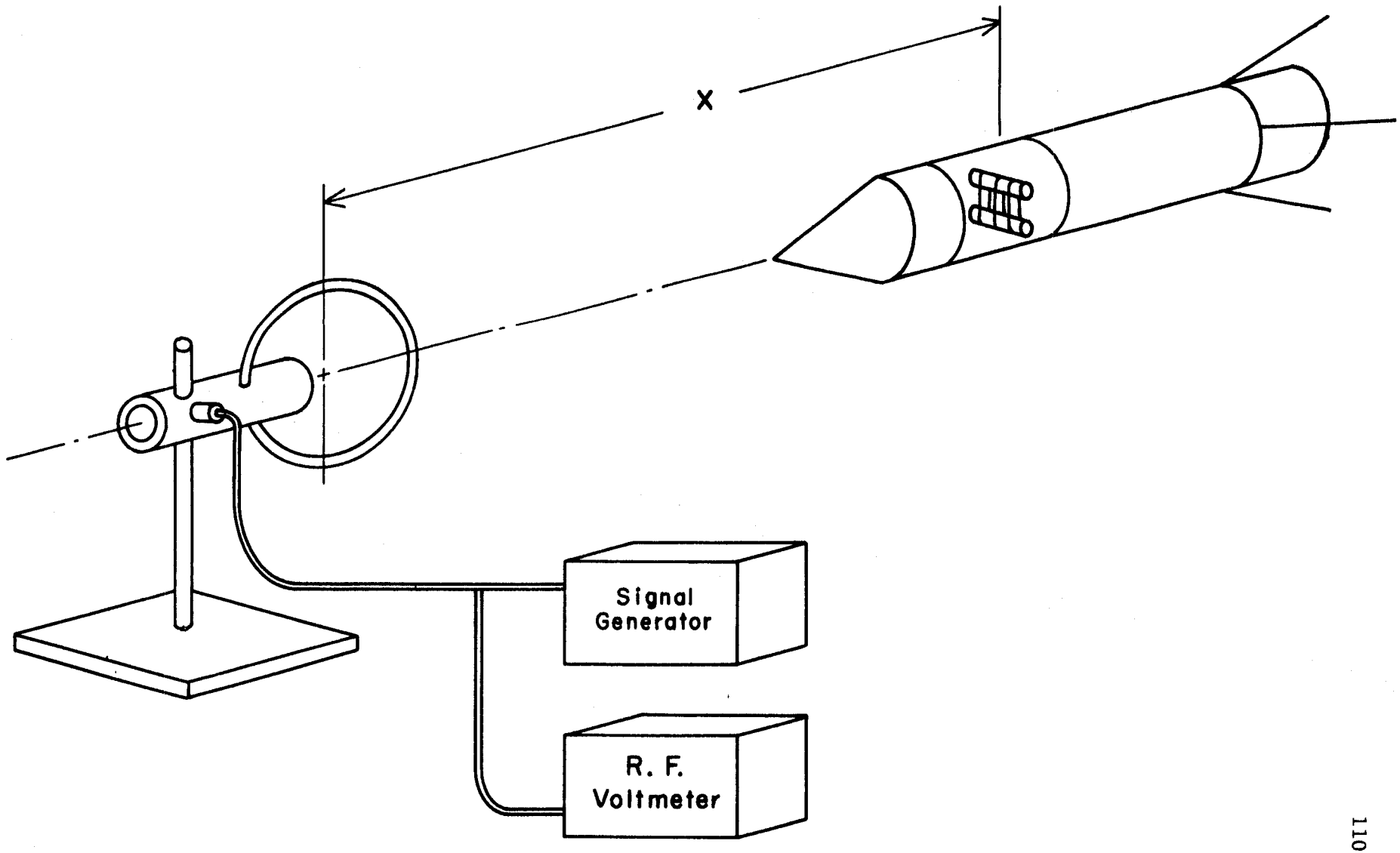

Figure 56
Schematic of System for Establishing a Given Electric Field at a Point

The payload receivers are calibrated in order to provide an indication of the change in field strength with altitude or the total attenuation during the rocket flight.

Both the detector dc output and the AGC output are calibrated as a function of receiver input. This calibration can be made in the laboratory under controlled conditions. A typical setup is shown in the block diagram of Fig. 57. The tunable crystal oscillator is used as a signal source because of its frequency stability. Commercial signal generators that were available in the laboratory drifted too much in frequency for accurate measurements with the narrow receiver bandwidth. The Hewlett-Packard 411A rf voltmeter establishes a reference signal level. This with the 50 ohm step attenuators gives a calibrated dbm input. Since the receiver input is designed to work into the antenna impedance of 300 to 700 ohms, a matching network is required to match the 50 ohm source.

An accurate dc meter is used to measure the output. At very low signal levels the output is rather noisy with the resulting loss in accuracy of the meter readings.

These measurements establish the characteristic detector output vs dbm input and AGC output vs dbm curves as shown in Figs. 33 and 58. Receiver tests were also made with signals simulating those used in the system. This test set is shown in the block diagram of Fig. 59. Two frequencies separated by 500 cps were generated by the tunable crystal controlled signal generator described in section III H. The relative amplitudes of these two signals were adjusted to give the effect of different per cent modulations. The per cent modulation is set by observing the modulation envelope of the combined signals on an oscilloscope. A 500 cps bandpass filter identical to that used in the servo system control filter

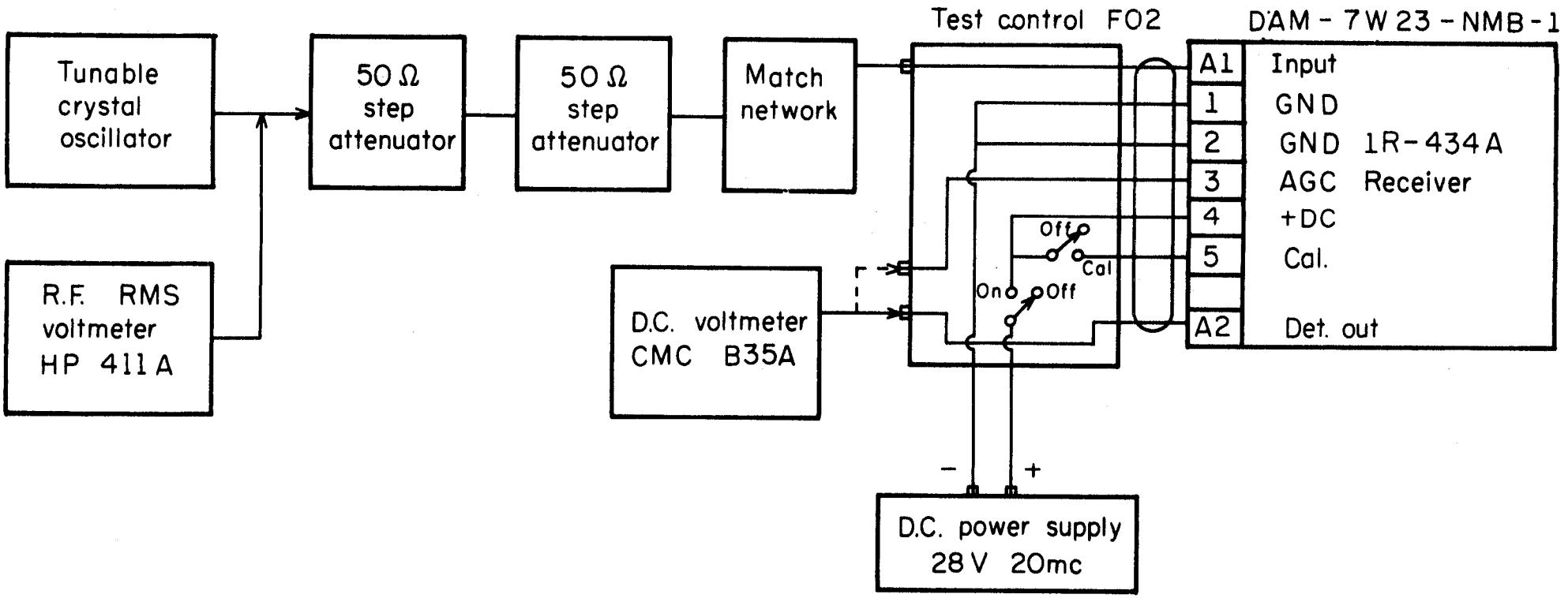

Figure 57
Block Diagram of System for Testing
the Rocket Receiver AGC and Detector

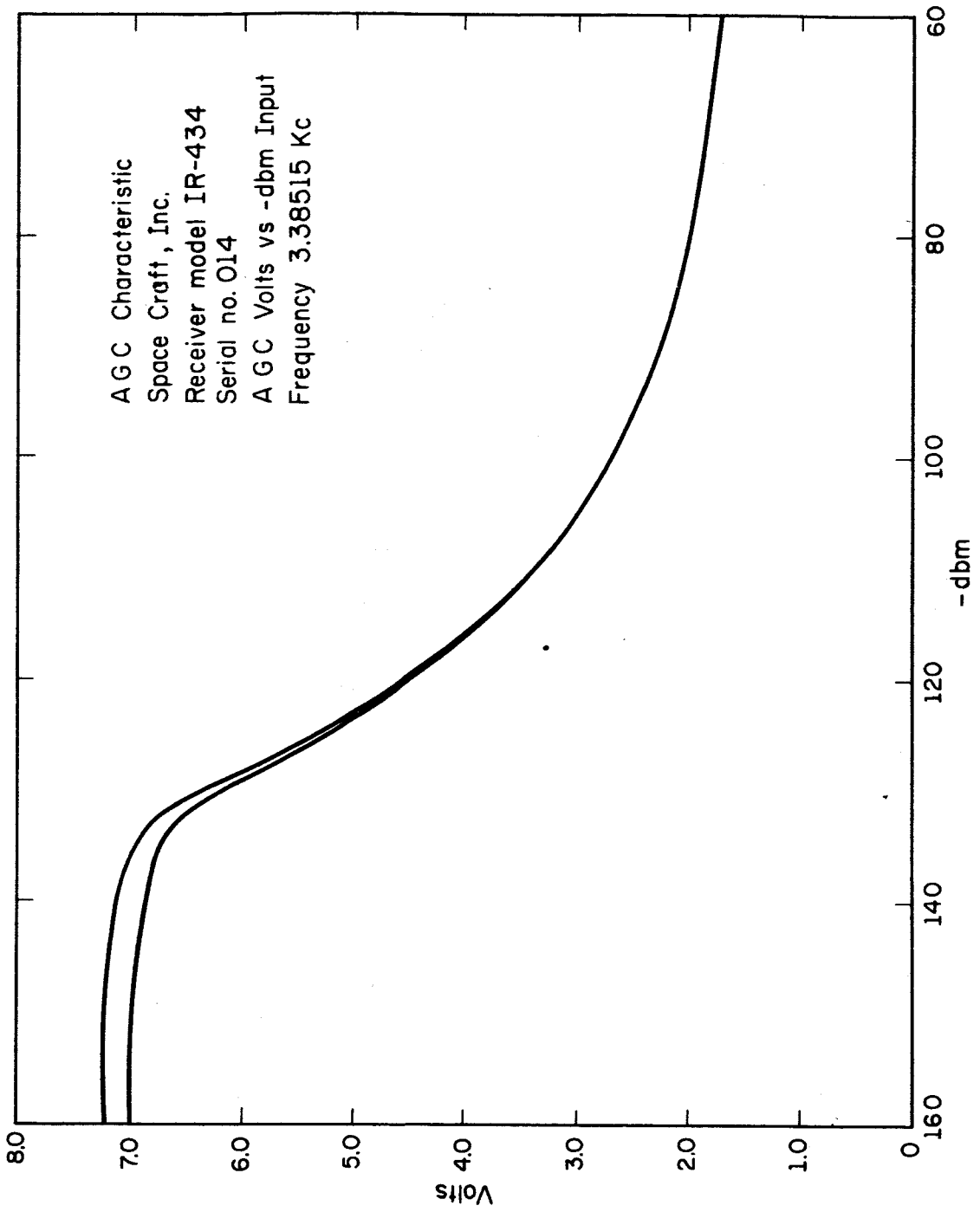

Figure 58
Rocket Receiver AGC Output vs dbm Input Characteristics

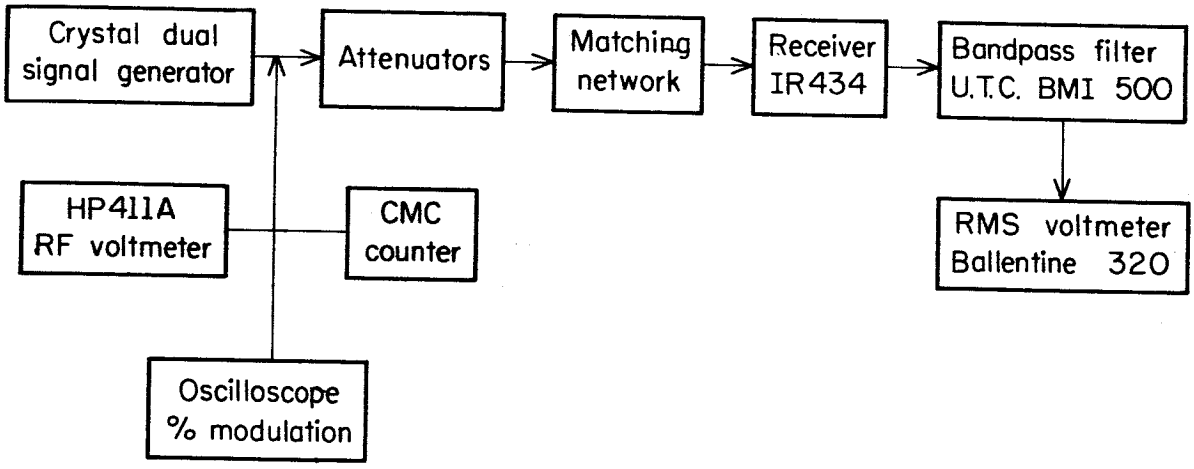

Figure 59

Block Diagram of System for Measuring
the Rocket Receiver Percent Modulation Characteristics

of Fig. 26 gives the 500 cps component of the receiver output which is measured by the rms voltmeter. A typical family of curves is shown in Fig. 60.

It is desired to have an overall calibration of the receiver and antenna, along with the AGC dividing network and the telemetry system, installed in the payload. One system that was used is shown in Fig. 56, where a General Radio type 1000-P10 test loop at a measured distance from the ferrite rod antenna is used to supply a known field strength. With the umbilical cable and the control console connected, the detector dc output and the AGC after the dividing network can be measured at several field strengths above the local noise level. By curve matching the dbm scales on the receiver curves can now be converted to equivalent field strength at the rocket. In other words, the gain of the payload antenna is measured.

While these measurements are being made the telemetry can be energized and the complete system calibration checked from the rf field strength at the payload to the telemetry chart recorders.

Similar rf checks are made during the countdown with the rocket on the launcher in both the horizontal and the vertical position. In this case a larger, more efficient shielded loop is used mainly because of its convenience. It is easily set up about 20 feet from the launcher, and if time does not allow its removal before launch it is not seriously damaged by the rocket blast. It can also be moved from launcher to launcher if a series of shots are scheduled. No attempt has been made to obtain absolute field strength calibration on the launcher. The effect of the launcher on the antenna is unknown and the exact distance and orientation of the loop and payload are difficult to control. However, by changing the field

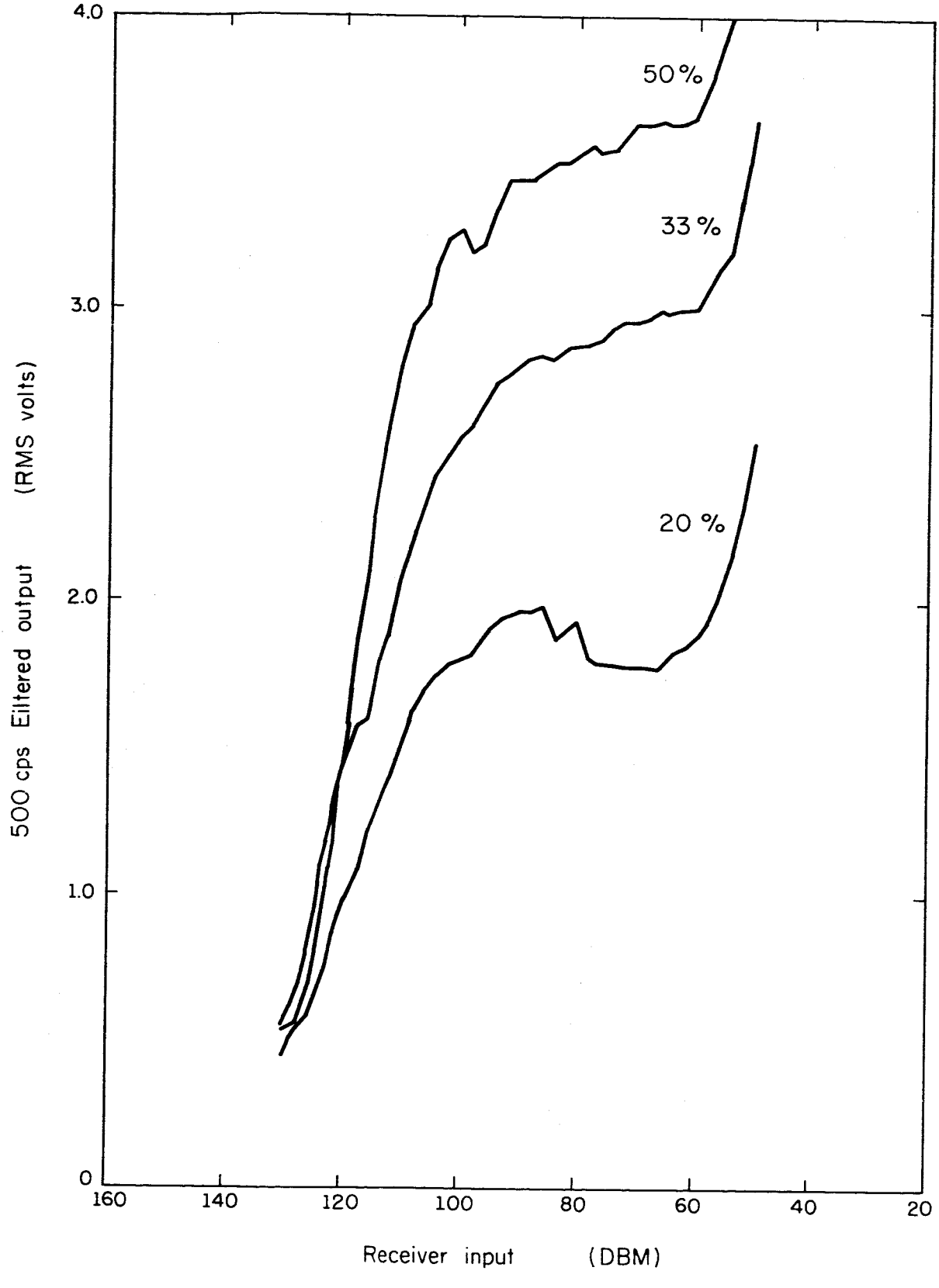

Figure 60

Rocket Receiver Percent Modulation Characteristics

strength in known increments the relative power level is calibrated through the complete system. The ground station transmitters should be off during these checks.

An additional incremental calibration of the complete system can be obtained during the ordinary and extraordinary potentiometer calibration by allowing the ground station transmitters to radiate.

E. Polarization Tests

After the antennas have been properly matched, the array checked and dressed for symmetry, and the transmitters tuned and warmed up for at least a half hour, the polarization tests can be performed. These can be divided into the rotating magnetic loop, the pulse reflection, and the helicopter tests. The first, unfortunately, can only give the near field antenna radiation patterns. With the second scheme, only the extraordinary wave can be adjusted. The third scheme gives the far field patterns but is complex and costly and consequently has only been used twice. These methods will be described in detail.

The first procedure is to set the X and O crystal oscillator drivers 500 cps apart by feeding the beat frequency output (500 cps reference) to a counter and adjusting the tuning capacitors shunting the crystals (Fig. 13). With the rotating dipole placed in the center of the array and one exciter set to -10 db, the other exciter is completely attenuated by its rf attenuator. One transmitter is turned on and the peak-to-peak amplitude of the 100 per cent modulated signal from the rotating dipole is noted. The two attenuator settings are then reversed and the peak-to-peak amplitude is adjusted to the noted value by the "rf output" control on the exciter chassis. The two exciters thus produce the same radiated power. At no time, however, must the full exciter outputs cause any transmitter overload relays

to be thrown. If this happens, both exciter outputs are reduced to fulfill the equal X and O radiated power requirements and to avoid any transmitter overloads. Methods for obtaining circular polarizations will first be described.

In the rotating loop method of setting the circular polarization both transmitters are turned on and the corresponding modulation envelope of the rotating dipole signal observed. In all our experiments the X-wave has always been chosen at the higher frequency but this is not a required condition. Transmitting only the X-mode, the X phase shifter and attenuator are alternately varied until the modulation has been reduced to a minimum. Usually, the modulation will appear as a first and second harmonic of the rotating loop frequency — the second harmonic corresponding to the ellipticity of the near-field antenna array radiation pattern and the first harmonic to the vertical radiation to which the rotating loop is also sensitive. Consequently, the X-mode attenuator and phase shifter is adjusted until all traces of the second harmonic component has been removed. The sense of rotation is now checked by counting the carrier signal frequency of the spinning loop, which is shifted by the loop spin frequency. In the northern hemisphere, the X-mode is counterclockwise looking up or cw rotation looking down. Hence, if the spinning loop rotates at 10 cps in a cw rotation looking down on it, the 500 cps carrier signal should be shifted downwards to 480 cps. The rotating loop can be spun in both directions so that the appropriate carrier frequency shifts in both directions should be checked.

After doing the same for the O-mode, which is cw looking up in the northern hemisphere, the X-mode polarization should be rechecked and readjusted if necessary. Then, the two exciter outputs of both modes should be reset to produce the same radiated power as described previously. The

foregoing procedure produces circular polarizations only for the near field and is reliable only for highly symmetrical antenna arrays that are far removed from unsymmetrically situated induced radiators.

The pulse reflection method is always used to check the X-mode polarization and is based on the fact that, during the day, this mode is strongly absorbed in the D region. Therefore, the X-mode phase shift and attenuator settings are adjusted for minimum reflected signal. A circuit for generating rf pulses of variable width and repetition frequency, described in section III E, is used in place of the crystal exciters and rf attenuators. A switch diverts the rf pulses into either the X or O mode channels. With a prf of about 5 to 30 pps, a reflection of the extraordinary pulsed wave can be observed in the daytime at a time delay of about 0.8 msec. The reflected signal is picked up by a loop antenna which is positioned to minimize the effect of the transmitted pulse. The loop antenna is placed as far from the transmitting antenna array as conveniently possible. The signal is then fed to a special wide band receiver which is described in section III E. If the X and O polarizations have been previously obtained with the rotating magnetic loop, a small adjustment of the X-mode phase shifter usually suffices to null the X-mode reflection completely into the receiver noise. With this method the O-mode has to be tuned for a maximum return, but the adjustments are too insensitive for practical use.

If a helicopter is available it allows the most accurate polarization adjustments to be made because the radiation patterns are made in the far field. A loop antenna, receiver, telemetry discriminator and transmitter must be mounted in a structure in which the loop antenna can be rotated. In CSL's tests a battery operated dummy payload containing all the above components was suspended from the helicopter in a harness with fins attached

so that aerodynamic forces rotated the dummy payload at about 2 rps. With this setup, the O and X polarizations were set and found to differ from the phase shifter settings obtained by the ground rotating loop method by the same amounts. However, for the X mode, settings obtained by the pulse reflection method were the same as those obtained by helicopter.

With these results in mind, the usual procedure for polarization adjustments when a helicopter is not available is to first obtain X and O polarizations by means of the rotating loop and record the attenuator and phase shift settings. Next, using the pulse reflection method during the daytime for the X mode, readjust the phase shifter only for complete null of the reflected wave and note the change in phase shifter setting. Apply this same change to the O phase shifter.

Another method for adjusting the polarization (for the cool-headed and quick-witted only) is possible for the first 30 seconds of a rocket flight, during which all the characteristics of the helicopter method are present and differential absorption and Faraday rotation have not yet begun. This method was never used.

For equatorial experiments, where linear polarizations must be used, the identical procedures are followed, except that the output of the rotating loop must exhibit 100 per cent modulation at twice the spin rate of the loop. The plane of polarization for either the X or O mode is rotated by adjusting the appropriate attenuator. A simple way to check this is to first adjust both phase and attenuation for maximum percent modulation with the loop rotating. Then, stop the loop and position it so that its plane is normal to the desired plane of polarization and adjust the phase for a minimum signal amplitude out of the loop. Repeat these two steps until further readjustment is unnecessary.

F. System

A crew of two technicians are usually sent to the rocket launch site about one week before launch to hook up the main power to the van, set up the antenna array, measure the antenna impedances, arrange to have the telemetry lines hooked up, and fire up and check out the transmitters. A few days before launch, one or two more people arrive to check out the telemetry lines, set the proper signal levels with telemetry personnel, adjust the X and O polarizations, check out the servo loop, test the rocket antenna and receiver, and perform a closed loop servo test using the rocket antenna and receiver to be launched. As much testing and adjusting is done before the horizontal and vertical rocket payload checks as possible. During the early stages of tests the antenna array must be made as symmetric as possible by stretching the dipoles tautly and tying down and arranging all feed lines and power cables to lie in straight runs, symmetrically placed with respect to the array. The importance of this has been observed both on land and aboard ship, since the greatest reliance has been placed on the near-field measurements for polarization adjustment.

During the night before launch all the equipment except the servo motor is left turned on. The transmitters are operated in the standby mode. One person sleeps in the van during this period and makes periodic checks on the equipment.

Four hours before launch the operating crew arrives and performs the following:

1) 500 cps difference frequency between the X and O exciters rechecked;

2) Transmitter tuning and exciter drive amplitudes rechecked. The maximum exciter drives must not cause any transmitter overload relay to be thrown;
3) Purity of X and O polarizations with the rotating loop rechecked and readjusted. Directions of rotation of circularly polarized waves rechecked;
4) Minimization of the X-wave reflection with the pulsing method readjusted;
5) Servo switched to "sweep mode" and tracking of X and O manual control knobs observed;
6) Telemetry line voltages rechecked, with special care given to channel E band edge amplitudes and offset voltage adjustment;
7) Check power supply voltages and currents;
8) Check for spurious radiation at frequency to be used;
9) Van's tape recorder input signals rechecked.

During the horizontal payload check, the following calibrations are performed and results recorded on the telemetry tapes:

1) The rocket receiver is calibrated, as described in section IV D.
2) X and O rf attenuators are calibrated by stepping each attenuator 5 or 10 db throughout its range and recording the audio output voltages on the proper telemetry channels and transmitting van tape recorder.
3) The rocket receiver is switched to calibration and the offset voltage at the servo chassis is rechecked or readjusted for zero error signal, as described in section IV C.

4) A closed loop servo test using the actual rocket payload is performed as described in section IV C.

5) After the rocket payload power has been turned off and the transistor receiver protected, the exciters are turned to maximum drive (zero db) for the X wave and -10 db for the O mode, and the transmitters are checked for overload.

These tests are all repeated for the vertical payload check, which usually occurs one hour before launch. In the intervening period the polarizations are rechecked and readjusted. One man is given the task of watching the transmitters during a rocket experiment to quickly reset any tripped overload relays should they occur, including the special over-riding switch installed by CSL on the back of the transmitters.

G. Data Lines

Six pairs of balanced data lines are used between the transmitter van and each of the telemetry stations. The following is a list of these data lines, their number designations, and the information carried by each.

Data Line	Information Carried
1	500 cps reference from transmitter van to TM station.
2	Extraordinary power level from transmitter van to TM station
3	Ordinary power level from transmitter van to TM station.
4	Magnetic aspect sensor from TM station to transmitter van.
5	Differential absorption receiver output from TM station to transmitter van.

Lines 1, 2, and 3 are driven through transformers at the transmitter van and so are kept balanced at the sending end, as described in section III F. This is necessary in order to balance out ac pickup voltages. These lines are terminated in a balanced transformer winding at the Wallops Island Readout Station (main base), this telemetry station being approximately eleven miles from the transmitter van. It was found unnecessary to terminate lines 1, 2, and 3 with balanced transformers at the Goddard Station A Telemetry Station, this station being less than one mile from the transmitter van. These lines, therefore, are terminated at the inputs of the tape and chart recorders of Station A and operate with a sufficiently low noise level.

Data lines 4, 5, and 6 are driven from the outputs of appropriate discriminators at the TM stations. They are terminated at the inputs of balanced differential input amplifiers[9] at the transmitter van. The lines are therefore balanced at the transmitter van end only. However, through careful adjustment of the differential amplifier common mode reject, noise levels are kept to a low level.

Data lines 1, 2, 3, 4, and 6 are twisted pair, unshielded lines. Data lines 5 are coax lines that run from the TM stations to a small block house located about 800 yards from the transmitter van. The remaining distance is spanned by twisted pair lines. It is necessary to use these special coax lines, as data line 5 carries the differential absorption receiver output which contains a dc component that could possibly cause damage to the loading coils contained in the other lines.

---

[9]Minneapolis-Honeywell Model 790714 Eight-Channel Differential-Amplifier.

Generally speaking, the data lines are allowed to remain intact between rocket launches. However, one is occasionally borrowed by other experimenters and all tend to change their characteristics with time so that it is necessary to check the performance of all the lines before each shot. The procedure for this check is as follows: The lines are connected in the same manner as for the launch (described above). The ac signals on data lines 1, 2, and 3 are turned to zero and a noise measurement made at the telemetry station end by means of a sensitive, calibrated oscilloscope. The discriminators that drive data lines 4, 5, and 6 are put on band center calibrate so that they have zero dc and zero signal volts output and a noise measurement is made at the transmitter van end. These lines are terminated in the differential input amplifier, whose "common mode adjusts" are at this time set for minimum noise. The "balance" controls of these amplifiers are also carefully adjusted and their gain set at 1/2, prior to the common mode adjustment. Following the noise measurement, the lines are driven with their normal signal levels and voltage measurements made on both ends of the line to determine their transmission characteristics. Following are tables of typical noise values and signal levels representing measurements made for the November, 1964, launches.

Data Lines to Goddard Station A

Data Line	Function	P-P Noise at Station A	P-P Noise at Van	Signal Level at Station A	Signal Level at Van
1	500 cps ref.	50 mV		(Rec) 8.0V P-P	(Send) 9.0V P-P
2	extraordinary power	25 mV		(Rec) 9.6V P-P	(Send) 10.0V P-P
3	ordinary power	30 mV		(Rec) 9.3V P-P	(Send) 10.0V P-P
4	magnetic aspect sensor		10 mV	(Send) 16.0V P-P	(Rec)[10] 8.0V P-P
5	D.A. receiver output		13 mV	(Send) 16.0V P-P	(Rec)[10] 5.0V P-P
6	D.A. receiver AGC		20 mV	(Send) 16.0V P-P	(Rec)[10] 8.0V P-P

These noise levels are acceptable, although data 1 has higher noise than is desirable. On subsequent launches, noise levels have been measured to be less than 10 millivolts. Dc transmission checks were also made which showed no attenuation.

---

10 With differential gain set at 1/2, and volume control on data line 5 (at input of differential amplifier) set at maximum.

Data Lines to Wallops Readout (Main Base)

Data Line	Function	P-P Noise at Main Base	P-P Noise at Van	Signal Level at Main Base	Signal Level at Van
1	500 cps ref.	40 mV		(Rec) 8.6V P-P	(Send) 9.0V P-P
2	extraordinary power	45 mV		(Rec) 10.0V P-P	(Send) 10.0V P-P
3	ordinary power	45 mV		(Rec) 10.0V P-P	(Send) 10.0V P-P
4	magnetic aspect sensor		35 mV[11]		
5	D.A. receiver output		20 mV[11]	(Send) 20.0V P-P	(Rec) 8.0V P-P[11]
6	D.A. receiver AGC		28 mV[11]		

As in the case of the Station A data lines, these noise levels are acceptable, although it is desirable to have them at the 10 millivolt level or below. These lines also displayed little or no dc attenuation. For the check out, and for the actual rocket shot, discriminators driving lines 4, 5, and 6 are set on the 10-20 volt output range with the verniers maximum clockwise. Any adjustment of the level of the voltage on data line 5 is made by means of the control on the input of the differential amplifier at the transmitter van. The polarities of the discriminator band edge voltages are opposite for the two telemetry stations (equipment manufactured by different companies) so that it is necessary to compensate for this difference on data

---

11 With differential amplifier gain set at 1/2 and volume control data line 5 (at input of differential amplifier) set at maximum.

lines 5 by connecting the lines oppositely to the differential amplifiers for the two lines concerned. Polarity is critical on this line as this is the differential absorption receiver output line that closes the servo loop for the system. Polarity is not critical on the other lines. Signal levels in the above tables are the levels used for the rocket shots.

FIGURE CAPTIONS

Distribution list as of March 1, 1965

1 Dr. Chalmers Sherwin
Deputy Director (Research & Technology)
DD&RE Rm 3E1060
The Pentagon
Washington, D. C. 20301

1 Dr. Edward M. Reilley
Asst. Director (Research)
Ofc. of Defense Res & Eng
Department of Defense
Washington, D. C. 20301

1 Dr. James A. Ward
Office of Deputy Director (Research and Information Rm 3D1037)
Department of Defense
The Pentagon
Washington, D. C. 20301

1 Director
Advanced Research Projects Agency
Department of Defense
Washington, D. C. 20301

1 Mr. Charles Yost, Director
for Materials Sciences
Advanced Research Projects Agency
Department of Defense
Washington, D. C. 20301

20 Defense Documentation Center
Cameron Station, Bldg. 5
Alexandria, Virginia 22314
Attn: TISIA

1 Director
National Security Agency
Fort George G. Meade, Maryland 20755
Attn: Librarian C-332

1 Chief of Research and Development
Headquarters, Department of the Army
Washington, D. C. 20310
Attn: Physical Sciences Division P & E

1 Chief of Research and Development
Headquarters, Department of the Army
Washington, D. C. 20310
Attn: Mr. L. H. Geiger, Rm 3A442

1 Research Plans Office
U. S. Army Research Office
3045 Columbia Pike
Arlington, Virginia 22204

1 Commanding General
U. S. Army Materiel Command
Attn: AMCRD-RS-PE-E
Washington, D. C. 20315

1 Commanding General
U. S. Army Strategic Communications Command
Washington, D. C. 20315

1 Commanding Officer
U. S. Army Materials Research Agency
Watertown Arsenal
Watertown, Massachusetts 02172

1 Commanding Officer
U. S. Army Ballistics Research Lab.
Aberdeen Proving Ground
Aberdeen, Maryland 21005
Attn: J. Richards

1 Commanding Officer
U. S. Army Ballistics Research Lab.
Aberdeen Proving Ground
Aberdeen, Maryland 21005
Attn: Keats A. Pullen, Jr.

1 Commanding Officer
U. S. Army Ballistics Research Lab.
Aberdeen Proving Ground
Aberdeen, Maryland 21005
Attn: George C. Francis, Computing Lab.

1 Commandant
U. S. Army Air Defense School
P. O. Box 9390
Fort Bliss, Texas 79916
Attn: Missile Sciences Div., C&S Dept.

1 Commanding General
U. S. Army Missile Command
Redstone Arsenal, Alabama 35809
Attn: Technical Library

1 Commanding General
Frankford Arsenal
Philadelphia, Pa. 19137
Attn: SMUFA-1310 (Dr. Sidney Ross)

1 Commanding General
Frankford Arsenal
Philadelphia, Pa. 19137
Attn: SMUFA-1300

1 U. S. Army Munitions Command
Picatinney Arsenal
Dover, New Jersey 07801
Attn: Technical Information Branch

1 Commanding Officer
Harry Diamond Laboratories
Connecticut Ave. & Van Ness St., N.W.
Washington, D. C. 20438
Attn: Mr. Berthold Altman

1 Commanding Officer
Harry Diamond Laboratories
Attn: Library
Connecticut Ave. & Van Ness St., N.W.
Washington, D. C. 20438

1 Commanding Officer
U. S. Army Security Agency
Arlington Hall
Arlington, Virginia 22212

1 Commanding Officer
U. S. Army Limited War Laboratory
Aberdeen Proving Ground
Aberdeen, Maryland 21005
Attn: Technical Director

1 Commanding Officer
Human Engineering Laboratories
Aberdeen Proving Ground, Maryland 21005

1 Director
U. S. Army EngineerGeodesy, Intelligence and Mapping, Research & Devel. Agency
Fort Belvoir, Virginia 22060

1 Commandant
U. S. Army Command and General Staff College
Fort Leavenworth, Kansas 66207
Attn: Secretary

1 Dr. H. Robl, Deputy Director
U. S. Army Research Office (Durham)
Box CM, Duke Station
Durham, North Carolina 27706

1 Commanding Officer
U. S. Army Research Office (Durham)
P. O. Box CM, Duke Station
Durham, North Carolina 27706
Attn: CRD-AA-IP (Richard O. Ulsh)

1 Commanding General
U. S. Army Electronics Command
Fort Monmouth, New Jersey 07703
Attn: AMSEL-SC

1 Director
U. S. Army Electronics Laboratories
Fort Monmouth, New Jersey 07703
Attn: Dr. S. Benedict Levin, Director
Institute for Exploratory Research

1 Director
U. S. Army Electronics Laboratories
Fort Monmouth, New Jersey 07703
Attn: Mr. Robert O. Parker, Executive
Secretary, JSTAC (AMSEL-RD-X)

1 Superintendent
U. S. Military Academy
West Point, New York 10996

1 The Walter Reed Institute of Research
Walter Reed Army Medical Center
Washington, D. C. 20012

1 Director
U. S. Army Electronics Laboratories
Fort Monmouth, New Jersey 07703
Attn: AMSEL-RD-DR

1 Director
U. S. Army Electronics Laboratories
Attn: AMSEL-RD-X
Fort Monmouth, New Jersey 07703

1 Director
U. S. Army Electronics Laboratories
Fort Monmouth, New Jersey 07703
Attn: AMSEL-RD-XL

1 Director
U. S. Army Electronics Laboratories
Fort Monmouth, New Jersey 07703
Attn: AMSEL-RD-XC

1 Director
U. S. Army Electronics Laboratories
Fort Monmouth, New Jersey 07703
Attn: AMSEL-RD-XS

1 Director
U. S. Army Electronics Laboratories
Fort Monmouth, New Jersey 07703
Attn: AMSEL-RD-NR

1 Director
U. S. Army Electronics Laboratories
Fort Monmouth, New Jersey 07703
Attn: AMSEL-RD-NE

1 Director
U. S. Army Electronics Laboratories
Fort Monmouth, New Jersey 07703
Attn: AMSEL-RD-NO

1 Director
U. S. Army Electronics Laboratories
Fort Monmouth, New Jersey 07703
Attn: AMSEL-RD-NP

1 Director
U. S. Army Electronics Laboratories
Fort Monmouth, New Jersey 07703
Attn: AMSEL-RD-SA

1 Director
U. S. Army Electronics Laboratories
Fort Monmouth, New Jersey 07703
Attn: AMSEL-RD-SE

1 Director
U. S. Army Electronics Laboratories
Fort Monmouth, New Jersey 07703
Attn: AMSEL-RD-SR

1 Director
U. S. Army Electronics Laboratories
Fort Monmouth, New Jersey 07703
Attn: AMSEL-RD-SS

1 Director
U. S. Army Electronics Laboratories
Fort Monmouth, New Jersey 07703
Attn: AMSEL-RD-PE

1 Director
U. S. Army Electronics Laboratories
Fort Monmouth, New Jersey 07703
Attn: AMSEL-RD-PT

1 Director
U. S. Army Electronics Laboratories
Fort Monmouth, New Jersey 07703
Attn: AMSEL-RD-PR

1 Director
U. S. Army Electronics Laboratories
Fort Monmouth, New Jersey 07703
Attn: AMSEL-RL-GF

1 Director
U. S. Army Electronics Laboratories
Fort Monmouth, New Jersey 07703
Attn: AMSEL-RD-ADT

1 Director
U. S. Army Electronics Laboratories
Fort Monmouth, New Jersey 07703
Attn: AMSEL-RD-FU#1

1 Commanding Officer
U. S. Army Electronics R&D Activity
Fort Huachuca, Arizona 85163

1 Commanding Officer
U. S. Army Engineers R&D Laboratory
Fort Belvoir, Virginia 22060
Attn: STINFO Branch

1 Commanding Officer
U. S. Army Electronics R&D Activity
White Sands Missile Range
New Mexico 88002

1 Director
Human Resources Research Office
The George Washington University
300 N. Washington Street
Alexandria, Virginia

1 Commanding Officer
U. S. Army Personnel Research Office
Washington 25, D. C.

1 Commanding Officer
U. S. Army Medical Research Laboratory
Fort Knox, Kentucky

1 Commanding General
U. S. Army Signal Center and School
Attn: Chief, Office of Academic Operations
Fort Monmouth, New Jersey 07703

2 Dr. Richard H. Wilcox, Code 437
Department of the Navy
Washington, D. C. 20360

1 Chief, Bureau of Weapons
Attn: Technical Library, DL1-3
Department of the Navy
Washington, D. C. 20360

1 Chief, Bureau of Ships
Department of the Navy
Washington, D. C. 20360
Attn: Code 680

1 Chief, Bureau of Ships
Department of the Navy
Washington, D. C. 20360
Attn: Code 732

1 Commander
U. S. Naval Air Development Center
Johnsville, Pennsylvania
Attn: NADC Library

1 Commanding Officer
Naval Electronics Laboratory
San Diego, California 92052
Attn: Code 2222(Library)

1 Commanding Officer
Naval Electronics Laboratory
San Diego, California 92052
Attn: Code 2800, C. S. Manning

1 Commanding Officer and Director
(Code 142 Library)
David W. Taylor Model Basin
Washington, D. C. 20007

6 Director
Naval Research Laboratory
Washington, D. C. 20390
Attn: Technical Information Office
(Code 2000)

1 Commanding Officer
Office of Naval Research Branch Office
219 S. Dearborn Street
Chicago, Illinois 60604

1 Chief of Naval Operations
Department of the Navy
Washington, D. C. 20350
Attn: OP-07T

1 Chief of Naval Operations
Department of the Navy
Washington, D. C. 20350
Attn: OP-03EG

1 Commanding Officer
Office of Naval Research Branch Office
1000 Geary Street
San Francisco, California 94109

1 Commanding Officer
U. S. Naval Weapons Laboratory
Asst. Director for Computation
Dahlgren, Virginia 22448
Attn: G. H. Gleissner (Code K-4)

1 Inspector of Naval Material
Bureau of Ships Technical Representative
1902 West Minnehaha Avenue
St. Paul 4, Minnesota

5 Lt. Col. E. T. Gaines, SREE
Chief, Electronics Division
Directorate of Engineering Sciences
Air Force Office of Scientific Research
Washington, D. C. 20333

1 Director of Science & Technology
Deputy Chief of Staff (R & D)
USAF
Washington, D. C.
Attn: AFRST-EL/GU

1 Director of Science & Technology
Deputy Chief of Staff (R & D)
USAF
Washington, D. C.
Attn: AFRST-SC

1 Karl M. Fuechsel
Electronics Division
Director of Engineering Sciences
Air Force Office of Scientific Research
Washington, D. C. 20333

1 Lt. Col. Edwin M. Myers
Headquarters, USAF (AFRDR)
Washington 25, D. C.

1 Director, Air University Library
Maxwell Air Force Base
Alabama 36112
Attn: CR-4803a

1 Commander
Research & Technology Division
AFSC (Mr. Robert L. Feik)
Office of the Scientific Director
Bolling AFB 25, D. C.

1 Commander
Research & Technology Division
Office of the Scientific Director
Bolling AFB 25, D. C.
Attn: RTHR

1 Commander
Air Force Cambridge Research Laboratories
Attn: Research Library
CRMXL-R
L. G. Hanscom Field
Bedford, Massachusetts 01731

1 Dr. Lloyd Hollingsworth
AFCRL
L. G. Hanscom Field
Bedford, Massachusetts 01731

1 Commander
Air Force Cambridge Research Laboratories
Attn: Data Sciences Lab
(Lt. S. J. Kahne, CRB)
L. G. Hanscom Field
Bedford, Massachusetts 01731

1 Commander
Air Force Systems Command
Office of the Chief Scientist
(Mr. A. G. Wimer)
Andrews AFB, Maryland 20331

1 Commander
Air Force Missile Development Center
Attn: MDSGO/Major Harold Wheeler, Jr.
Holloman Air Force Base, New Mexico

1 Commander
Research & Technology Division
Attn: MAYT (Mr. Evans)
Wright-Patterson Air Force Base
Ohio 45433

1 Directorate of Systems Dynamics Analysis
Aeronautical Systems Division
Wright-Patterson AFB, Ohio 45433

1 Hqs. Aeronautical Systems Division
AF Systems Command
Attn: Navigation & Guidance Laboratory
Wright-Patterson AFB, Ohio 45433

1 Commander
Rome Air Development Center
Attn: Documents Library, RAALD
Griffiss Air Force Base
Rome, New York 13442

1 Commander
Rome Air Development Center
Attn: RAWI-Major W. H. Harris
Griffiss Air Force Base
Rome, New York 13442

1 Lincoln Laboratory
Massachusetts Institute of Technology
P. O. Box 73
Lexington 73, Massachusetts
Attn: Library A-082

Continued next page

Distribution list as of March 1, 1965 (Cont'd.)

1 Lincoln Laboratory
Massachusetts Institute of Technology
P. O. Box 73
Lexington 73, Massachusetts
Attn: Dr. Robert Kingston

1 APGC (PGAPI)
Eglin Air Force Base
Florida

1 Mr. Alan Barnum
Rome Air Development Center
Griffiss Air Force Base
Rome, New York 13442

1 Director
Research Laboratory of Electronics
Massachusetts Institute of Technology
Cambridge, Massachusetts 02139

1 Polytechnic Institute of Brooklyn
55 Johnson Street
Brooklyn, New York 11201
Attn: Mr. Jerome Fox
Research Coordinator

1 Director
Columbia Radiation Laboratory
Columbia University
538 West 120th Street
New York, New York 10027

1 Director
Coordinated Science Laboratory
University of Illinois
Urbana, Illinois 61803

1 Director
Stanford Electronics Laboratories
Stanford University
Stanford, California

1 Director
Electronics Research Laboratory
University of California
Berkeley 4, California

1 Professor A. A. Dougal, Director
Laboratories for Electronics and Related
Science Research
University of Texas
Austin, Texas 78712

1 Professor J. K. Aggarwal
Department of Electrical Engineering
University of Texas
Austin, Texas 78712

1 Director of Engineering & Applied Physics
210 Pierce Hall
Harvard University
Cambridge, Massachusetts 02138

1 Capt. Paul Johnson (USN Ret.)
National Aeronautics & Space Agency
1520 H. Street, N. W.
Washington 25, D. C.

1 NASA Headquarters
Office of Applications
400 Maryland Avenue, S.Q.
Washington 25, D. C.
Attn: Code FC Mr. A. M. Greg Andrus

1 National Bureau of Standards
Research Information Center and Advisory
Serv. on Info. Processing
Data Processing Systems Division
Washington 25, D. C.

1 Dr. Wallace Sinaiko
Institute for Defense Analyses
Research & Eng. Support Div.
1666 Connecticut Avenue, N. W.
Washington 9, D. C.

1 Data Processing Systems Division
National Bureau of Standards
Conn. at Van Ness
Room 239, Bldg. 10
Washington 25, D. C.
Attn: A. K. Smilow

1 Exchange and Gift Division
The Library of Congress
Washington 25, D. C.

1 Dr. Alan T. Waterman, Director
National Science Foundation
Washington 25, D. C.

1 H. E. Cochran
Oak Ridge National Laboratory
P. O. Box X
Oak Ridge, Tennessee

1 U. S. Atomic Energy Commission
Office of Technical Information Extension
P. O. Box 62
Oak Ridge, Tennessee

1 Mr. G. D. Watson
Defense Research Member
Canadian Joint Staff
2450 Massachusetts Avenue, N. W.
Washington 8, D. C.

1 Martin Company
P. O. Box 5837
Orlando, Florida
Attn: Engineering Library MP-30

1 Laboratories for Applied Sciences
University of Chicago
6220 South Drexel
Chicago, Illinois 60637

1 Librarian
School of Electrical Engineering
Purdue University
Lafayette, Indiana

1 Donald L. Epley
Dept. of Electrical Engineering
State University of Iowa
Iowa City, Iowa

1 Instrumentation Laboratory
Massachusetts Institute of Technology
68 Albany Street
Cambridge 39, Massachusetts
Attn: Library WI-109

1 Sylvania Electric Products, Inc.
Electronics System
Waltham Labs. Library
100 First Avenue
Waltham 54, Massachusetts

2 Hughes Aircraft Company
Centinela and Teale Streets
Culver City, California
Attn: K. C. Rosenberg, Supervisor
Company Technical Document Center

3 Autonetics
9150 East Imperial Highway
Downey, California
Attn: Tech. Library, 3041-11

1 Dr. Arnold T. Nordsieck
General Motors Corporation
Defense Research Laboratories
6767 Hollister Avenue
Goleta, California

1 University of California
Lawrence Radiation Laboratory
P. O. Box 808
Livermore, California

1 Mr. Thomas L. Hartwick
Aerospace Corporation
P. O. Box 95085
Los Angeles 45, California

1 Lt. Col. Willard Levin
Aerospace Corporation
P. O. Box 95085
Los Angeles 45, California

1 Sylvania Electronic Systems-West
Electronic Defense Laboratories
P. O. Box 205
Mountain View, California
Attn: Documents Center

1 Varian Associates
611 Hansen Way
Palo Alto, California 94303
Attn: Tech. Library

1 Huston Denslow
Library Supervisor
Jet Propulsion Laboratory
California Institute of Technology
Pasadena, California

1 Professor Nicholas George
California Institute of Technology
Electrical Engineering Department
Pasadena, California

1 Space Technology Labs., Inc.
One Space Park
Redondo Beach, California
Attn: Acquisitions Group
STL Technical Library

1 The Rand Corporation
1700 Main Street
Santa Monica, California
Attn: Library

1 Miss F. Cloak
Radio Corp. of America
RCA Laboratories
David Sarnoff Research Center
Princeton, New Jersey

1 Mr. A. A. Lundstrom
Bell Telephone Laboratories
Room 2E-127
Whippany Road
Whippany, New Jersey

1 Cornell Aeronautical Laboratory, Inc.
4455 Genesee Street
Buffalo 21, New York
Attn: J. P. Desmond, Librarian

1 Sperry Gyroscope Company
Marine Division Library
155 Glenn Cove Road
Carle Place, L. I., New York
Attn: Miss Barbara Judd

1 Library
Light Military Electronics Dept.
General Electric Company
Armament & Control Products Section
Johnson City, New York

1 Dr. E. Howard Holt
Director
Plasma Research Laboratory
Rennselaer Polytechnic Institute
Troy, New York

1 Battele-DEFENDER
Battelle Memorial Institute
505 King Avenue
Columbus 1, Ohio

1 Laboratory for Electroscience Research
New York University
University Heights
Bronx 53, New York

1 National Physical Laboratory
Teddington, Middlesex
England
Attn: Dr. A. M. Uttley, Superintendent,
Autonomics Division

1 Dr. Lee Huff
Behavioral Sciences
Advanced Research Projects Agency
The Pentagon (Room 3E175)
Washington, D. C. 20301

1 Dr. Glenn L. Bryan
Head, Personnel and Training Branch
Office of Naval Research
Navy Department
Washington, D. C. 20360

1 Instituto de Fisica Aplicado
"L. Torres Quevedo"
High Vacuum Laboratory
Madrid, Spain
Attn: Jose L. de Segovia

1 Stanford Research Institute
Attn: G-037 External Reports
(for J. Goldberg)
Menlo Park, California 94025

REVISED U. S. ARMY DISTRIBUTION LIST

(As received at the Coordinated Science Laboratory 27 July 1965)

1 Dr. Chalmers Sherwin
Deputy Director (Research & Technology)
DD&RE Rm 3E1060
The Pentagon
Washington, D. C. 20301

1 Dr. Edward M. Reilley
Asst. Director (Research)
Ofc. of Defense Res. & Eng.
Department of Defense
Washington, D. C. 20301

1 Dr. James A. Ward
Office of Deputy Director (Research and Information Rm 3D1037)
Department of Defense
The Pentagon
Washington, D. C. 20301

1 Director
Advanced Research Projects Agency
Department of Defense
Washington, D. C. 20301

1 Mr. E. I. Salkovitz, Director for Materials Sciences
Advanced Research Projects Agency
Department of Defense
Washington, D. C. 20301

1 Colonel Charles C. Mack
Headquarters
Defense Communications Agency (333)
The Pentagon
Washington, D. C. 20305

20 Defense Documentation Center
Attn: TISIA
Cameron Station, Building 5
Alexandria, Virginia 22314

1 Director
National Security Agency
Attn: Librarian C-332
Fort George G. Meade, Maryland 20755

1 U. S. Army Research Office
Attn: Physical Sciences Division
3045 Columbia Pike
Arlington, Virginia 22204

1 Chief of Research and Development
Headquarters, Department of the Army
Attn: Mr. L. H. Geiger, Rm 3D442
Washington, D. C. 20310

1 Research Plans Office
U. S. Army Research Office
3045 Columbia Pike
Arlington, Virginia 22204

1 Commanding General
U. S. Army Materiel Command
Attn: AMCRD-RS-PE-E
Washington, D. C. 20315

1 Commanding General
U. S. Army Strategic Communications Command
Washington, D. C. 20315

1 Commanding Officer
U. S. Army Materials Research Agency
Watertown Arsenal
Watertown, Massachusetts 02172

1 Commanding Officer
U. S. Army Ballistics Research Laboratory
Attn: V. W. Richards
Aberdeen Proving Ground
Aberdeen, Maryland 21005

1 Commanding Officer
U. S. Army Ballistics Research Laboratory
Attn: Keats A. Pullen, Jr.
Aberdeen Proving Ground
Aberdeen, Maryland 21005

1 Commanding Officer
U. S. Army Ballistics Research Laboratory
Attn: George C. Francis, Computing Lab.
Aberdeen Proving Ground, Maryland 21005

1 Commandant
U. S. Army Air Defense School
Attn: Missile Sciences Division, C&S Dept.
P. O. Box 9390
Fort Bliss, Texas 79916

1 Commanding General
U. S. Army Missile Command
Attn: Technical Library
Redstone Arsenal, Alabama 35809

1 Commanding General
Frankford Arsenal
Attn: SMUFA-1310 (Dr. Sidney Ross)
Philadelphia, Pennsylvania 19137

1 Commanding General
Frankford Arsenal
Attn: SMUFA-1300
Philadelphia, Pennsylvania 19137

1 U. S. Army Munitions Command
Attn: Technical Information Branch
Picatinney Arsenal
Dover, New Jersey 07801

1 Commanding Officer
Harry Diamond Laboratories
Attn: Mr. Berthold Altman
Connecticut Avenue and Van Ness St.,N.W.
Washington, D. C. 20438

1 Commanding Officer
Harry Diamond Laboratories
Attn: Library
Connecticut Avenue and Van Ness St.,N.W.
Washington, D. C. 20438

1 Commanding Officer
U. S. Army Security Agency
Arlington Hall
Arlington, Virginia 22212

1 Commanding Officer
U. S. Army Limited War Laboratory
Attn: Technical Director
Aberdeen Proving Ground
Aberdeen, Maryland 21005

1 Commanding Officer
Human Engineering Laboratories
Aberdeen Proving Ground, Maryland 21005

1 Director
U. S. Army Engineer Geodesy, Intelligence & Mapping
Research and Development Agency
Fort Belvoir, Virginia 22060

1 Commandant
U. S. Army Command and General Staff College
Attn: Secretary
Fort Leavenworth, Kansas 66207

1 Dr. H. Robl, Deputy Chief Scientist
U. S. Army Research Office (Durham)
Box CM, Duke Station
Durham, North Carolina 27706

1 Commanding Officer
U. S. Army Research Office (Durham)
Attn: CRD-AA-IP (Richard O. Ulsh)
Box CM, Duke Station
Durham, North Carolina 27706

1 Superintendent
U. S. Army Military Academy
West Point, New York 10996

1 The Walter Reed Institute of Research
Walter Reed Army Medical Center
Washington, D. C. 20012

1 Commanding Officer
U. S. Army Electronics R&D Activity
Fort Huachuca, Arizona 85163

1 Commanding Officer
U. S. Army Engineers R&D Laboratory
Attn: STINFO Branch
Fort Belvoir, Virginia 22060

1 Commanding Officer
U. S. Army Electronics R&D Activity
White Sands Missile Range, New Mexico 88002

1 Director
Human Resources Research Office
The George Washington University
300 N. Washington Street
Alexandria, Virginia 22300

1 Commanding Officer
U. S. Army Personnel Research Office
Washington, D. C.

1 Commanding Officer
U. S. Army Medical Research Laboratory
Fort Knox, Kentucky 40120

1 Commanding General
U. S. Army Signal Center and School
Fort Monmouth, New Jersey 07703
Attn: Chief, Office of Academic Operations

1 Dr. S. Benedict Levin, Director
Institute for Exploratory Research
U. S. Army Electronics Command
Fort Monmouth, New Jersey 07703

1 Director
Institute for Exploratory Research
U. S. Army Electronics Command
Attn: Mr. Robert O. Parker, Executive Secretary, JSTAC (AMSEL-XL-D)
Fort Monmouth, New Jersey 07703

1 Commanding General
U. S. Army Electronics Command
Fort Monmouth, New Jersey 07703

Attn: AMSEL-SC
RD-D
RD-G
RD-MAF-I
RD-MAT
RD-GF
RD-MN (Marine Corps LnO)
XL-D
XL-E
XL-C
XL-S
HL-D
HL-L
HL-J
HL-P
HL-O
HL-R
NL-D
NL-A
NL-P
NL-R
NL-S
KL-D
KL-E
KL-S
KL-T
VL-D
WL-D

1 Mr. Charles F. Yost
Special Assistant to the Director of Research
National Aeronautics & Space Admin.
Washington, D. C. 20546

1 Director
Research Laboratory of Electronics
Massachusetts Institute of Technology
Cambridge, Massachusetts 02139

1 Polytechnic Institute of Brooklyn
55 Johnson Street
Brooklyn, New York 11201
Attn: Mr. Jerome Fox
Research Coordinator

1 Director
Columbia Radiation Laboratory
Columbia University
538 West 120th Street
New York, New York 10027

1 Director
Stanford Electronics Laboratories
Stanford University
Stanford, California 94301

1 Director
Electronics Research Laboratory
University of California
Berkeley, California 94700

1 Director
Electronic Sciences Laboratory
University of Southern California
Los Angeles, California 90007

1 Professor A. A. Dougal, Director
Laboratories for Electronics and Related Science Research
University of Texas
Austin, Texas 78712

1 Professor J. K. Aggarwal
Department of Electrical Engineering
University of Texas
Austin, Texas 78712

1 Division of Engineering and Applied Physics
210 Pierce Hall
Harvard University
Cambridge, Massachusetts 02138

Security Classification

DOCUMENT CONTROL DATA R&D

(Security classification of title, body of abstract and indexing annotation must be entered when the overall report is classified)

1. ORIGINATING ACTIVITY (Corporate author)
University of Illinois
Coordinated Science Laboratory
Urbana, Illinois 61801

2a. REPORT SECURITY CLASSIFICATION
Unclassified

2b. GROUP

3. REPORT TITLE

HIGH RESOLUTION RADIO FREQUENCY MEASUREMENTS OF FARADAY ROTATION AND DIFFERENTIAL ABSORPTION WITH ROCKET PROBES.

4. DESCRIPTIVE NOTES (Type of report and inclusive dates)

5. AUTHOR(S) (Last name, first name, initial)

Knoebel, Howard W.; Skaperdas, Dominic G.; Gooch, Jay D.; Kirkwood, Bill D.; and Krone, Henry V.

6. REPORT DATE
December, 1965

7a TOTAL NO. OF PAGES
131

7b. NO. OF REFS.
6

8a. CONTRACT OR GRANT NO.
DA 28 043 AMC 00073(E)

b. PROJECT NO.
20014501B31F

c. Also National Aeronautics and Space Administration under

d. Grant No. NsG 504

9a. ORIGINATOR'S REPORT NUMBER(S)
R-273

9b. OTHER REPORT NO(S) (Any other numbers that may be assigned this report)

10. AVAILABILITY/LIMITATION NOTICES

Qualified requesters may obtain copies of this report from DDC.
This report may be released to OTS.

11. SUPPLEMENTARY NOTES

12. SPONSORING MILITARY ACTIVITY
U. S. Army Electronics Command
Ft. Monmouth, New Jersey 07703

13. ABSTRACT

A highly essential system for lower ionosphere radio propagation measurements, using probe rockets, developed by the Coordinated Science Laboratory, is described in detail. Unique features include 1) feedback around a closed loop consisting of the rocket and ground stations employed in a null-seeking technique, which increased absorption measurement accuracy and 2) artificial rotation of the ground based antenna which extends the range over which Faraday rotation can be resolved from layer reflection phenomena. The rocket borne and ground station equipment has been shown to work reliably during a series of 14 rocket measurements made from both land-based facilities and the NASA seagoing mobile launch platform during the International Quiet Sun Years. Complete engineering information is given in the hope that other investigators may easily duplicate the measurements. Data processing techniques for smoothing and improving the accuracy as well as some typical data are described.

This system was developed by a group of scientists and engineers who are primarily interested in aerospace instrumentation, measurement control, and data handling techniques working in cooperation with the ionosphere scientists at the University of Illinois Electrical Engineering Department who were responsible for the basic research program. It is felt that the application of sound engineering principles to this program of basic measurement will greatly aid in obtaining an understanding of our atmosphere.

DD FORM 1 JAN 64 1473

Security Classification

Security Classification

KEY WORDS	LINK A		LINK B		LINK C	
	ROLE	WT	ROLE	WT	ROLE	WT
Faraday rotation						
differential absorption						
lower ionosphere						
radio propagation measurements						
aerospace instrumentation						
measurement control						
data processing techniques						
International Year of the Quiet Sun						
electron density in the D region of the ionosphere						
collision frequency in the D region of the ionosphere						

INSTRUCTIONS

1. ORIGINATING ACTIVITY: Enter the name and address of the contractor, subcontractor, grantee, Department of Defense activity or other organization (corporate author) issuing the report.

2a. REPORT SECURITY CLASSIFICATION: Enter the overall security classification of the report. Indicate whether "Restricted Data" is included. Marking is to be in accordance with appropriate security regulations.

2b. GROUP: Automatic downgrading is specified in DoD Directive 5200.10 and Armed Forces Industrial Manual. Enter the group number. Also, when applicable, show that optional markings have been used for Group 3 and Group 4 as authorized.

3. REPORT TITLE: Enter the complete report title in all capital letters. Titles in all cases should be unclassified. If a meaningful title cannot be selected without classification, show title classification in all capitals in parenthesis immediately following the title.

4. DESCRIPTIVE NOTES: If appropriate, enter the type of report, e.g., interim, progress, summary, annual, or final. Give the inclusive dates when a specific reporting period is covered.

5. AUTHOR(S): Enter the name(s) of author(s) as shown on or in the report. Enter last name, first name, middle initial. If military, show rank and branch of service. The name of the principal author is an absolute minimum requirement.

6. REPORT DATE: Enter the date of the report as day, month, year; or month, year. If more than one date appears on the report, use date of publication.

7a. TOTAL NUMBER OF PAGES: The total page count should follow normal pagination procedures, i.e., enter the number of pages containing information.

7b. NUMBER OF REFERENCES: Enter the total number of references cited in the report.

8a. CONTRACT OR GRANT NUMBER: If appropriate, enter the applicable number of the contract or grant under which the report was written.

8b, 8c, & 8d. PROJECT NUMBER: Enter the appropriate military department identification, such as project number, subproject number, system numbers, task number, etc.

9a. ORIGINATOR'S REPORT NUMBER(S): Enter the official report number by which the document will be identified and controlled by the originating activity. This number must be unique to this report.

9b. OTHER REPORT NUMBER(S): If the report has been assigned any other report numbers (either by the originator or by the sponsor), also enter this number(s).

10. AVAILABILITY/LIMITATION NOTICES: Enter any limitations on further dissemination of the report, other than those imposed by security classification, using standard statements such as:

(1) "Qualified requesters may obtain copies of this report from DDC."

(2) "Foreign announcement and dissemination of this report by DDC is not authorized."

(3) "U. S. Government agencies may obtain copies of this report directly from DDC. Other qualified DDC users shall request through

_____."

(4) "U. S. military agencies may obtain copies of this report directly from DDC. Other qualified users shall request through

_____."

(5) "All distribution of this report is controlled. Qualified DDC users shall request through

_____."

If the report has been furnished to the Office of Technical Services, Department of Commerce, for sale to the public, indicate this fact and enter the price, if known.

11. SUPPLEMENTARY NOTES: Use for additional explanatory notes.

12. SPONSORING MILITARY ACTIVITY: Enter the name of the departmental project office or laboratory sponsoring (paying for) the research and development. Include address.

13. ABSTRACT: Enter an abstract giving a brief and factual summary of the document indicative of the report, even though it may also appear elsewhere in the body of the technical report. If additional space is required, a continuation sheet shall be attached.

It is highly desirable that the abstract of classified reports be unclassified. Each paragraph of the abstract shall end with an indication of the military security classification of the information in the paragraph, represented as (TS), (S), (C), or (U).

There is no limitation on the length of the abstract. However, the suggested length is from 150 to 225 words.

14. KEY WORDS: Key words are technically meaningful terms or short phrases that characterize a report and may be used as index entries for cataloging the report. Key words must be selected so that no security classification is required. Identifiers, such as equipment model designation, trade name, military project code name, geographic location, may be used as key words but will be followed by an indication of technical context. The assignment of links, roles, and weights is optional.

DD FORM 1 JAN 64 1473

Security Classification